POLITECNICO DI MILANO

School of Industrial and Information Engineering

Department of Chemistry, Materials and Chemical Engineering

"Giulio Natta"

Surface Tension Assisted Devices For Drugs And Cells Delivery Using Hydrogels

Advisor: Prof. Filippo Rossi

Co-Advisors: Prof. Mark W. Tibbitt

Dr. Arianna Rossetti

Mr. Elia Guzzi

Viola Chiozzi, 918238

Anno accademico 2018/2019

Ringraziamenti

Ringraziamenti alle persone e alle istituzioni che hanno collaborato al lavoro di tesi. Lunghezza: da poche righe a una pagina.

Abstract

The drug delivery field is a branch in continuous development and research by the scientific community, due to the utility in the practical life for disease treatments, tissue regeneration, tailored therapeutics releasing. Cells "in loco" delivery is also a deeply investigated field, especially for anti-tumour treatments and wound healing.

These objectives can be achieved using combinations of different solutions or exploiting composite materials, made of two or more different constituents with distinct chemical or physical properties of other two or more systems. This allows to exploit the best characteristics from a great quantities of technologies.

In this work we investigated the uses of 3D- printed devices, that thanks to superficial tension, can be tightly coated with drug or cells loaded hydrogels. The aim is to have both the on-target delivery of different types of cells and diffusion-based release of both hydrophilic and hydrophobic drugs loaded in a hydrophilic hydrogel matrix.

In the Macromolecular Engineering Laboratory of ETH ZÜRICH, the biocompatible support made of polycaprolactone has been 3D printed and coated with two different hydrogels, methacrylated gelatin (GelMa) and sodium alginate. Regarding the metallic support, this has been printed in DL60 resin by the +LAB of Politecnico di Milano and metallized by the SEE Lab of Politecnico di Milano, using the layer by layer teqnique.

Considering the cells delivery part, NIH/3T3 (ATCC® CRL-1658™) fibroblasts have been encapsulated in GelMa. For the drug delivery part of the project we loaded two types of model drugs:

- Rhodamine B Isothiocyanate, hydrophilic, loaded thanks to steric phenomena

- Oil Red O, hydrophobic, loaded into GelMa and sodium alginate using polymeric nanoparticles of polyethylene glycol linked to polylactic acid (PEG-PLA Nanoparticles).

The crosslinking kinetic has been evaluated through rheologic analysis for both the systems.
The entire experimental work has been carried out at ETH ZÜRICH.

For further experimentation, at the end of the project, we started to synthesized, in liquid phase, the RGD peptide sequence (arginylglycylaspartic acid), with the future outlook of chemically linked it to the sodium alginate molecules using amidic bonds, in order to analyse which of the two systems between GelMa and sodium alginate would be better for cells delivery application.

Sommario

Il settore del "*drug delivery*" è una branca in costante sviluppo e ricerca da parte della comunità scientifica, grazie all'utilità nella vita pratica per i trattamenti delle malattie, la rigenerazione dei tessuti, il rilascio di terapie su misura. Anche la consegna "in loco" delle cellule è un campo profondamente studiato, in particolare per i trattamenti anti-tumorali e la guarigione delle ferite. Questi obiettivi possono essere raggiunti utilizzando combinazioni di soluzioni diverse o sfruttando materiali compositi, costituiti da due o più componenti diversi con proprietà chimiche o fisiche distinte di altri due o più sistemi. Ciò consente di sfruttare le migliori caratteristiche da una più grande quantità di tecnologie.

In questo lavoro abbiamo studiato gli usi dei dispositivi stampati in 3D che, grazie alla tensione superficiale, possono essere saldamente rivestiti con idrogels contenenti farmaci o cellule. L'obiettivo è quello di avere sia la consegna in uno specifico punto di diversi tipi di cellule sia il rilascio basato sulla diffusione di farmaci idrofili e idrofobici caricati in una matrice idrofila o idrofoba.

Nel laboratorio di ingegneria macromolecolare dell' ETH ZÜRICH, il supporto biocompatibile in policaprolattone è stato stampato in 3D e rivestito con due diversi idrogels, la gelatina metacrilata (GelMa) e l'alginato di sodio. Per quanto riguarda il supporto metallico, questo è stato stampato in resina DL60 dal + LAB del Politecnico di Milano e metallizzato dal SEE Lab del Politecnico di Milano, utilizzando la tecnica del *layer by layer*.

Per la parte del progetto riguardante il trasporto in loco di cellule, sono stati incapsulati fibroblasti NIH / 3T3 (ATCC® CRL-1658 ™) direttamente

nell'hydrogel di GelMa. Per la parte relativa alla consegna dei farmaci invece, abbiamo caricato due tipi di molecole "modello":

• Rodamina B, idrofila, caricata grazie a proprietà steriche

• Oil Red O, idrofobo, caricato sia nel GelMa che nell'alginato di sodio usando nanoparticelle polimeriche di polietilenglicole legate all'acido polilattico (nanoparticelle PEG-PLA).

La cinetica di crosslinking è stata valutata mediante analisi reologiche per entrambi i sistemi.

L'intero lavoro sperimentale è stato svolto presso l'ETH ZÜRICH.

Per ulteriori sperimentazioni, alla fine del progetto, abbiamo iniziato a sintetizzare, in fase liquida, la sequenza peptidica RGD (acido arginilglicilaspartico), in prospettiva futura di legarlo chimicamente alle molecole di alginato di sodio usando legami amidici, al fine di analizzare poi quale dei due sistemi tra GelMa e alginato di sodio sarebbe più indicato per il trasporto ed il supporto cellulare.

INDEX

LIST OF FIGURES

LIST OF TABLES

CHAPTER 1

INTRODUCTION

Nowadays, in the scientific world, one of the primary goals is to develop always smarter and newer therapeutic innovations to increase the efficiency of medical treatments and at the same time improving the patient feedbacks.

The past approach of conventional drug delivery sees a non- selective methodological approach, based on transportation by physiological systems, for example through digestive system or blood circulation. Sometimes, in these cases, there are problems due to high administration frequencies and possibilities of overdosages and/or underdosages.

A way to try to solve these issues is to focus researches on targeted drug delivery systems, thanks to which it is possible to released with a controlled and selective approach involving in:

- Improving the lifetime of the pharmaceutical effect while decreasing side-effects

- Reducing the waste of medicines

- Increasing patients approval diminishing administration frequencies and invasiveness

Regarding the cells *in vitro* culture and in loco delivery, since the forties, them have been cultured in 2D, essentially attached to plastic surfaces or glass. Nowadays, there is the need of giving them a more realistic extra cellular matrix environment, both to better understand their behaviours and functions and to investigate on cancer formation of malignant cells. In fact, forcing the cells to adapt themselves to a 2D layer, implies a possible alteration of metabolism and changing or reducing some aspects of their functionalities. The goal of regenerative medicine is to create a local artificial environment for cells' life

where proliferation and differentiation are efficiently accomplished in the way to induce the healing of damaged tissues. At the same time, natural polymers can be successfully engineered to release growth factors in order to imitate the human healing process and to favour fast tissue regeneration.

The topic of this thesis project is to design an artificial system that, supported by the phenomena of superficial tension, could transport and delivery in loco both cells and drugs with the same hydrogel matrix.

The following chapters focus on the devices fabrication, the hydrogels choices and mechanical aspects, the cells response and the drug delivery part with both an hydrophilic model drug (Rhodamine B) and an hydrophobic one (Oil Red O) encapsulated using polymeric nanoparticles.

In particular, the work will be structured as follows:

- The 3D printing of both the PCL device and the metallic one, the former performed in the Macromolecular Engineering Laboratory (MEL) of ETH Zürich, the latter printed by the +LAB of Politecnico di Milano, exploiting the technique of micro stereolithography (µSLA) with DL260 resin as support material. The metallization of this one was operated in the SEE Lab of Politecnico di Milano by wet metallization technique to make it biocompatible and magnetic, using a layer by layer electroless approach.

- The synthesis and functionalization of methacrylated gelatin, its rheological properties and polymerization process

- The cells viability studies, carried out both with PCL devices and metallic ones

- The drug releasing part of the hydrophobic mimic drugs, Oil Red O, loaded in the hydrogel solution through polymeric nanoparticles, characterized in size and Zeta Potential by DLS

- The drug releasing part of the hydrophilic mimic drugs, Rhodamine B Isothiocyanate, sterically loaded in the hydrogel solution

- The degradation analysis of Rhodamine B due to the combination of the photo-initiatior and UV light

The adhesion of the hydrogel liquid solution to the two different types of supports has been performed using planar grids in the way to coat them easier and to incubate them in common well-plates. Anyhow, the shape of the support could be whatever is desired to be, because the superficial tension would work with every different shape. The supports with holes are in fact designed in a way that, printing them also with other shapes or geometries, can still support the hydrogel matrix thanks to interfacial forces.

The hydrogel precursor solution has been formulated with three different GelMA percentages to test which one would has been better for the cellular life.

The drugs release profiles have been investigated at two different timings to check the influence of the mesh size of the hydrogels matrix.

3D PRINTING AND METALLIZATION

2.1 3D Printing

3D printing is an operation that generates 3D objects by adding material layer after layer. It is very flexible and permit to create an object of shape and dimension that we desire.

2.2 Process

For the metallic devices, everything start creating a CAD (computer aided design) model. Then the 3D structures are fabricated by means of stereolithography, SLA, that is based on the polymerization of a photocurable resin using a UV laser source, computer-controlled by galvano-mirrors. [1] At this point the photocurable resin is transformed into polymer inside a 2D layer. Then, consequently, the platform lowers, and the next not polymerized resin is applied.

Epoxy and acrylic resins are the typical polymers used for SLA, as well as UV absorbers or photo initiator to manipulate the rate and the quality of polymerization.

One of the drawbacks, in particular for biological application, is the risk ok cytotoxicity of the residues of photo initiators and/or uncured resin.[2]

In addition to SLA, that is included in the group of the Light polymerized family, we can mention also other families like Power Bed and Material Extrusion.

In the former there is a continuous layer of granules coupled with a moving head that works by binding with a gluing or a laser a zone of the surface. Afterwards, other layer after layer of granules are deposited .

About Material Extrusion (figure 2.1), it is used a thermoplastic material, heated up to its melting temperature and then extruded on a support by means of a pressurized nozzle. When in contact with lower temperatures, the melted material rapidly hardens. The nozzle shifts through the plane while extruding material
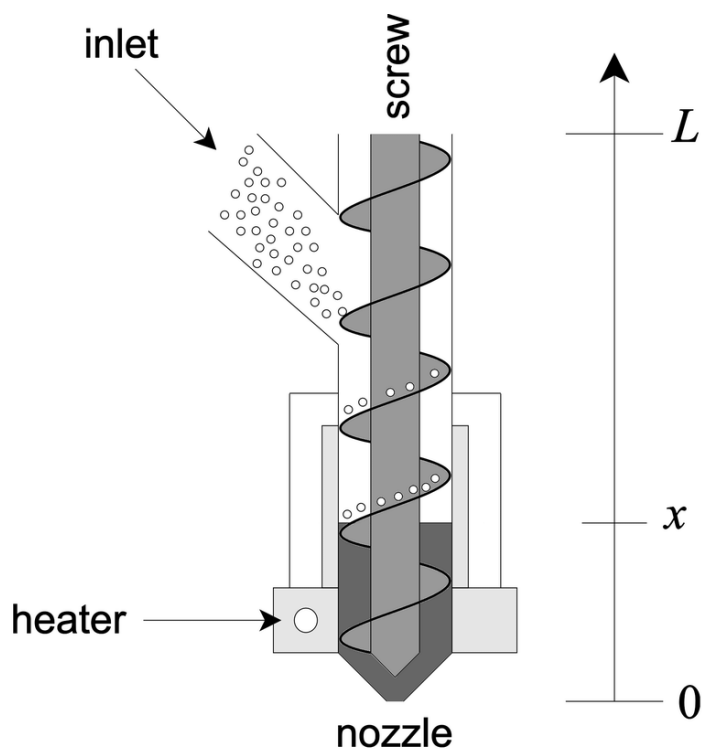
Figure 2.1 – 3D Printing with Material Extrusion

2.3 Electroless Deposition

It is a technique used to apply a metallic coating over a semi conductive or conductive surface, without using any external current, as it is done for common electro deposition. Metals, alloys or composites can be deposited with this process. This particular operation, aim at improving superficial hardness, corrosion resistance or to transform the surface of the metal in a magnetic surface.

The process is based on redox reactions and it is requested that the $\Delta G°$ is negative.

$$\Delta G = -zFE$$

Where z is the number of electrons taking part in the redox mechanism, F is the faraday's constant and E is the standard electrode potential.

Two different mechanisms exist through which the process can take place:

- Galvanic Displacement
- Autocatalytic Deposition

2.3.1 Galvanic Displacement
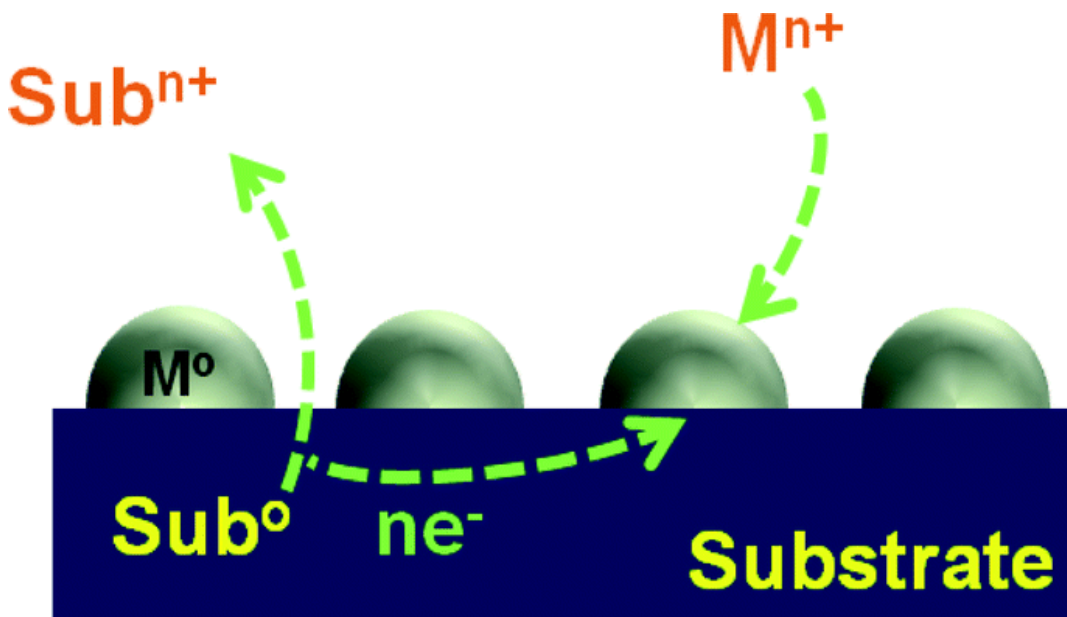
Figure 2.2 – Mechanism of galvanic displacement

~ 7 ~

It is due to the coupling of a less noble metal immersed in a solution containing ions of a more noble metal.

The chemical reactions that take part in the process are:

$$M_2^{n+} + ne^- = M_2 \text{ Reduction}$$

$$M_1 = M_1^{n+} + ne^- \text{ Oxidation}$$
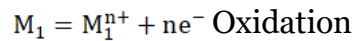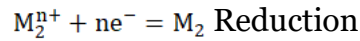
Where M_1 is the less noble metal and M_2 is the more noble metal. During the procedure, the atoms on the surface of the less noble metal are replaced by the ones of the more noble. Theoretically only a mono- layer could be deposited with this method but thicker deposits can be created because the deposited metal could be porous or there are differences in dissolution and deposition rate among the two metals.

2.3.2 Autocatalytic Deposition

Also this process is operated through a redox reaction, in the solution we dissolved the metal to be deposited as positive ions. Then there is the reducing agent that provides the electrons for the reduction, for example formaldehyde, hydrazine, sodium hypophosphite. As the name says, the reaction catalysed itself by depositing film. The reaction that take place is:

$$M^{n+} + RedAg^{m-} = M + RedAg^{n-m}$$
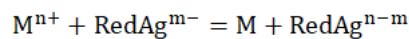
Where RedAg is the reducing agent and M is the metal to be deposited. Differently from galvanic displacement, with the autocatalytic deposition the film thickness cannot be theoretically limited.

2.4 CoNiP

This alloy made of Cobalt, Nickel and Phosphorous, of which our metallic devices are made, it is of particular interest in the electroless deposition procedures also because shows magnetic properties together with good corrosion resistances and hardness. The chemical bath can be made in the following way: "$NiSO_4·6H_2O$ and $CoSO_4·6H_2O$ were used as the source of nickel and cobalt, respectively. $NaH_2PO_2·H_2O$ was used as a reducing agent, which also forms the source of phosphorus in the deposit. $Na_3C_6H_5O_7$ was used as the complexing agent to control the rate of release of free metal ions for the reduction reaction. In addition to other constituents, ammonia solution was added to control the bath pH and the bath was operated at a constant temperature 35 ± 1 °C during the deposition process."[3]

2.5 Polycaprolactone and 3D Printing

Polycaprolactone is a biodegradable polyester with melting point around 60°C , glass transition temperature of around -60°C and decomposition temperature of 350°C.
Lately, this polymer has earned a lot of attention. Among synthetic polymers in fact, is one of the easiest to manipulate and to process into a wide rage of sizes and shapes, thanks to its low melting temperature and its considerable viscoelastic properties. It has been exploited in tissue engineering and drug delivery applications.
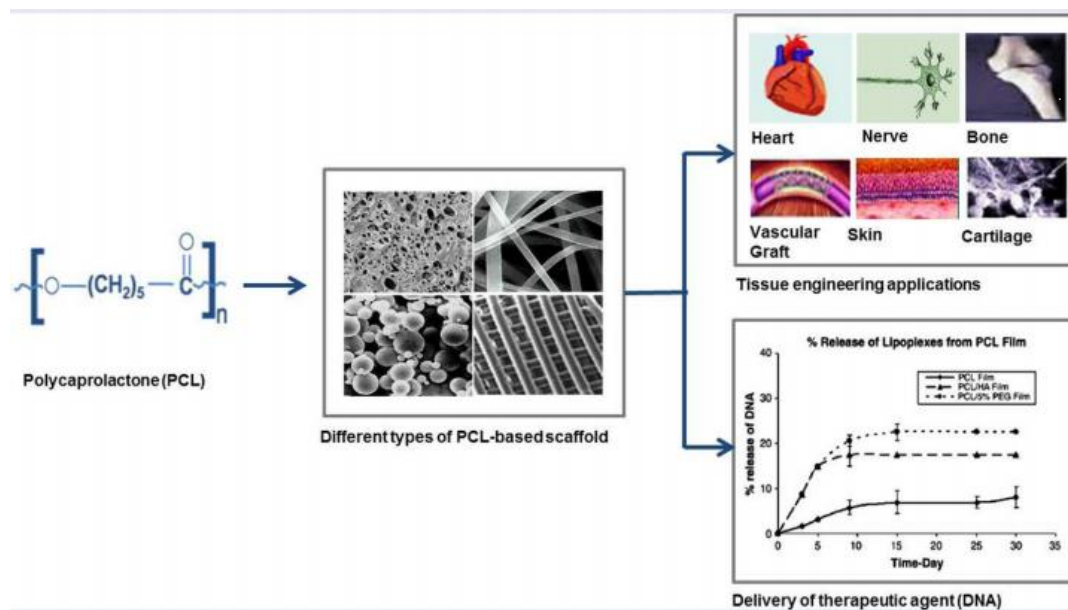
Figure 2.3 - PCL Scenario

In particular, this material has been defined as implantable biomaterial for medical application, considering also nerve regeneration, wound dressing and bone tissue engineering. In addition, it is exploited as a vehicle for controlled therapeutics molecules delivery (drugs, proteins, genes).

PCL is an hydrophobic linear aliphatic polyester, semi crystalline, relatively slow-degrading polymer, thermoplastic and with a good stability at ambient conditions.[4]

A lot of different processes have been improved to design and fabricate 3D PCL scaffolds, including solvent casting, fibre bonding, membrane lamination, temperature- induced phase separation, gas foaming and obviously three-dimensional printing. Anyway, none of these techniques have permitted researchers to fabricate scaffolds with totally interconnected pore network and with a highly solvent- free reproducibility, regarding the scaffold morphology.

These features are essential to facilitate cells differentiation and proliferation, mimic the extracellular matrix and flow of nutrient sand wastes.[5]

CHAPTER 3
HYDROGELS

3.1 Structure

Hydrogels are 3D networks of hydrophilic polymers that can usually swell in water and maintain their structure due to chemical or physical cross-linking of individual chains. By definition, they posses at least 10% of their total weight in water and highly degree of flexibility. The hydrophilic groups like -OH, -COOH, -NH2, -CONH and – SO_3H ensure the hydrophobicity of the network.

Usually, under the influence of certain chemical or physical stimuli, they undergo to a significant sol-gel transition. As physical stimuli we can include temperature, electromagnetic fields, light intensity and pressure. For the chemical type, pH, ions or particular chemical composition. The response to the external stimuli is determined for the most part by the nature of the monomer, degree of crosslinking, charge density. In the most cases, such transitions are reversible.[6]

The property to avoid network dissolution is guaranteed by the crosslinking between the polymeric chains that establish a matrix which retains the liquid.
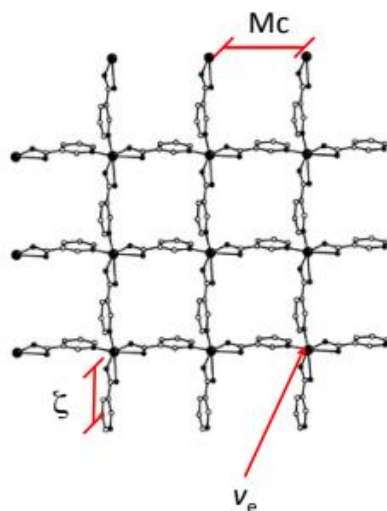
Figure 3.1 – Gel   Matrix

Figure 3.1 is an example of matrix, where M_c is the average molecular weight between two crosslinked chains, ξ is the mesh size and v_e is the density of the cross-links. M_c is function of X, which is the degree of cross linking of the gel, and M_o, that is the molecular weight of the monomer unit, via the following formula:

$$M_c = \frac{M_o}{2X}$$

The mesh size ξ is the distance between two sequential points of cross-linking and thus, is useful to estimate the space in which a cell or a molecule could eventually diffuse through the gel matrix.

$$\xi = v_s^{-\frac{1}{3}} * C \left(\frac{M_c}{M_o}\right)^{\frac{1}{2}} = v_s^{-\frac{1}{3}} * C \left(\frac{1}{2X}\right)^{\frac{1}{2}}$$

In the formula above, C is a constant depending on the polymer and the solvent, and v_s is the polymer volume fraction in the swollen state, defined as the ratio between the volume of the polymer and the volume of the swollen gel.

The density of cross-links ν_e corresponds to the ratio between the density of the polymer and the molecular weight between two crosslinked chains:

$$\nu_e = \frac{\rho_p}{M_c} = \frac{2\rho_p X}{M_o}$$

Where ρ_p is the density of the dry polymer.

3.1.1 Swelling

The amount of water it can retain an hydrogel it is called swelling behaviour. It is possible to characterized it with a parameter called volumetric swelling behaviour Q:

$$Q = \frac{V_{wet}}{V_{dry}}$$

Where V_{wet} is the volume of the hydrogel when is totally filled with water, and V_{dry} is the volume when the hydrogel is dry. The ratio for the volumetric swelling depends on pH, temperature and osmosis. The phenomena starts
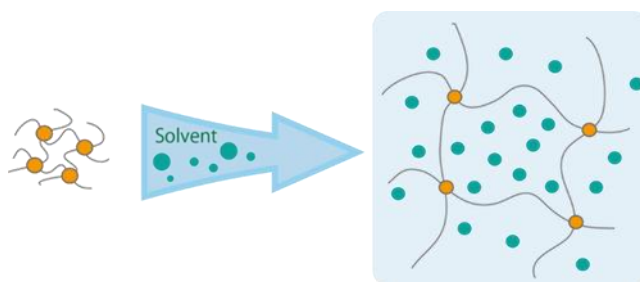
Figure 3.2 - Hydrogel Swelling

putting a dry hydrogel into the water, which interact directly with the hydrophilic groups of the polymer, and will compose the primary bound water. Subsequently, the hydrophobic groups are exposed and interact with the water molecules, building hydrophobically bound water. In the end, the osmotic force will cause the absorption of additional water, the free water that is included in the hydrogel network without being bonded chemically. The swelling equilibrium is reached when the elastic retraction force of the network is balanced by the osmotic force that causes the stretch of the matrix.

3.1.2 Degradation

Due to some factors like temperature, enzymatic hydrolysis or pH, there is the possibility for the hydrogel to degrade. It happens when there is a breakage on the chains or o the cross-linking points.
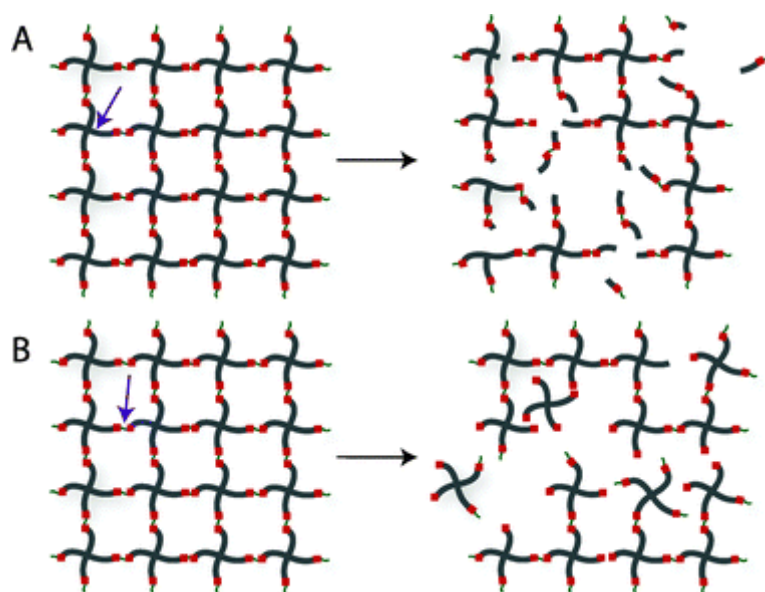
Figure 3.3 – Hydrogel network degradation: A) Cleavage of polymer chain
B) Cleavage of cross-linking point

In the field of biomaterial engineering, biodegradation is an important feature, especially when hydrogels are used as drug delivery systems, artificial tissues or parts of organs. Furthermore, it is also a key parameter for cells migration and proliferation and for drug delivery application where the progressive disruption of the gel matrix permits the release of the encapsulated molecules in function of space and time. The releasing kinetic is governed by bulk or surface erosion. The former occurs with a rate of water diffusion faster than hydrolysis reactions; on the contrary, the latter is characterized by

degradation reactions that are faster than diffusion rate into the network, so water is absorbed on the surface before it can penetrate in the gel's bulk.[6]

3.1.3 Porosity

This characteristic is a sum of three different parameters that are not easy to estimate, due to their dependence on solvent or temperature, that cause the hydrogel matrix to swell, varying the results. Otherwise, these estimations necessitate a mathematical approach and, consequently, approximations and assumptions.[6]

As another important factor, the porosity handles the rate of diffusion of matter outside the gel.

Considering porosity, hydrogels can be classified in the following categories:

➢   Non porous gels

➢   Micro porous gels (100 Å < Pore Size < 1000 Å)

➢   Macro porous gels (0.1 µm < Pore Size < 1 µm)

➢   Super porous gels (pore size of several hundreds of micrometers)

3.2 Preparation

The formation of the hydrogel starts with a physical or chemical mechanism, where a cross- linking agent connects monomers with chains. It is possible to manipulate the properties of the gel just controlling the degree of cross-linking.[7],[8]

3.2.1 Physical cross-linking

The advantages of this method are that there is no need for a cross linking agent, which could be toxic or affect the integrity of the gel and, in addition, need to be removed after the usage.
Due to the less strong physical bond respect to the chemical ones, physical cross-linked gels are usually less stable. The bond their chains through:

• Hydrogen bonds
• Amphiphilic graft and block polymers, that have the ability to self-assembled in aqueous media to form polymeric micelles and hydrogels
• Crystallization; usually occurs with a decreasing of the temperature
• Ionic interactions; usually depends on pH and temperature
• Protein interactions

3.2.2 Chemical cross-linking

• Chemical reactions between complementary groups, like condensation or addition reactions
• Energy radiation, that can polymerized unsaturated substances

• Free radical polymerization; using energy as temperature of light, radicals are formed and then start to propagate among the solution and at a certain point the polymeric matrix starts to be formed

• Enzymes

3.2.3 Environmentally responsive hydrogels

This kind of hydrogels can shift from solution to gel and opposite, when some certain environmental circumstances are met[9].

Thermoresponsive are whose gel that jellified through temperature changes. Above the lower critical solution temperature (LCST), they start to become hydrophobic and experiment a separation from the solution. On the opposite, other hydrogels start to form when the temperature decreases below the upper critical solution temperature (UCST).

pH is another factor that affect hydrogels' properties, in particular the swelling behaviour. It is very common for ionic gels, for which low pH enhances swelling in acid gels, caused be repulsion between ions of the same charge. On the other side, basicity triggers an acid gel to shrink.

3.3 Classification

It is possible to divide hydrogels considering:

• Source: natural (gelatine, chitosan, fibrin, alginate), synthetic (polyacryl amide, polyethylene glycol diacrylate), hybrid.

• Composition. Referring to monomers: homopolymeric or copolymeric, with a single o two or more monomers species respectively, arranged as blocks or randomly.

• Configuration: crystalline, semi-crystalline, amorphous

• Cross- linking type

• Physical appearance: microsphere, film, matrix

- Electrical charge: ionic, non-ionic, zwitterionic, amphoteric
- Biocompatible or not

3.4 Gelatin

Gelatin is a protein-based material obtained by hydrolytic degradation of naturally collagen. It is soluble in water (T>40°C) , but due to its thermo-responsive behaviour, when temperature decreases, gels are normally formed, creating a partial recover of the collagen triple-helix structure.[10]

Gelatine does not shown antigenity. Moreover, due to its large quantity of functional groups, can easily undergo chemical cross-linking. Considering the chemical crosslinkers, we can utilize reagents such as diisocyanate, glutaraldehyde, carbodiimides, acyl azides. Gelatin can be cured also by UV treatment, if the material is previously modified with methacrylamide and a photo initiator is added in the precursor solution.

Figure 3.4 – Gelatine Monomer Structure

3.4.1 Methacrylated Gelatin – GelMa

Methacrylated gelatin (GelMa) hydrogels have enough high melting point to maintain their physical shape at body temperature for a sufficiently long time.[10] It shows important features like cells adhesion, thanks to the RGD sequences (arginine- glycine- aspartic acid) naturally present. The methacryloyl

functionalization can be adjusted via a feed ratio of gelatin to methacrylic anhydride (MMA) and is one of the main

parameters that can tune biophysiochemical properties of GelMa and its photo-crosslinked hydrogels. It has been noticed that the higher the degree of modification, the lower the G' modulus (storage modulus).[11]

.
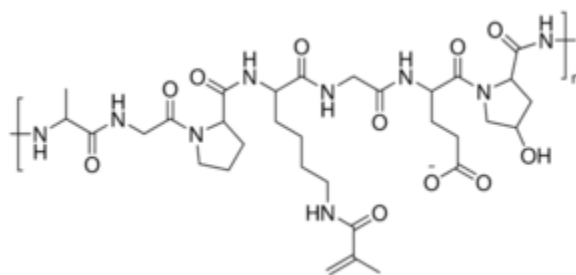
Figure 3.5 – GelMa Monomer Structure

Common photoinitiators include 2-hydroxy-1-[4-(2-hydroxyethoxy)phenyl]-2-methyl-1-propanone (Irgacure 2959) and lithium acylphosphinate salt (LAP). The reactions occurring in the photocrosslinking of GelMA to form hydrogel networks start with the formation of free radicals that are generated from photoinitiators, which initiate the chain polymerization of the methacryloyl substitutions. Propagation occurs between methacryloyl groups, which are located on the same chain and/or on different chains. Termination occurs between two propagating chains or between one propagating chain and a second radical, as showed in figure 3.6
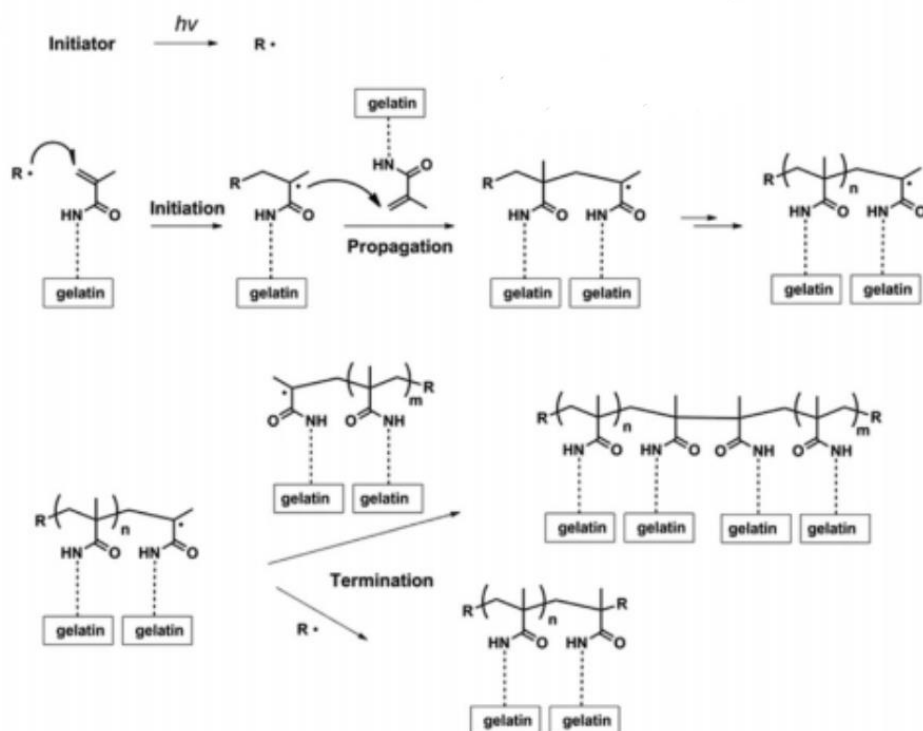
Figure 3.6 – Polymerization Mechanism

3.5 Sodium Alginate

Sodium alginate is a polymer extracted from seaweed, in particular the class of the brown algae (Phaeophyceae). The algae are treated with NaOH and then filtered, adding calcium or sodium chloride as precipitating agent. Then after various purification processes, it is obtained sodium alginate powder [12].

3.5.1 Structure and Gelation

Alginate is a polymer composed by L-guluronate (G) and D-mannuronate (M). The weight percentages of the two compounds and their arrangement depend on the source of the alginate itself. In particular, only the G

~ 20 ~

units seem to be responsible of crosslinking. The molecular weight can vary between 32.000 and 400.000 g/mol. The higher the molecular weight, the better the physical properties compared with lower weight. As drawback, it could also produce a highly viscous aqueous solution, which can disturb the crosslinking process.

This polymer is water-soluble, thanks to the presence of polar groups, and it has consequently poor solubility in organic media.
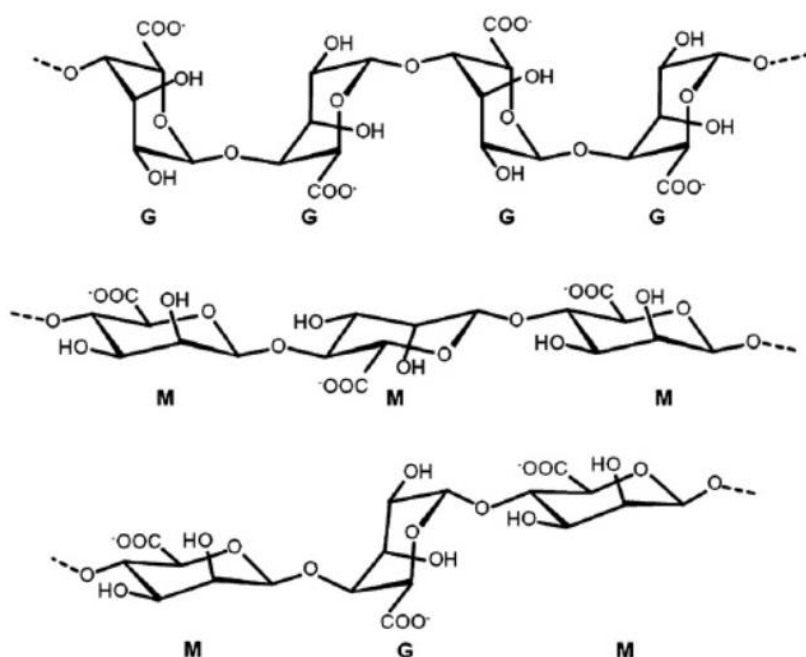
Figure 3.7 – Molecular structure of sodium alginate and its blocks

The solubility is influenced by the degree of protonation of the carboxylic groups. HCl can be added to promote protonation, forming Alginic acid, insoluble in polar solvents. Adding NaOH instead, reverses the process back to the sodium alginate form. The gelation can be obtain through the addition of an ionic cross-linking agent, like Ca^{2+}. This kind of cations links with the carboxylic groups of the guluronate units exploiting a mechanism called egg-box gelation model.
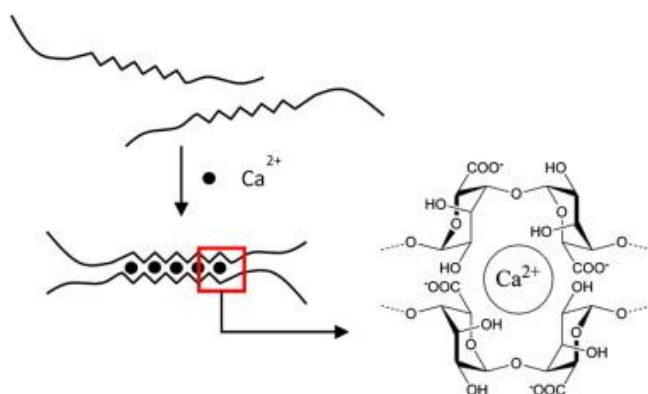
Figure 3.8 – Egg- Shell Gelation Mechanism

The reactants that provide calcium ions, usually are calcium chloride or calcium acetate, which is used for edible applications. Due to the high solubility in water and so the high number of cations of these compounds, gelation kinetic can be uncontrolled. For this reason, it is advised to use a buffer that slows the gelation competing with the reaction of the carboxylate groups. Temperature is another factor that influences strongly the gelation: the lower the temperature, the lower will be the reactivity of the cations, thus the gelation will be slower. This involves a greater order in the hydrogel network, so better mechanical properties.

CHAPTER 4
SURFACE TENSION

Surface tension is a propensity of fluid surfaces to shrink into the minimum surface area possible. At air-liquid interfaces, surface tension become greater than attraction between liquid molecules (cohesion phenomena) and greater then to the molecules in the air (adhesion phenomena). Practically, it is a force per unit length. If F is the force necessary to prevent a side from starting to slide, then this is also the force that would maintain the side in the state of sliding at a steady speed.
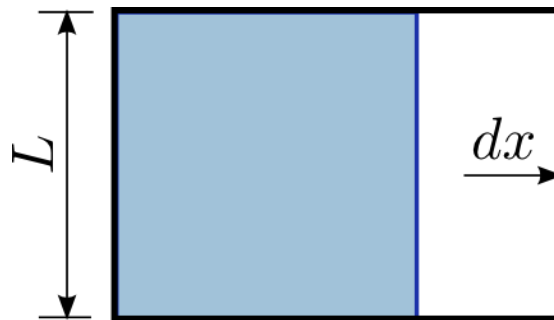
Figure 4 – Force necessary to expand the surface area

But if the side is moving to the right (in the direction the force is applied), then the surface area of the stretched liquid is increasing while the applied force is doing work on the liquid. This means that increasing the surface area increases

the energy of the film. The work performed by the force F in pushing the side by distance Δx is $W = F\Delta x$; at the same time the total area of the film rises by $\Delta A = 2L\Delta x$. Therefore, multiplying both the numerator and the denominator of $\gamma = 1/2F/L$ by Δx, we get

$$\gamma = \frac{F}{2L} = \frac{F\Delta x}{2L\Delta x} = \frac{W}{\Delta A}.$$

This work W is interpreted as being stored as potential energy.

CHAPTER 5
DRUG DELIVERY

5.1 Introduction

The field of drug delivery represents all the formulations, technologies and systems designed to target and regulate therapeutics administration. It involves the carrying of the drug into the body to the desired target and the enhancement of pharmacokinetics and pharmacodynamics.
The goals of controlled and targeted drug delivery are:

- Improving the time of the therapeutic effect[13]
- Reduce administration frequency[14] while rising patient fulfilment[15]
- Optimized management of pharmaceutical active principles
- Diminished side effects[16]

To minimize the probability for side effects and be most effective, the drug quantity in the plasma has to be kept into the range of the minimum effective concentration (MEC) and the minimum toxic concentration (MTC). Under the MEC, the therapeutic will be mostly ineffective and higher than MTC there is the risk of unwelcome side effects. Each time a new dosage is administrated, the

concentration in the blood of the drug itself rockets, reaching a peak and then dropping after some time. At this point a new dose is introduced and so on. With this sudden adjustments of concentration, it is simple to decline under the MEC value .
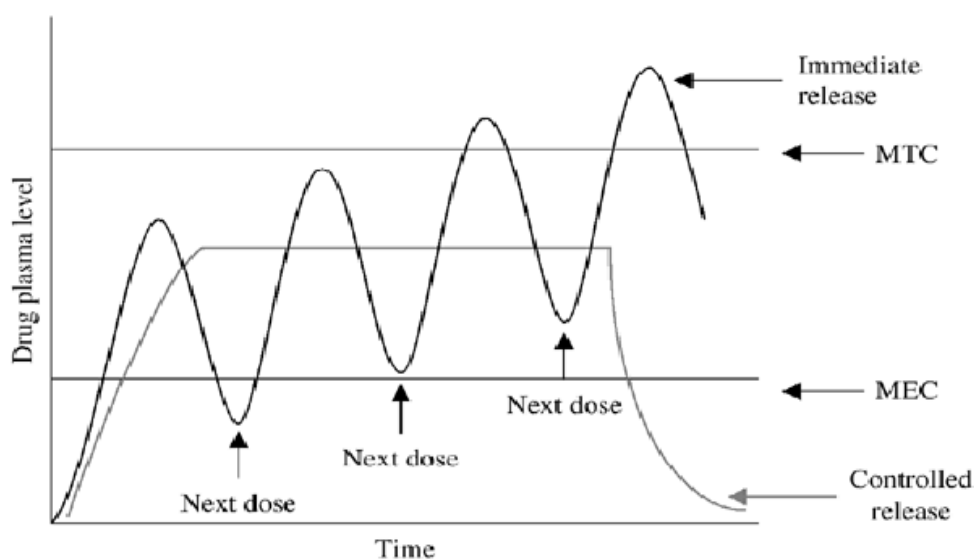
Figure 5 – Releasing Thresholds

In addition, it is common in this case, that due to the necessity of a new dose, the previous one could be not adequately disposed and this can bring to overdosages.

A smart solution in these cases, is controlled drug delivery, which can be tuned to maintain the correct therapeutic level among the two critical regions, avoiding wasting of product and side effects of overdosages.

5.2 Absorption

The absorption performance of a drug into the body is predominantly governed by its hydrophilic/hydrophobic properties

which are influenced by polarity or ionization. Considering the absorption behaviour, it is possible to select the right method to administer the drug.

Highly polar drugs find obstacles in passing through the stomach wall barrier and so they are administered via injections rather than oral way. On the other side, non-polar drugs are absorbed only by fat tissues, because of their poor solubility in aqueous solutions.

The most common techniques operated to tune and modify the drugs' substituents are:

• Alteration of acyl/alkyl substituents to alter the polarity. By adding extra lipophilic groups for example, it is possible to reduce the drug polarity. This has to be achieved without damaging or covering the functional groups of the pharmacophore, that are the ones active for the interaction with the binding sites.

• Modification of polar functional groups to change the drug polarity.

• Modification of *N*-alkyl substituents to vary pKa. It is possible to vary the ionization properties by adding extra alkyl substituents close to the electron donating group (EDG) to bring the pKa in the range required by the specific case.

• Changing of the aromatic substituents to modify pKa, by increasing the number of EWG or EDG. Considering EWG, the more we add them, the lower is pKa and so the higher is the acidity. About EDG, the more them are added, the higher pKa and so the more is basicity.

• Utilization of bio-isosteres as substituents for important functional groups. To improve the pharmacodynamics of a drug, it is possible to use a correlated bio-isostere to overcome pharmacodynamics problems while guaranteeing the proper pharmacodynamics. This new bio-isostere has similar physiochemical properties as the substituted one. The aim of changing these structures is to enhance the physical or biological characteristics of a molecule without modifying the chemical structure itself.

5.3 Drug delivery routes

5.3.1 Ocular

The ocular delivery route is preferred for eyes diseases therapies, but due to the several physiological barriers in the eye, this is not usually easy to perform, as well as for the sensibility of the organ itself, for which is difficult to maintain the required drug concentration in the target tissue.
Modulation of conventional ocular drops administration has been enhanced by permeation and viscosity enhancers that help the delivery to the anterior part of the eyes. For the back instead, nanoformulations or drug releasing devices to treat vitreoretinal diseases have been developed.[17–20]

5.3.2 Pulmonary and Nasal

These routes are mainly exploited to treat pulmonary and nasal diseases, in particular through pressurized dose inhalers or dry powder inhalers. The carrier that bring the therapeutic into the lungs can be solid, liquid or gaseous, like microemulsions, suspensions, liposomes, cyclodextrine. [21,22]

5.3.3 Dermal and Transdermal

Considering in which position the drug is active, it is common to subdivide the skin delivery route in dermal, if the drug is active topically or with a small thickness of penetration, or transdermal, if the necessary thickness that permits the drug to enter the systemic distribution system goes over the skin first layer. The skin itself is an hard physiological barrier to overcome by the

drug, that to be delivered needs to have acceptable lipophilicity and a molecular weight of less than 500 Da. [23]

5.3.4 Parenteral

This administration practise which involve the direct injection of the drug typically subcutaneous, intravenous and intramuscular. Due to the fact that the medicine bypass automatically all the barriers, it makes this method the most effective. Researches have been focused mostly in the formulation branch, to enhance the drug solubility, especially to let them to be administered by blood, that is indeed an aqueous media. [24]

5.3.5 Oral

Between the numerous delivery routes, the most frequently adopted is definitely the oral one. In particular because of the patient compliance and the easiness of admission. The gastrointestinal tract, on the other side, acts opposing barriers like pHs and residence times that differ in each zone, as it can be seen in the figure 5.1.

For several drugs, there is a better absorption in the upper tract due to the bigger surface area of the stomach but the finest one is reached by tuning the release from the drug delivery system.
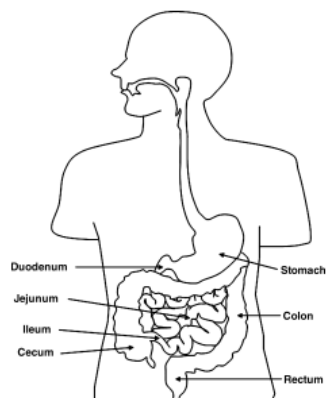
Anatomical Site	pH	Transit Time (h)
Stomach	1–3.5	0.25
Duodenum	5–7	0.26
Jejunum	6–7	1.7
Ileum	6.6–7.4	1.3
Cecum	6.4	4.5
Colon	6.8	13.5

Figure 5.1 – pH in Different Part of the Gastrointestinal Tract

5.4 Mechanism of Drug Release from Polymers

The releasing from polymers follow different paths and is function of several parameters, organised in the table 5.1 e 5.2

Table 5.1 - Mechanisms of drug release by polymers

Mechanism	Variations
Osmosis[25]	• Controlled porosity osmotic pump • Multichambered and modified osmotic pumps • Elementary osmotic pump
Ion exchange	• Polymeric coatings (release rate control) • Relation between small-scale design (particle size) and big-scale design • Ion-exchange resins (anion/cation)
Diffusion	• Swelling and diffusion • Basic diffusion, monolithic system • Matrix degradation and diffusion • Diffusion with rate controlling membrane

Table 5.2 - Main factors affecting drug release by polymers

Material matrix	Release medium	Drug compounds
• Structure	• Temperature	• Solubility
• Composition	• pH	• Charges
• Degradation	• Ionic strength	• Interaction with matrix
• Swelling	• Enzymes	• Stability

5.4.1 Osmosis

This phenomenon, represented in figure 5.3, is based on osmotic force. There is a central core that hosts the medical principle, bounded by a semi-permeable polymeric membrane, with an orifice. When the device is immersed in an aqueous solution, the inner fluid goes across the polymer and dissolves the drug. At this point, the combination of solution and drug exits from the orifice.
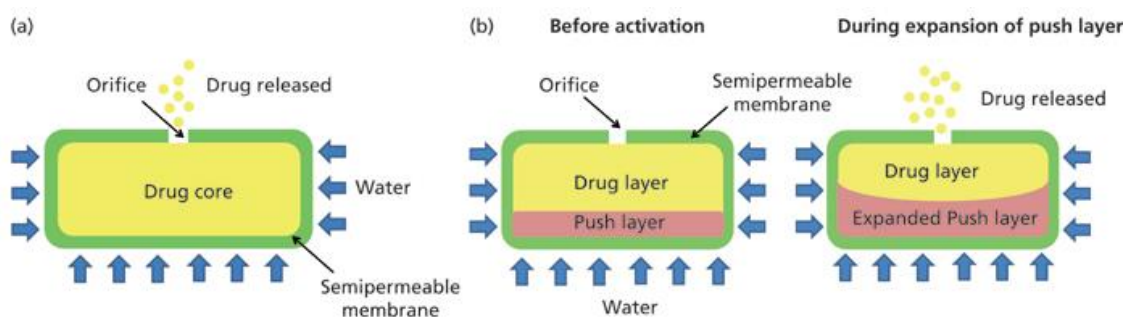
Figure 5.2 – Osmosis Drug Delivery Mechanism

5.4.2 Ion Exchange

It exploits the electrostatic interaction between a water insoluble polymeric material containing ionic groups with opposite charges, commonly ion exchange resins[26], and the ionic drug, as shown in figure 5.4.
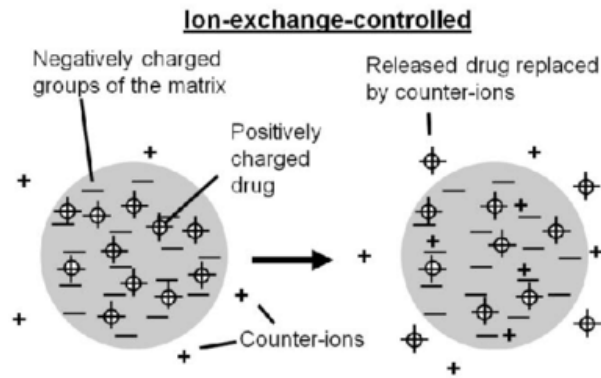
Figure 5.3 - Ion Exchange

The medicine is released by the ion exchange resin and is going to be substituted by other electrolytes dissolved in the surrounding system, usually K+ or Na+ and Cl-, for cationic drugs and anionic drugs respectively. The velocity of the releasing depends on the crosslinking density of the resin, on the ionic strength of the surface of diffusion of the drug resin link and on the surface of diffusion of the device. Matrix tables or fast disintegrating tablets can by used for this delivery way.

5.4.3 Diffusion

This way of drug delivery is driven by a concentration gradient between the outside and the inside of the device. The releasing is function of temperature, steric hindrance, pH, viscosity and so on. Nevertheless, in general, the total release of the drug from the inner of the device is pretty quick, because of the high grade of acceptance from the human body.

The concentration gradient is the driving force for the release itself, that obeys the Fick's law, according to the following law:

$$\frac{\partial C_i}{\partial t} = \nabla(D\nabla C_i)$$

Where D is the diffusion coefficient and Ci is the concentration of the i-th species. It explains the dynamic release of a generic drug molecule from a polymeric matrix, which is assumed not to undergo any changes in terms of chemical and/or physical properties and that it does not degrade on a time scale analogous to the one linked to the diffusion process. Considering also the geometry of the device, diffusion coefficient and doing the proper approximations, we can end up with the Peppas equations, that describes the diffusion-based release models.

$$\frac{M_t}{M_0} = kt^n$$

M_0 is the whole amount of drug loaded in the device at time t=0, M_t is the quantity of drug released at time t, k is the release kinetic constant which is mostly a function of the geometrical parameters of the device itself and of the therapeutic diffusion coefficient inside the polymeric matrix; n is a geometrical parameter, that is chosen considering the geometry of the releasing object and it can be 0.5 for thin-film, 0.45 for cylindrical geometries or 0.43 used for spherical geometries. In function of the exponent n, the release has distinct characteristics, according to the values:

- 1.0, the drug release rate is independent of time and this case relates to zero-order release kinetics, in which the drug release rate is constant
- 0.5, the diffusion is pure Fickian, the law is known as Higuchi equation, that is considered as empirical model, so it is the easiest to use specially for short release times, or low M_t/M_0 ratios. Anyway, it is important to highlight that, going to higher release times, Higuchi equation becomes more complex and the functional dependence of the drug release on the geometrical parameter varies significantly.

An example is the release from a rounded disk type drug delivery system made of undegradable polymeric matrix, of thickness h, in which the release equation has different terms depending on the release time and the ratio M_t/M_0 varies its dependence on both time and geometrical parameter as it is clear in the formulas below:

- $\dfrac{M_t}{M_0} = 4\left[\dfrac{D\,t}{\pi\,h^2}\right]^{1/2}$ when $0 \leq M_t/M_0 \leq 0.6$

- $\dfrac{M_t}{M_0} = 1 - \left(\dfrac{8}{\pi^2}\right)\exp\left[\dfrac{-\pi^2\,D\,t}{h^2}\right]$ when $0.4 \leq M_t/M_{0z} \leq 1.0$
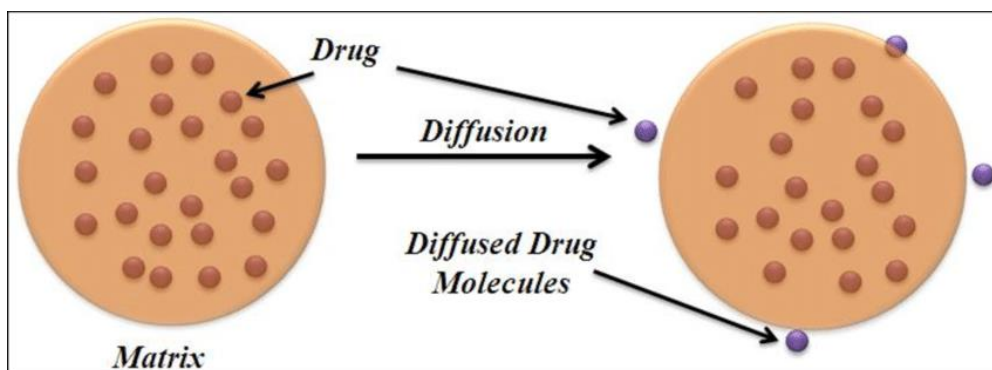
Figure 5.4 - Diffusion drug release

• Diffusion with membrane that controls the rate of release, also identified as reservoir type. These devices have an inert coating material that has the role of rate-controlling polymeric membrane, which can be microencapsulation-type or coated-type, on a drug-loaded centre. Due to this conformation, it is commonly possible to load an high amount of active principle in the coated core and tuning the thickness of the membrane is possible to set the rate of releasing[27]. The diffusion through the polymeric stratum, release across the water- filled pores and the osmotic driving force: these are the factors involving in the mechanism. Firstly, the aqueous solution enters the coating and gets to the core, secondly the

drug is dissolved and released thanks the concentration gradient. An osmotic pressure is generated because of the water entering, and a stress/strain field is created due to the polymer swelling properties and the different core. These produce the follow two mechanisms.

$$\frac{dm_i}{dt} = D_{app} \, A \, K \, \frac{C_i}{d}$$

One dimension-model balance equation, where A is the surface accessible for diffusion, D_{app} is the apparent diffusion coefficient of the drug in the polymeric film, K is the partition coefficient of the drug among the aqueous solution and polymeric phase, and d is the width of the coating.

The release via water-filled openings, that are the part of the polymeric coating layer due to numerous causes, for example due to cracks produced by the hydrostatic pressure created inside these systems by water.

$$\frac{dm_i}{dt} = D_p \, A \, \frac{\varepsilon}{\tau} \, \frac{C_i}{d}$$

In the formula above, ε is the volume part of the pores, D_p is the diffusion coefficient of the drug in the solution present inside the pores, τ the tortuosity of the pores. The drug tended to be pushed out by the osmotic effect, from the drug delivery device. This release can be explained as:

$$\frac{dV}{dt} = \frac{A \, \theta \, \Delta\pi}{l}$$

Where dV/dt indicates the water stream, l the membrane thickness, A the membrane surface area, θ the permeability of the polymeric membrane and $\Delta\pi$ the difference in osmotic pressure, ignoring the counteracting hydrostatic force.

These processes can continue lonely on in combination, but a crucial role on the release rate is performed also by the core/coat swelling behaviour.

• Swelling mechanism. In the field of controlled drug delivery of swellable polymers, the drug is spread into the polymeric phase and when the latter is in contact with an suitable solvent, swelling occurs beginning the drug release in the nearby environment. This happens because usually in the non-swelled configuration the drug is incapable to diffuse over the polymer network in any significant amount but when the swell reaches a proper degree, the network hinderance diminish due to the relaxation of the polymer chains and manages to elongate between the network junctions because of the solvent-polymer interactions, then the drug begins to be released.

• Degradation and diffusion routs. The degradation of the polymer carrier characterizes these systems, and it is designed to degrade into gradually smaller and biocompatible compounds. Normally, biodegradable polymer chains contain • amide, ester, and/or anhydride bonds which are predisposed to degradation inside the organism, generally via enzymatic action or hydrolysis. The conventional parameter used to calculate the degradation progression in function of the time is the difference in average molecular mass of the polymer due to the breakage of its chains on the labile links, the most broadly used degradation kinetic equations are:

$$\text{Zero-order} \quad MW_r(t) = MW_{r0}k_{degr}t$$

$$\text{Pseudo first-order} \quad MW_r(t) = MW_{r0}\exp{(-k_{degr}t)}$$

Where $MW_r(t)$ and MW_{r0} are the average polymer molecular mass at time t and time zero, k_{degr} is the apparent degradation rate constant of the polymer.
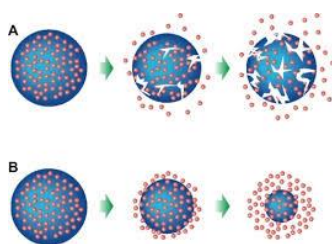
Figure 5.5 - Bulk degradation, surface degradation

Considering the time of polymer degradation and water diffusion, we can subdivide the degradation mechanism in two types:

• Bulk degradation ($\tau_{diff}<<\tau_{degr}$). Here the degradation effect occurs homogeneously all the way through the material and the drug is released gradually.

Surface degradation ($\tau_{diff}>>\tau_{degr}$). This is described by a degradation restricted to the outer surface of the device and the drug is released constantly in the same way the erosion process continues in the centre of the object. These type of releases are simpler to model and forecast respect to the bulk degradation ones, if we take into account in particular the assumption of a "layer by layer" degradation or the theory of a moving "degradation front". In literature exist a lot of release models but the easiest is the Hopfenberg's model which is centered on the formula below:

$$\frac{M_t}{M_0}=1-\left(1-\frac{k_0 t}{C_0 a}\right)^n$$

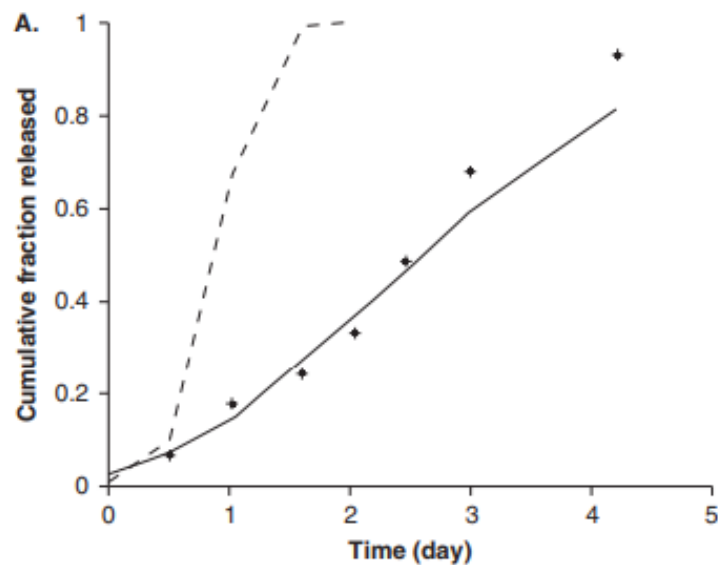Where M_t and M_0 are the amounts of drug released respectively at time t and

Figure 5.6 - Degradation-Based Release Rate

at infinite time, c_0 is the starting drug concentration contained by the matrix, the constant k_0 denotes the erosion rate, a is the radius of a cylinder or sphere or the half-thickness of a slab. In conclusion, n is a 'shape factor' representing slab (n = 1), cylindrical (n = 2) or spherical geometry (n = 3). The widespread trend in the degradation-based release rate is described in figure 5.7 where it can be highlight that the bulk degradation release (solid line) is much slower than the surface erosion one (dotted line). This is typically due to the fact that the characteristic time of degradation in the surface degradation release mechanism is much smaller than the one correlated to the solvent diffusion. That is why from these devices the drug is released in a faster way than in those devices focused on a bulk-degradation mechanism.

CHAPTER 6
MATERIALS AND METHODS

6.1 Devices fabrication

The goal we wanted to achieve, designing the device, was to obtain a 3D easily and fast printable biocompatible object, with which it could has been possible to guarantee certain features and uses:

- Superficial tension- based
- Not expensive
- Easy to manage during experimental activities
- Mild 3D printing conditions (temperature, pressure) and flexibility of the printing method itself

That is way it was decided to choose a perforate planar grid in polycaprolactone (PCL), a synthetic biodegradable semi crystalline polymer, cheap, simply available on the chemicals market and capable to host and adequate amount of hydrogel solution for research activities.

However, with this process design, it is possible to print whatever 3D structure, just adjusting the printing code that tells the machine how and where to eject the material.

As future outlook, we thought about creating different 3D structure shapes in order to apply or use them in part as a vehicle for drugs of cells within the human body, as it has been lately done with bones in the field of Tissue Engineering.[28,29]

Figure 6 - PLA/PCL/TiO$_2$ Composites for Cancellous Bone

6.1.1 3D Printing Process

6.1.1.1 3D Printer

The printer we used in the Macromolecular Engineering Laboratory (MEL) at ETH ZÜRICH, was an high- tech 3D Bioprinter BIOx produced by the Swedish company Cellink, shown in the figure 6.1 with the following features:

• Cooled printheads.

• Heated print bed.

• Cooled print bed.

• Clean Chamber Technology.

• Piston-driven syringe head.

- Pneumatic printheads.

- Multi well-plate printing.

Figure 6.1 – BioX 3D Printer

With this 3D bioprinter, it is possible to print both thermoplastic material, like PCL, or gel-like material that polymerized directly into the printer itself. It is a named as "bio" because it was designed to print materials with cells encapsulated into it as well. The 3D printing operating pressure range goes from 0 to 700 KPa and the temperature from 4 to 250°C.

6.1.1.2 Experimental Section

6.1.1.2.1 PCL Grids

The 3D printing of the PCL grids starts with the creation of a G-Code, a file that gives informatic instruction to the printing machine. To generate it, it is possible to exploit a CAD software or, for simpler geometries like our

device, just a text input file. The commands are divided through letters, as it follows in the table 6.

Table 6 – Letters/ Meaning

Letter	Meaning
Gnnn	Standard G-code command, such as move to a point
Mnnn	RepRap-defined command, such as turn on a cooling fan
Tnnn	Select tool nnn. In RepRap, a tool is typically associated with a nozzle, which may be fed by one or more extruders.
Snnn	Command parameter, such as time in seconds; temperatures; voltage to send to a motor
Pnnn	Command parameter, such as time in milliseconds; proportional (Kp) in PID Tuning
Xnnn	A X coordinate, usually to move to. This can be an Integer or Fractional number.
Ynnn	A Y coordinate, usually to move to. This can be an Integer or Fractional number.
Znnn	A Z coordinate, usually to move to. This can be an Integer or Fractional number.
U,V,W	Additional axis coordinates (RepRapFirmware)
Innn	Parameter - X-offset in arc move; integral (Ki) in PID Tuning
Jnnn	Parameter - Y-offset in arc move
Dnnn	Parameter - used for diameter; derivative (Kd) in PID Tuning
Hnnn	Parameter - used for heater number in PID Tuning
Fnnn	Feed- rate in mm per minute. (Speed of print head movement)
Rnnn	Parameter - used for temperatures
Qnnn	Parameter - not currently used
Ennn	Length of extrudate. This is exactly like X, Y and Z, but for the length of filament to consume.
Nnnn	Line number. Used to request repeat transmission in the case of communications errors.
*nnn	Checksum. Used to check for communications errors.

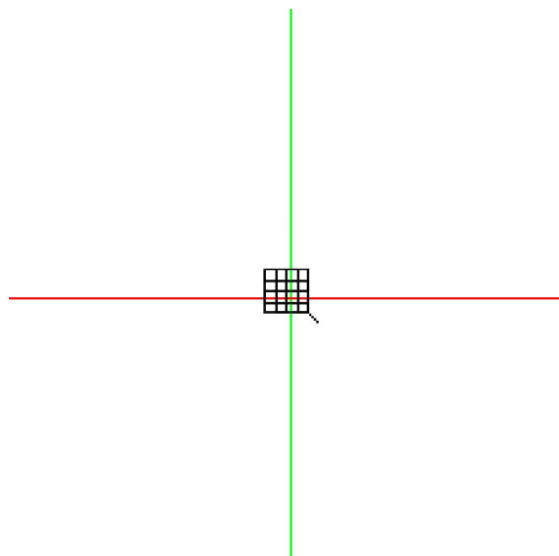The 2D figure obtained is presented below (figure 6.2)

Figure 6.2 – Grid 2D Model

After have given the 3D printer the code, the operational parameters, like pressure, temperature and extruding velocity have to be settled. After some tests performed, we decided to use these printing layout:

- Pressure of 180 KPa
- Temperature of 80°C
- Thermoplastic printing head velocity of 4- 5 mm/sec

The polycaprolactone used was purchased from Sigma-Aldrich.

The grids were then printed on a glass slide, as it can be seen in the figure 6.3 below.
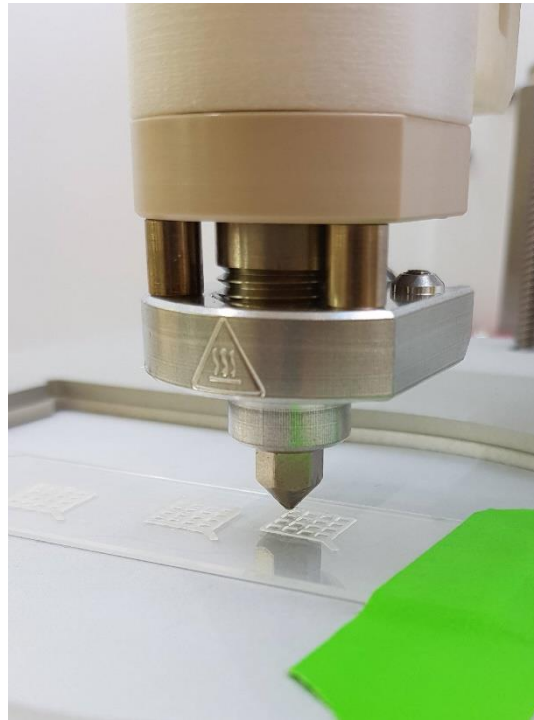
Figure 6.3 - Grids printed on a glass slide

6.1.1.2.2 **Metallic Devices**

These grids, showed in figure 6.4 , made by the +LAB and metallized by the SEE Lab of Politecnico di Milano, have been produced with DL260 resin using the SLA printing technique already described, while the metallization was made by deposit CoNiP layer and gold layer to ensure biocompatibility. The process has been widely and accurately described in the literature.[30]
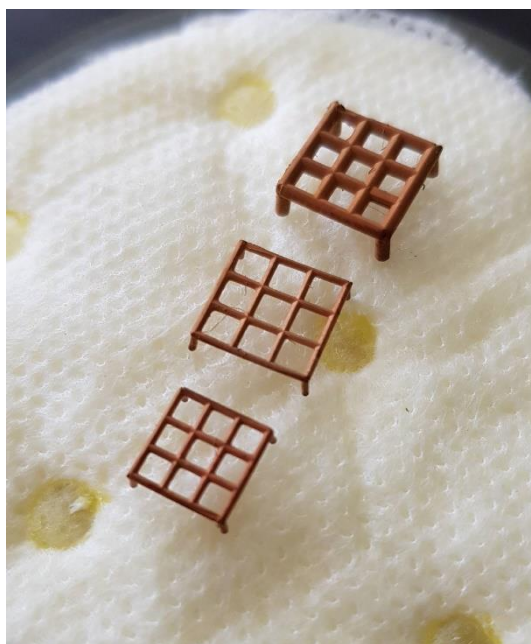
Figure 6.4– Metallic Grids

6.2 Methacrylated Gelatin

We decided to use this material because thanks to the arginine-glycine-aspartic acid (RGD) peptide sequence which favors certain cell behaviors (such as adhesion, differentiation and proliferation) and a matrix metalloproteinase (MMP) degradation sequence, promotes cell enzymatic degradation, as well as biophysicochemical properties that resemble the native extracellular matrix (ECM)[31]. In addition, also controlled drug release is another area where the use of GelMA hydrogels has been explored.[32]

6.2.1 GelMa Syntesis

The chemicals used for the reaction are presented in table 6.1

- Gelatin from porcine skin, type A, gel strength 300 bloom (Sigma-Aldrich G2500, RT)

- Methacrylic anhydride (MW: 154.17 g/mol; CAS #760-93-0; Sigma-Aldrich 276685; RT)
- Sodium bicarbonate (NaHCO3; MW: 84.01 g/mol; CAS #144-55-8; Sigma-Aldrich S6014; RT)
- Sodium citrate monobasic (MW: 214.11 g/mol; CAS #18996-35-5; Sigma-Aldrich 71498; RT)
- Glycerol (MW: 92.09 g/mol; CAS #56-81-5; Sigma-Aldrich G5516; RT)

Table 6.1 - Compounds and quantities for reaction

Compound	Quantity	MW [g/mol]	n [mol]
Gelatin from porcine skin, type A	20g	~100000	$2*10^{-4}$
$C_8H_{10}O_3$	12.0g	65.0099	0.184
$NaHCO_3$	-	154.165	3.89
$HOC(COONa)(CH_2COOH)_2$	-	214.11	q.s.
$C_3H_8O_3$	-	92.09	q.s.
H_2O	200 ml	18	q.s.

As first steps, it is prepared a 500 mL round bottom flask and is add gelatin (20.0 g) to the flask and dilute to 10 wt% in deionized water (200 mL). Then the mixture is stirred moderately for around 1 h to facilitate dissolution and heated up to 50 °C and until the gelatin is completely dissolved. At this point, methacrylic anhydride (12.0g; 3.89 mmol per gram of gelatin) is added to the solution, that is subsequently allows to spin as a homogenous suspension for 1.5 h at 50 °C.

It is important to highlight that the degree of functionalization (DoF - calculated after purification, as explained in Chapter 7.1) will depend on the ratio of methacrylic anhydride to gelatin, the temperature of the reaction, and the duration of the reaction period. After the reaction period, the solution is transferred to 50 mL conical tubes and the unreacted methacrylic anhydride and methacrylic acid are removed by centrifugation at 3.500 rcf for 5 min at room temperature. The methacryloyl gelatin (GelMA)-containing supernatant is let to decant into a glass beker (200-500 mL) and the opaque 'pellet', which contains unreacted methacrylic anhydride and methacrylic acid, is discarded. The GelMa solution is then diluted with twice its quantity of preheated (40 °C) deionized water. At last, the solution is transferred to dialysis tubing and dialyzed against 3500 mL of deionized water at 40 °C for 5 days in a fume hood.

For a week, the dialysis water is changed two times per day. At the end of the dyalisis period, the pH of the dialyzed GelMA solution is adjusted to 7.4 using 1 M NaHCO3 and the solution is then filter-sterilized the using a 0.2 µm span style vacuum filtration nits with a PES membrane. During this latter step, the GelMA solution is divided into aliquots in 50 mL conical tubes and snap-freezed in liquid nitrogen. As last stage, the samples are transfered to a lyophilizer and lyophilized until completely dryness.

6.2.2 GelMa Characterization

To check if the functionalization reaction was occurred, we used ^{1}H NMR spectroscopy. The samples were dissolve in D_2O and the number of scans operated
by the machine was 132. The ^{1}H NMR spectra was analysed to determine the extent of conversion of free amino groups (degree of methacrylation, DM)

6.2.3 Rheological Characterization

It has been seen that the higher the degree of methacrylation, the lower the storage modulus G'. This is probably due to the fact that the incorporation of vinyl side groups along the gelatin chain interferes with the polymer helix formation[10]. To analysed the rheological properties of the methacrylated gelatin, after deep researches in the literature, we decided to investigate on three different GelMa concentration in the hydrogel precursor solution, 4% w/w, 5% w/w, 6% w/w respectively [33] .

6.2.3.1 Experimental Section

To explore the properties of the three precursor solution, we used the Anton Paar Modular Compact Rheometer. It has low-friction air bearing, integrated normal force sensor and mechanical features presented in table 6.3.

Table 6.2 - Rheometer Features

Data	Unit	MCR 502 S
Bearing		Air
Maximum torque	mNm	300
Min. torque, rotation	mNm	100
Min. torque, oscillation	mNm	100
Angular deflection (set value)	μrad	0.05 to ∞
Min. angular velocity	rad/s	10^{-9}
Max. angular velocity	rad/s	220
Max speed	1/min	2100
Min. angular frequency	rad/s	10^{-7}
Max. angular frequency	rad/s	628
Normal force range	N	0.01-70
Normal force resolution	mN	1
Max. temperature range	°C	-160 to +1000

The GelMa hydrogel properties analysed were the three temperature sweeps of the three percentages, i.e. the storage modulus (G') and the loss modulus (G") in function of time, decreasing constantly the operational temperature, from 37°C to 14°C. The shear strain utilized was of 0.1% and the rotational frequency 5 [rad/sec]. The gap between the sample and the plate geometry tool used (diameter of 20 mm) was of 0.5 mm.

The solution we wanted to analyse was composed by the dried methacrylated gelatin and the rest was phosphate buffer solution, no photo initiator was added because for these analysis we just wanted to check the gelation behaviour of the three mixture in order to understand if at room temperature we could have easily exploited the liquid behaviour of the solution to cover, thanks to superficial tension, the holes of the PCL grids.

6.2.4 Crosslinking Rheological Characterization

After have checked the gelation behaviour and the liquid-like material range temperatures, we started to analysed the rheological performances of the hydrogel itself, beginning from a liquid state solution to get to the gel in the end of the experiment, while the rheometer extracts the data.

To do that, the precursor solution has been prepared adding the photo- initiator fraction of 0,1% w/w. This quantity has been chosen after researching on the literature the commonly amounts of photo-initiators used, also in case of usages and contact with cells or other biological organisms.[10],[33]

Typically, in case of photopolymerizations, the photo-initiator quantity fluctuates between 0,5% w/w to 0,001 % w/w. In the literature, the most utilized compounds are the Irgacure (2-hydroxy-1-[4-(2-hydroxyethoxy) phenyl]-2-methyl-1-propanone) hoto- initiators (2959/651) and the lithium phenyl-2,4,6-trimethylbenzoylphosphinate LAP).

The photopolymerization was operated by using UV light, in the wavelength range between 365 and 405 nm, as reported in the figure 6.10. Absorbing that wavelengths, the molecule cleavage mechanism is initiated and so the polymerization reaction. [34]
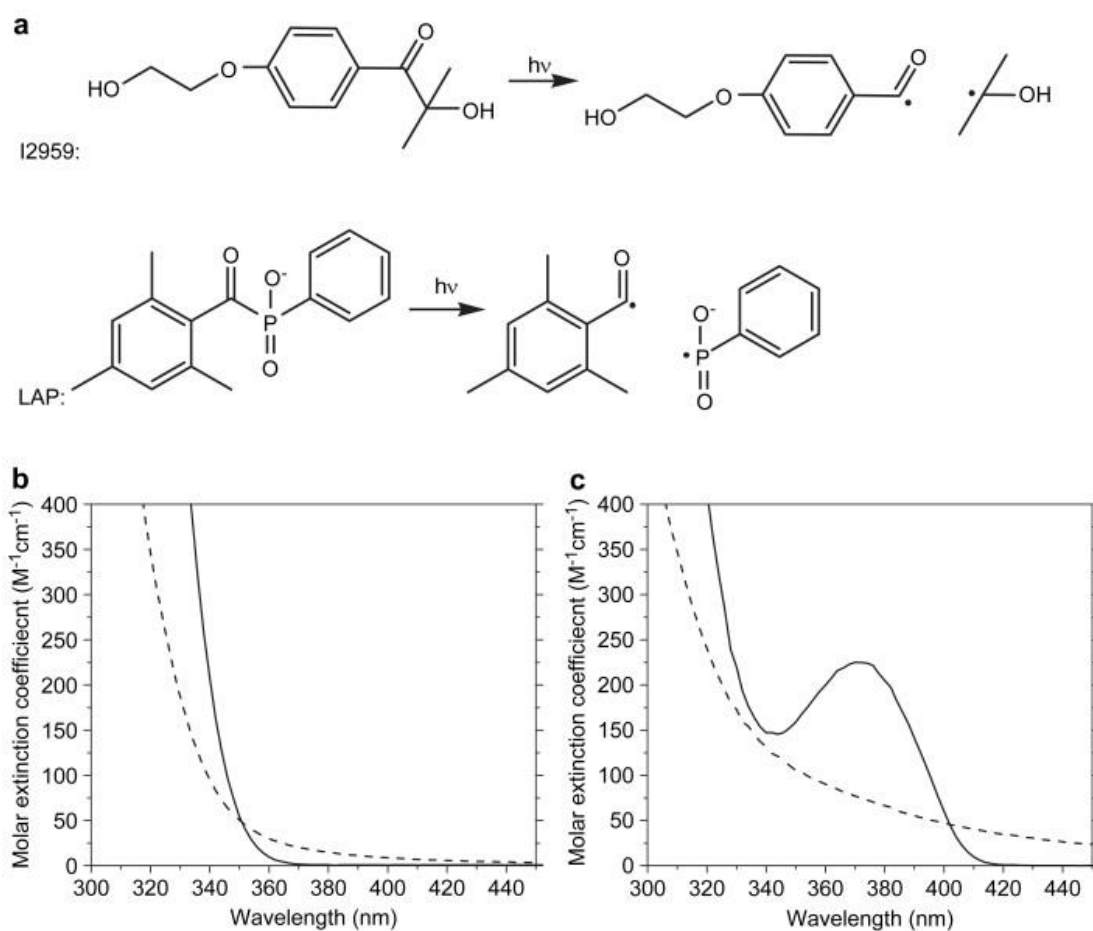
Figure 6.5 - (a) Cleavage of Irgacure 2959 and LAP into substituent radicals following photon absorption. (b) Molar absorptivities of the Irgacure 2959 (solid line) and cleavage products (dashed line). (c) Molar absorptivities of LAP (solid line) and cleavage products (dashed line).

We chose to use LAP initiator because was already present in the chemicals supply. The excitation wavelength applied was the 405 nm due to the fact that, we would have worked with cells and so staying in the visible light range to operate the polymerization was the best options to avoid any DNA modification or damaged by UV light. The intensity used for every experiments and polymerization conditions was of 10 mW/cm^2. Underneath, the graphs of G' and G'' are reported in function of time in the figures 6.11, 6.12, 6.13, again for 4%, 5%, 6% w/w GelMa. In this case, the temperature has been maintained constant at 37°C, value at which we would have worked for cells experiments.

The UV Light was on always after 2 minutes (120 sec) from the beginning of the test.

6.3 3D Cells Encapsulation in GelMa

After the rheological analysis, we wanted to control if the devices in their entirety (GelMa+ PCL grid or GelMa+ Metallic grid) were biocompatible and which of the three conditions of hydrogels (4%, 5%, 6% w/w of GelMa) would have been the most suitable for cells' life, aggregation and proliferation.

6.3.1 Experimental Part

The cells used for the experiments were NIH 3T3 fibroblasts and the quantity used was around 800.000 cells/ml of hydrogel precursor solution.
Viability tests have been performed with Live/Dead assay using Calcein-AM and Ethidium Homodimer as fluorescent tracers. The imaging was performed with a Leica fluorescence microscope. Excitation and emission wavelengths of Calcein-AM are 488 nm/520 nm respectively, Ethidium bromide has the highest UV absorbance peak at 300 and 360 nm, and an emission maximum at 590 nm. The amount of dyes used were 5 uL of 4 mM Calcein AM and 20 uL of 2 mM EthD-III to 10 mL of PBS. Some of the images we got are showed in figure 6.12, 6.13, 6.14.
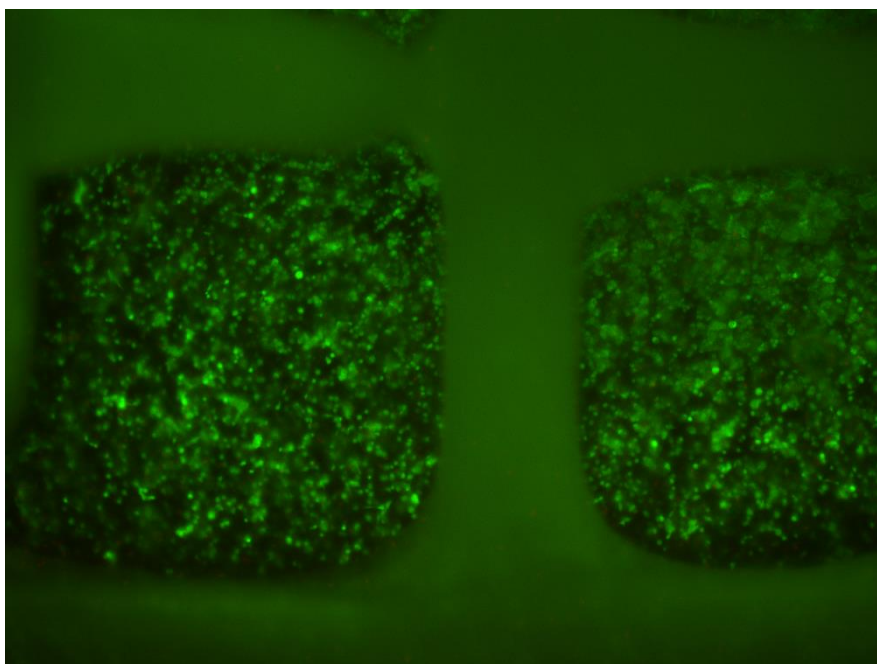
Figure 6.6 – 5% GelMa, day 1, 4X, PCL
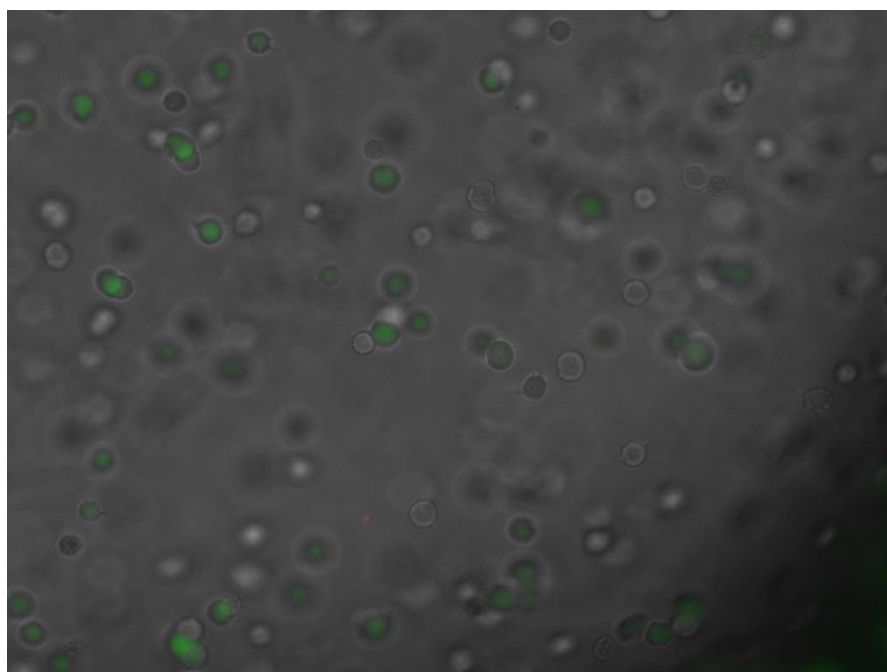
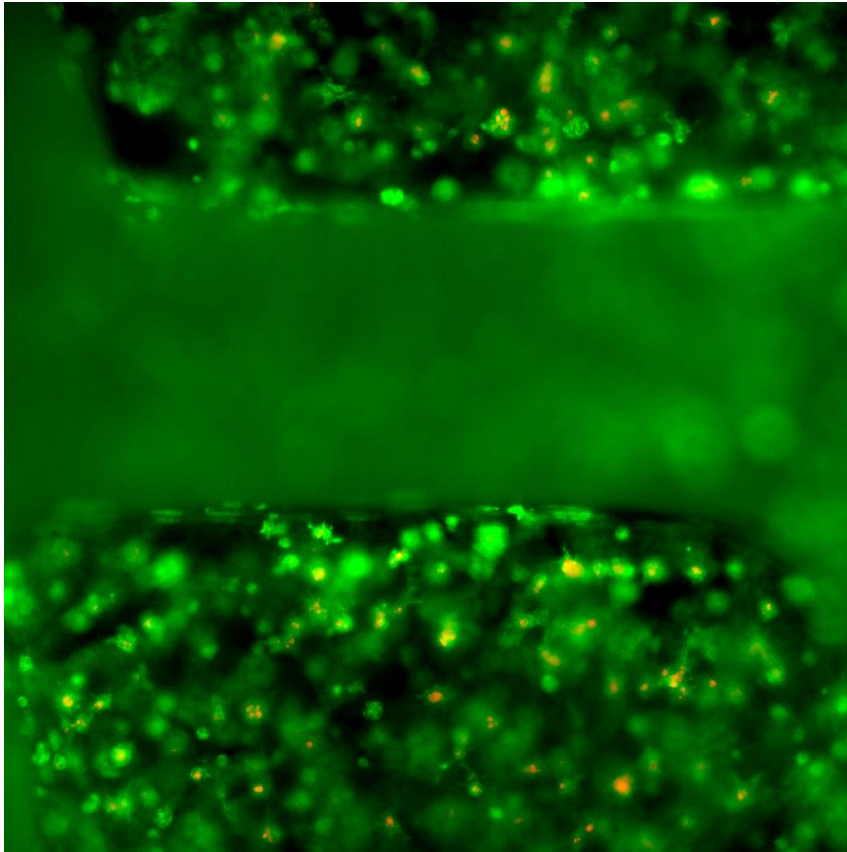**Figure 6.7** – 4% GelMa, day 1, 20X, PCL

~ 59 ~

Figure 6.8 – 4% GelMa, day 2, 4X, PCL

The L/D assay was done once per day for 3 and 2 day for PCL grids samples and metallic grids samples respectively. The day the cells encapsulation was performed is considered as Day 0.

6.4 Drug Delivery

6.4.1 Introduction

After having detected which was the best cellular environment, we chose the 4% w/w GelMa hydrogels to investigate on the drug releasing properties. For the analyses, the drugs selected were both hydrophobic and hydrophilic, Oil Red

O and Rhodamine B isothiocyanate respectively. The molecular structures are presented in figure 6.15 and 6.16
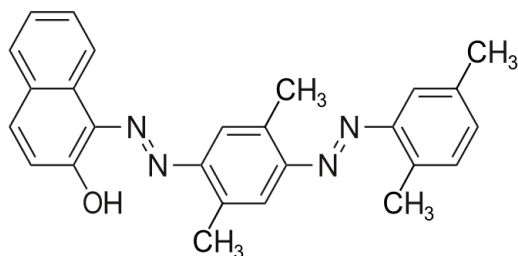
Figure 6.9 – Oil Red O
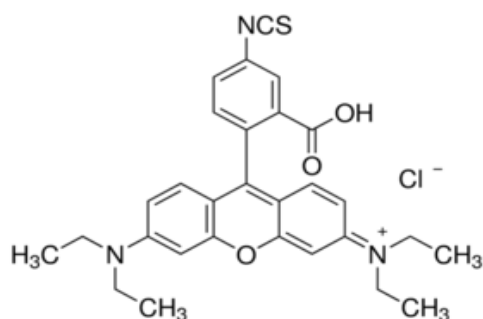
Figure 6.10 – Rhodamine B Isothiocyanate

6.4.2 Hydrophobic Model Drug

Due to its non-polarity, this molecule cannot be loaded into the hydrogel just dissolving it in the precursor solution. The approach we adopted was therefore to use polymeric nanoparticles (PNPs) to encapsulate the Oil Red O and then mixing the PNPs concentrated solution into the hydrogel precursor one. PNPs permit the loading thanks to their amphiphilic nature. In fact, as showed in figure 6.17, they have an outer layer hydrophilic and an inner one hydrophobic, that allows to encapsulate the molecule.
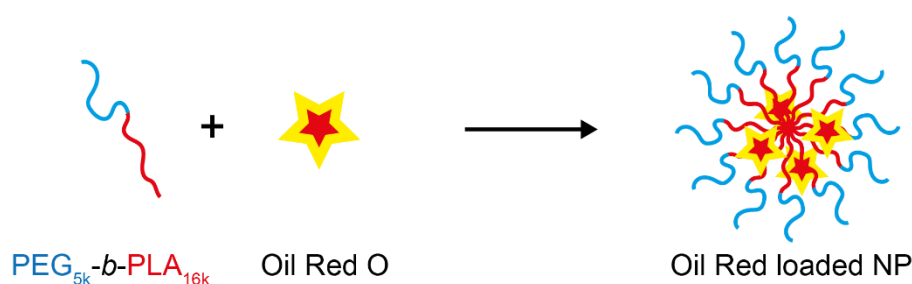
Figure 6.11 – Encapsulation Mechanism

6.4.3 Experimental Part

The polymeric nanoparticles have been made with AK54 (PolyEthileneGlycol 5 kDa – b - PolyLacticAcid 16 KDa), using batch nanoprecipitation.

As first trial we decided to load, into the PNPs, 1% of Oil Red O considering the weight of the AK54. The quantities commonly used to prepare the samples are listed in table 6.6.

Table 6.6 – Chemicals for PNPs Preparation

Chemical	Amount
AK54	70 mg
Oil Red O	7 mg
Acetone	10 ml

Oil Red O is firstly dissolve in 10 ml od acetone to reach a concentration of 0,7 mg/ml. From this solution A 1 ml is taken and used to dissolved AK54, to get to solution B.

To obtain the nanoparticles the solution B is nanoprecipitate in 10 ml of Millipore water (Milli-Q), with a digital dripper that makes aliquots of 15 ug for each drop, as presented in figure 6.18.
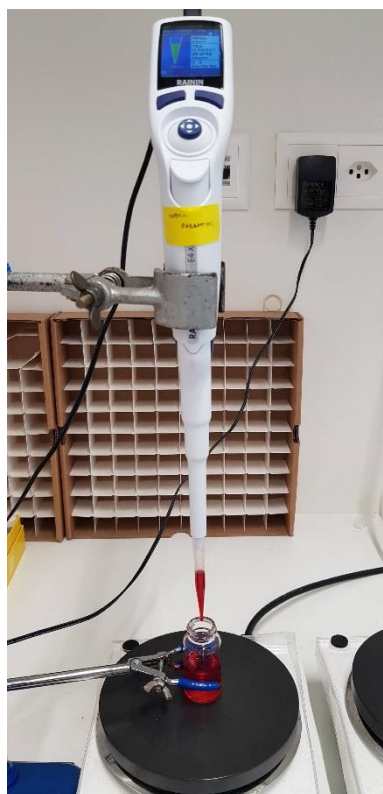
Figure 6.11 – Nanoprecipitation Setting

The stirring operates with 650 rpm room temperature. After the precipitation, acetone is letting evaporate for one day. Subsequently, the batch is transferred in empty filtering falcon (Amicon Ultra 15 Centrifugal Filter Unit – 30 KDa Molecular Weight Cut-Off) and centrifuged for 1 our and 10 minute at 4500 rcf. The retentate collected is then diluted with milli- Q water to get to a concentration of 20% w/w of PNPs loaded with Oil Red O.

A mass balance is then operated to be able to quantify the drug released. To do that, a small amount of 20% solution with nanoparticles is mixed with 95% of acetonitrile and its absorbance is measured and registered.

The calculation made to calculate the encapsulation efficiency, i.e. the extent od Oil Red O encapsulated, are reported in the table 6.7 below.

	Polymer Mass	Initial Drug Mass	mg OilRed Mass in Sample	% Encapsulation Efficiency
Name	AK54	OR	0.295	84.15%
%	-	1.00%	0.265	75.63%
mg / mL	35	0.35	0.375	107.05%
			Average	88.94%
			Standard deviation	16.25%

Table 6.7 – Encapsulation Efficiency Results

The encapsulation efficiency percentages are calculated divided the ORo mass we found remained in the sample by the initial drug mass loaded, multiplied by 100.

After the first drug release test we noticed that some particles of not encapsulated Oil Red O were present in the samples, as it appears in the figure 6.19. For this reason we decided to let the non-encapsulated ORo to crystallize at 4°C for one day and then centrifuged for 20 minutes at 4500 rcf. We did this procedure with three different ORo percentages (0,5% , 1%, 2%) and checked the effective efficiency of the loading using mass balance and spectrophotometric analysis.
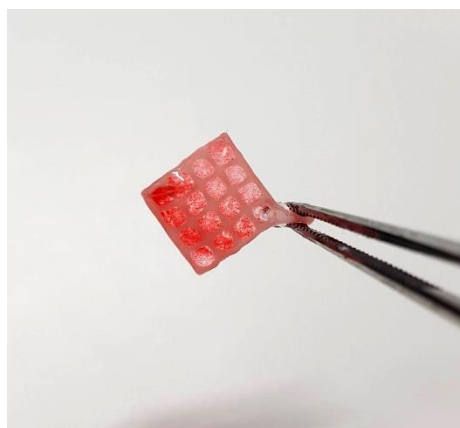
Figure 6.13– Oil Red O Microparticles

The results obtained are listed in the table 6.8.

Table 6.8 - Encapsulation Efficiencies After Precipitation

Drug Loading	Encapsulation Efficiency after precipitation
0,5%	68.11%
1%	70.81%
2%	99.7%

6.4.3.4 Releasing Profile of Oil Red O

The drug release studies of the devices in PCL and metallic have been completed for both gelatin methacrylated hydrogels and sodium alginate hydrogels, for two different crosslinking times.

- ## GelMa and Oil Red O

To analysed the releasing behaviour of the hydrophobic model drug- loaded polymeric nanoparticles, samples in triplicate have been produced and weighted with the polymerized solution onto them and let them release the nanoparticles for several days. The withdrawals collected have been diluted with the same quantity in volume of acetonitrile to brake the PNPs and let the Oil Red O contained to exit from them. After this step, colorimetric analysis with spectrophotometer have been performed, checking absorbance between 500 and 530 nm of wavelength.

- ## Sodium Alginate and Oil Red O

Sodium alginate hydrogels releasing behaviour has been investigated too, in particular to highlights the differences with methacrylated gelatin and with the two devices material used for the grids. The hydrogel has been crosslinked with calcium chloride (1.5% w/w of H_2O). The procedure used to calculate the amounts of drug released is the same as for the PCLs grids.

6.4.4 Hydrophilic Model Drug

Thanks to its polarity, this molecule can be loaded into the hydrogel just dissolving it in the precursor solution. The approach we adopted was to mix it with the other compounds and after depositing the liquid solution on the grids, we lighted them up with the UV lamp. Due to the fact that the combination of sodium alginate and rhodamine B had been already widely investigated, it has been decided to analysed the releasing behaviour of rhodamine B only from GelMa hydrogels, for both PCL and metallic grids.

6.4.4.1 Experimental Part

To prepare rhodamine B isothiocyanate–loaded hydrogels we formulated the precursor solution as indicated in the table 6.9.

Table 6.9 – Quantities Used for RhBI Grids Samples

Chemical	Amount
GelMa	4% w/w
Rhodamine B Isothiocyanate	0.5% w/w
LAP Photoinitiatior	0.1% w/w
Phosphate Buffer Solution	95.4% w/w

After that, the grids have been polymerized for two different crosslinking times, 8 and 16 minutes. With the former the hydrogel has lower stiffness, with the latter is in the plateaux range i.e. has the highest G'.

To guarantee always the same light intensity of 10 mW/cm², the UV lamp has been fixed has demonstrated in figure 6.20.
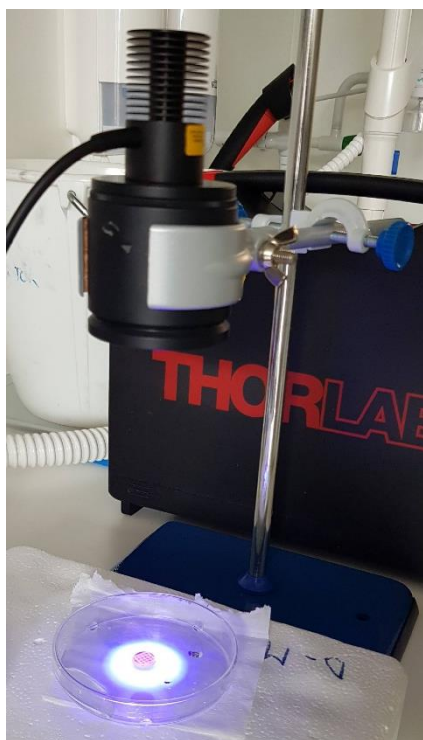
Figure 6.14 – Polymerization Setting

The samples prepared have been consequently placed in 1.5 ml releasing bath of PBS and analysis have been done every 2 hours for the first six after the polymerization, then after eight, one day, two days and 4 days. For each analysis, 620 µl were taken out from each wells and 620 µl of new phosphate buffer solution were added. These quantities had then been taken into account in the releasing evaluation. The appearance of the samples is showed in figure 6.21.
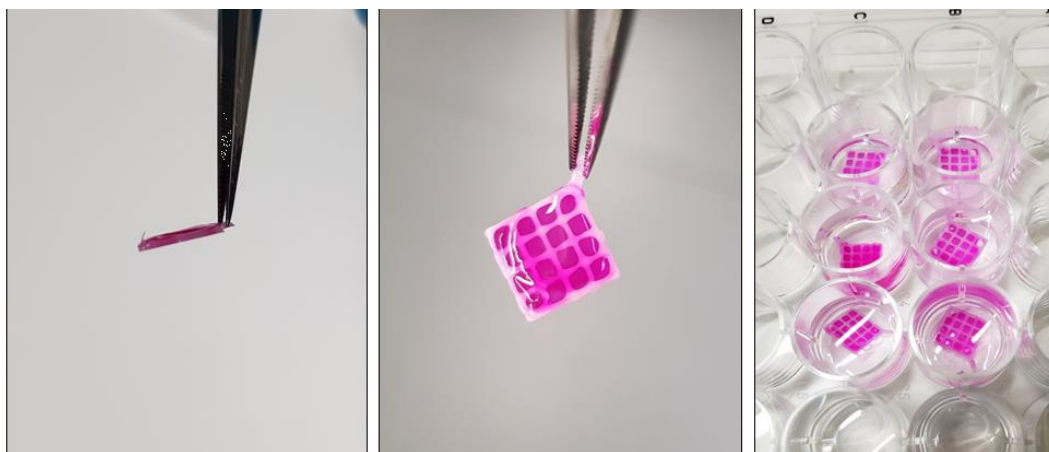
Figure 6.15 – Prepared Samples with loaded Rhodamine

6.4.4.1.1   Rhodamine   B   Isothiocyanate Photocatalytic Degradation

During the releasing experiments with rhodamine B isothiocyanate, confused by the low release detected, we wanted to check if something influenced the release or the detection of the rhodamine itself. That is way we began to check in the literature and we found that UV light in some condition and with particular compound like TiO_2 [35] or ZnO [36], degrades photocatalytically rhodamine B.

To check the effective degradation phenomena, two different solution where firstly prepared: one with photoinitiator, rhodamine B isothiocyanate and PBS and the other without photoinitiator. The initial rhodamine B isothiocyanate concentration was of 50 μg/ml of solution for both the solution prepared. The absorbance was firstly measured a time 0, before starting to irradiate the sample. Then, the absorbances were registered after 30 seconds of irradiation and subsequently for 1, 2, 4, 6, 8, 10, 12, 14, 16 and 20 minutes.

6.4.4.1.2 Rhodamine B Photocatalytic Degradation

The same analysis has been accomplished also for classic Rhodamine B, which molecular structure is presented in figure 6.22.
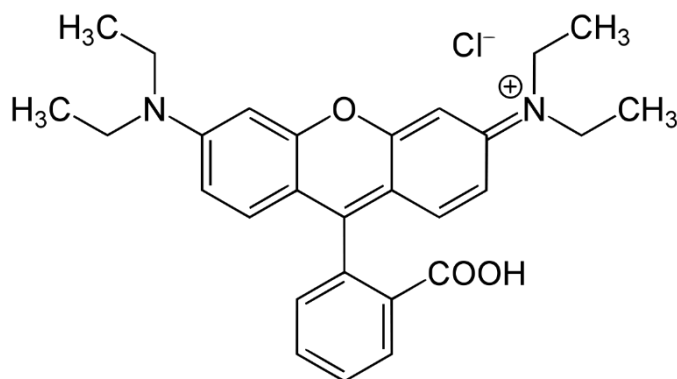
Figure 6.16 – Rhodamine B

For this case, after having checked the degradation with the photoinitiator in solution, we investigated the effect of the GelMa hydrogel itself on the degradation, checking the absorbance at time zero and during the polymerization time, after 30 seconds, then 1, 2, 3 minutes, at which we have the crossover point.

At last, the releasing behaviour of Rhodamine B has been analysed for three PCL samples to detect the differences. To prepare rhodamine B – loaded hydrogels we have formulated the precursor solution as indicated in the table 6.9.

Table 6.9 – Quantities Used for RhB Grids Samples

Chemical	Amount
GelMa	4% w/w
Rhodamine B Isothiocyanate	0.5% w/w
LAP Photoinitiatior	0.1% w/w
Phosphate Buffer Solution	95.4% w/w

CHAPTER 7

RESULTS AND DISCUSSION

The results of the products characterizations, the cells' viability tests and the drug release tests, performed on the hydrogel-coated grids are collected and commented in this chapter. In particular, it is underlined the difference in behaviour between GelMa hydrogels and alginate hydrogels also considering the two mimic drug used. All the drug release analysis were repeated several times in the same conditions, in order to increase the reliability of the results obtained. Furthermore, also all the characterization tests have been done in triplicate and the results presented are the mean of each of the three values obtained.

7.1 GelMa Characterization

To check if the functionalization reaction was occurred, we used 1H NMR spectroscopy. The samples were dissolve in D2O and the number of scansion operated by the machine was 132. The ^{1}H NMR spectra was analysed to determine the extent of conversion of free amino groups (degree of methacrylation, DM). In the figure 7 and 7.1 below are illustrated the obtained spectra.

Results and Discussion
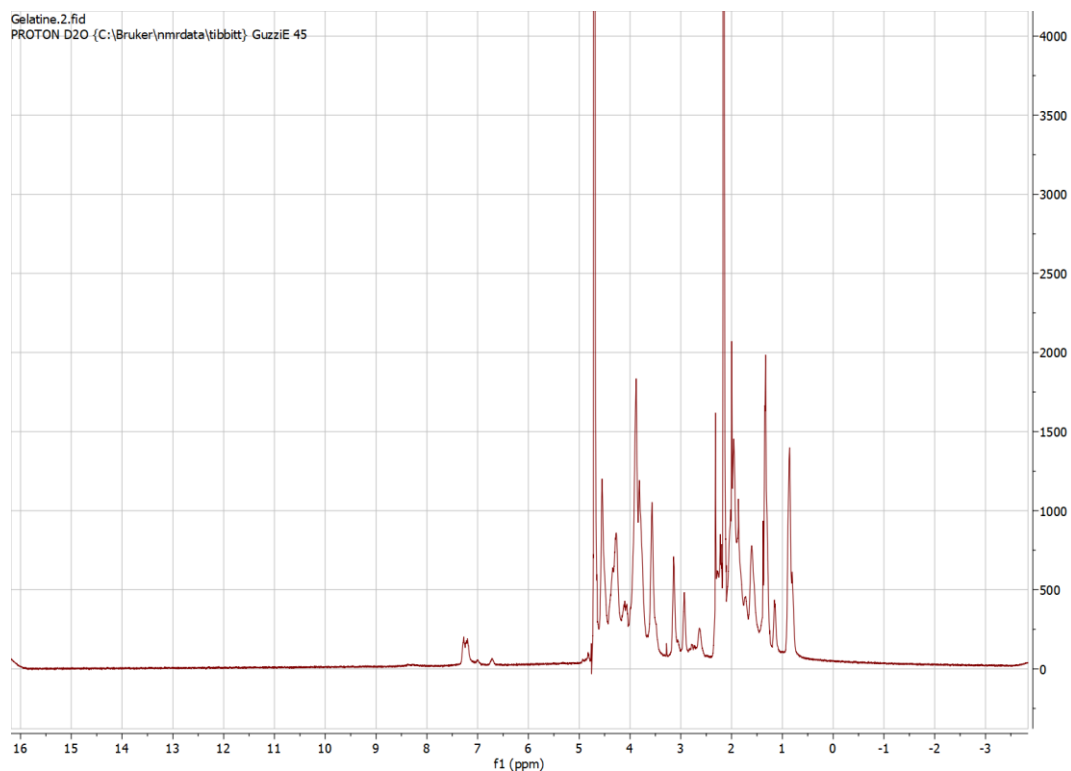
Figure 7 – Gelatin NMR
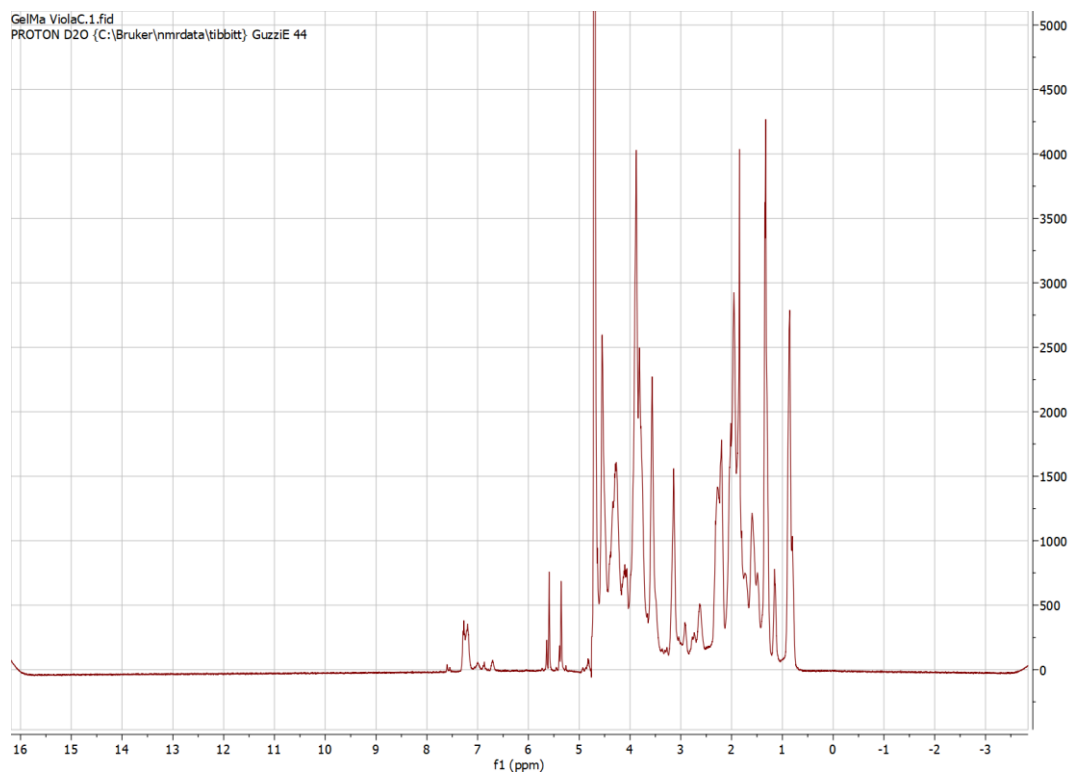
Figure 7.1 – GelMa NMR

The degree of methacrylation (DM) was defined as the percentage of ε-amino groups of gelatin (lysine, hydroxylysine) that are modifed in GelMa. For the quantification of the DM by 1H NMR the spectra were normalized to the phenylalanine signal (6.9–7.5 ppm), which characterizes the concentration of gelatin.

Consequently, the lysine methylene signals (2.8–2.95 ppm) of gelatin spectra and GelMa spectra were integrated to obtain the areas [*A(lysine methylene of unmodified gelatin)*] and [*A(lysine methylene of GelMa)*].[37] The degree of methacrylation of the different GelMa batches were calculated as follows, explained also in the figure 7.2 :

DM [%] = [1 − (*A (lysine methylene of GelMa)*/ *A (lysine methylene of unmodified gelatin*)] x 100
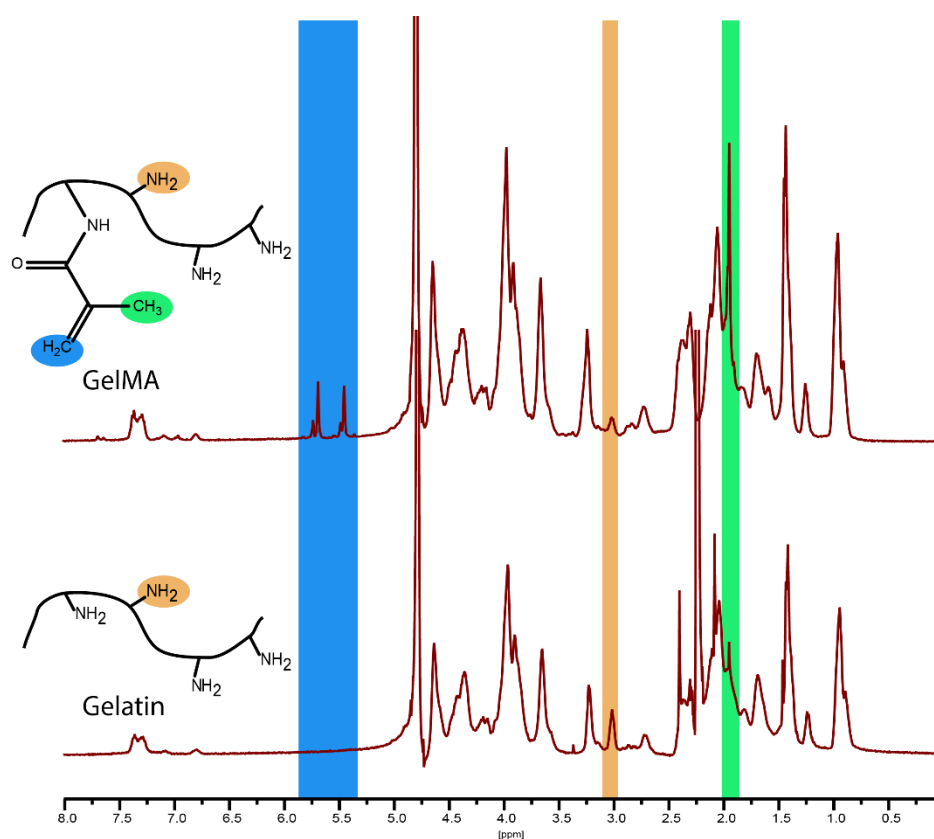
Figure 7.2– DM integral calculation

Table 7 – DoF Calculation

	Ppm Interval	Gelatin Absolute Area	GelMA Absolute Area	DoF	Lysine / Phenylananine
Phenylananine	7.1 - 7.4	132369211		0.77	0.77301416
Lysine Methylene	2.8 - 3.0		102323275		

As calculated in the table 7 , the degree of functionalization is around 77%.

7.1.1 Gelatin and GelMa Rehological Characterization

We firstly investigated on the gelation properties of gelatine to understand its behaviour in function of temperature. The results obtained from the rheology are reported in the graphs below, in the figure 7.3, 7.4 and 7.5. At

room temperature, all the three hydrogels precursor solutions, showed G">G'. This means that the material is liquid and it is possible to coat easily the devices, exploiting superficial tension.
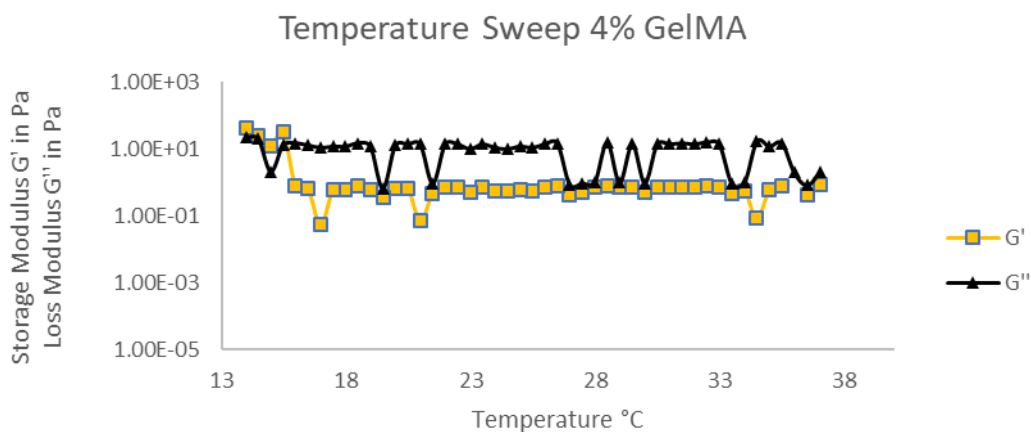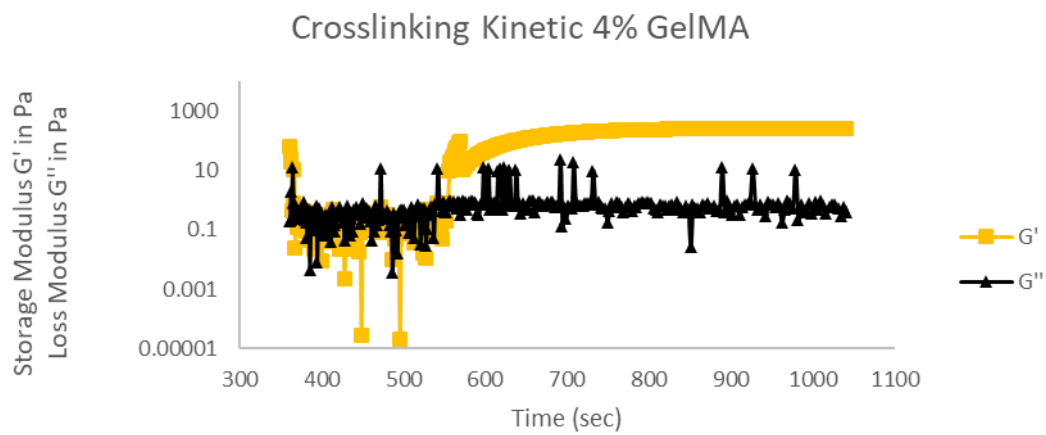

Figure 7.3 - G' and G" of 4% GelMa solution
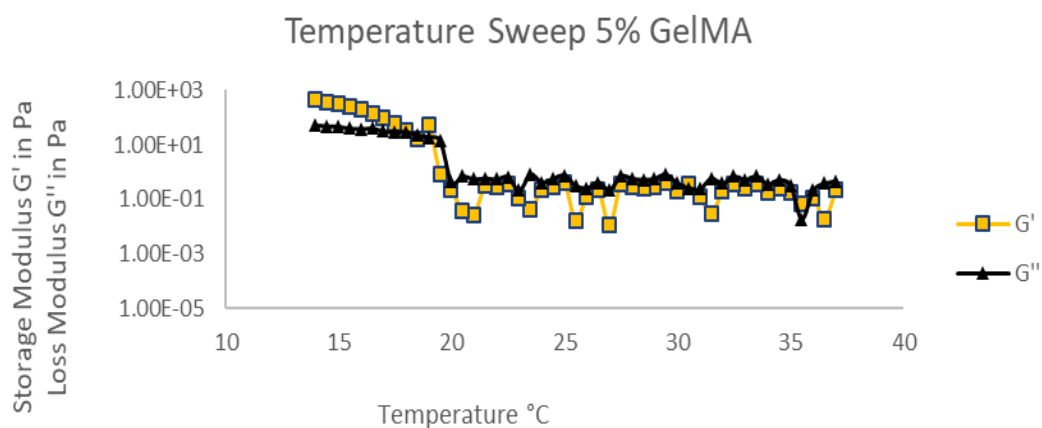
Figure 7.4 - G' and G" of 5% GelMa solution
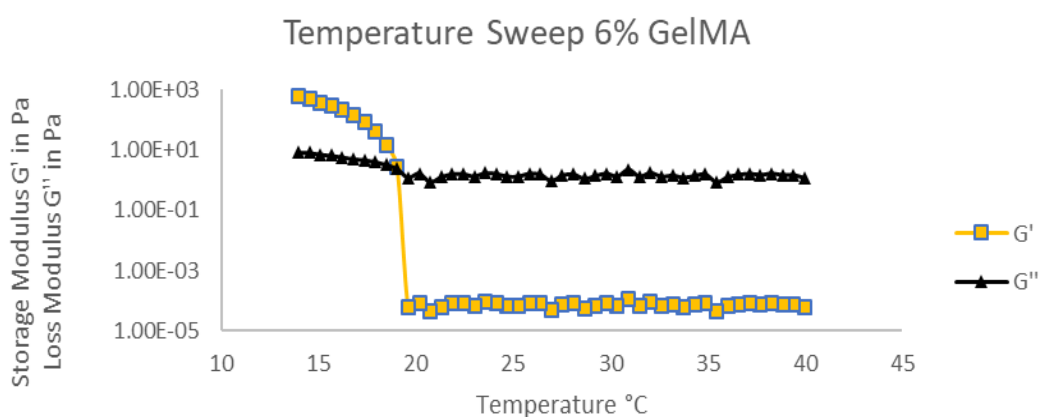
Figure 7.5 - G' and G" of 6% GelMa solution

The sol-gel crossover temperatures, i.e. that temperature from which the gelation starts and we enter in the viscoelastic regime, are registered in the table 7.1 below.

Table 7.1 – Sol-Gel Transition Temperatures

Condition	T (G'>G")
GelMA 4 wt%	15.5 °C
GelMA 5 wt%	19.0 °C
GelMA 6 wt%	19.0 °C

Considering then the crosslinking kinetic, we checked after how many seconds we got to the cross-over point, i.e. that point from which the viscous regime is predominant respect to the elastic one, and the sample can be considered a gel. Underneath, in the graphs of G' and G" are reported in function of time in the figures 7.6, 7.7, 7.8 , again for 4%, 5%, 6% w/w GelMa, . In this case, the temperature has been maintained constant at 37°C, value at which we would have worked for cells experiments.

Figure 7.6 - G' and G" of 4% GelMa solution
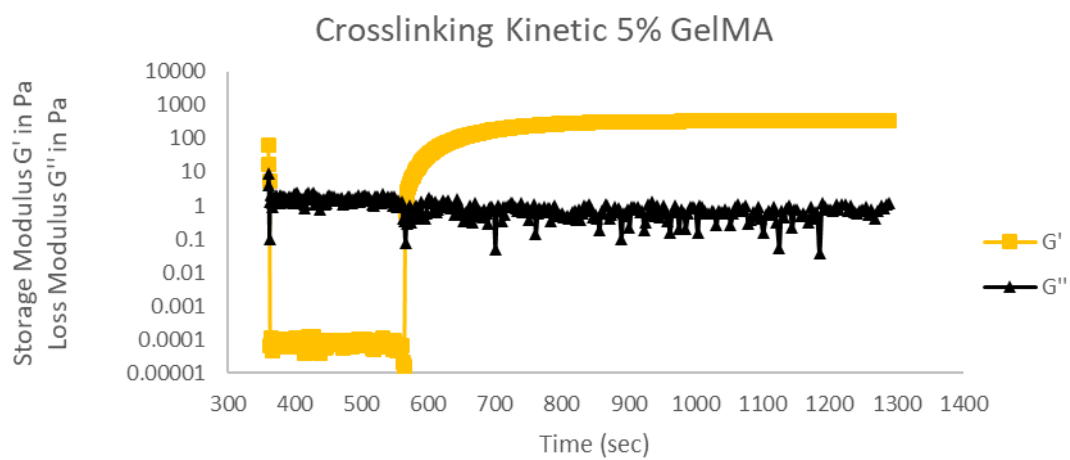
Figure 7.7 - G' and G" of 5% GelMa solution

~ 79 ~
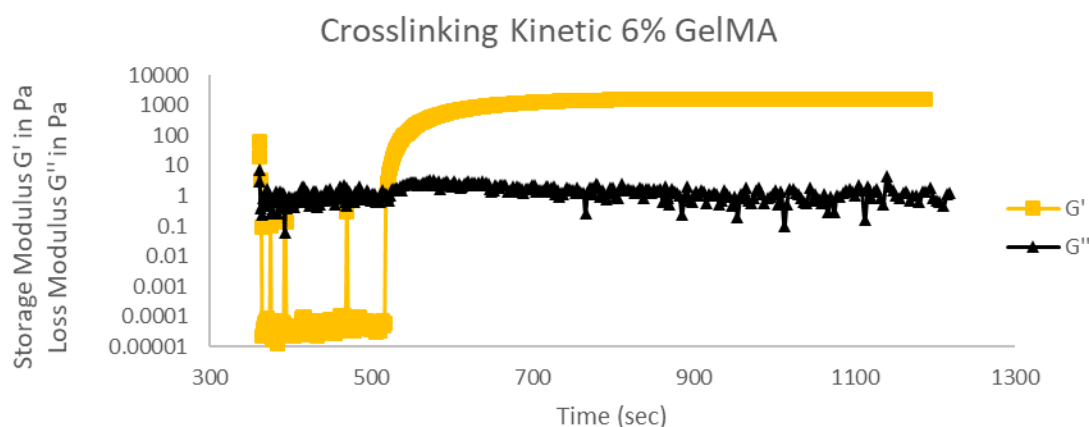
Figure 7.8 - G' and G" of 6% GelMa solution

The UV Light was on always after 2 minutes (120 sec) from the beginning of the test. The crossover times of the three different samples are reported in the table 7.2.

Table 7.2 – Times of Crossover Points

Condition	Crossover Point
GelMa 4 wt%	~75 sec
GelMa 5 wt%	86 sec
GelMa 6 wt%	40 sec

The plateaux range, i.e. the maximum value of G' at which the hydrogel gets to highest stiffness, changes in function of the GelMa percentages. As this increases, intermolecular connections become more feasible. An higher amounts of physical cross-links diminish the average molecular weight between cross-links and rise the storage modulus. The polymer concentration affects the values of G' also because the concentration of methacrylamide groups rises with

growing polymer concentration, and more chemical crosslinks per unit volume can be formed.[10] As presented in the table 7.3, G' modulus increases also from 4% to 6% w/w GelMa concentration.

Table 7.3 – Storage Modulus in the Plateaux Range

GelMa Concentration	G' (Storage Modulus)
4%	255 [Pa]
5%	328 [Pa]
6%	1655 [Pa]

7.2 3D Cells Encapsulation in GelMa

After the rheological analysis, we wanted to control if the devices in their entirety (GelMa+ PCL grid or GelMa+ Metallic grid) were biocompatible and which of the three conditions of hydrogels (4%, 5%, 6% w/w of GelMa) would have been the most suitable for cells' life, aggregation and proliferation.

The life/dead assay results, show that the polycaprolactone is not a cytotoxic material for the cells, as it is possible to understand comparing the control groups viability results with the one from PCL. Different is the case for the metallic grids, that probably the poor compliance revealed, was caused by the entering in solution of ions of nickel or cobalt from the sub-layers of the metallic grid, because, for some reasons, the outer gold layer was damaged and the underneath strata became exposed to the cells, causing the death for cytotoxicity[38], as it is possible to see in figure 7.9.
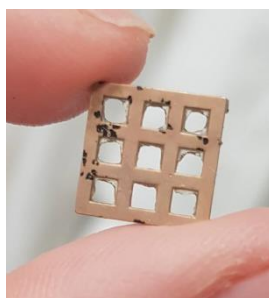
Figure 7.9 – Damaged Gold Layer

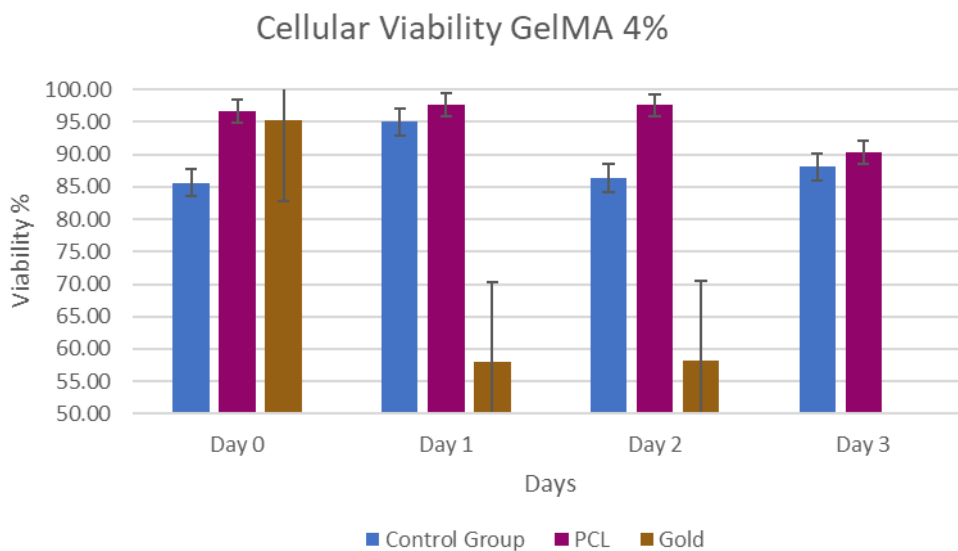The viability test results are reported in the figures 7.10, 7.11, 7.12 below.

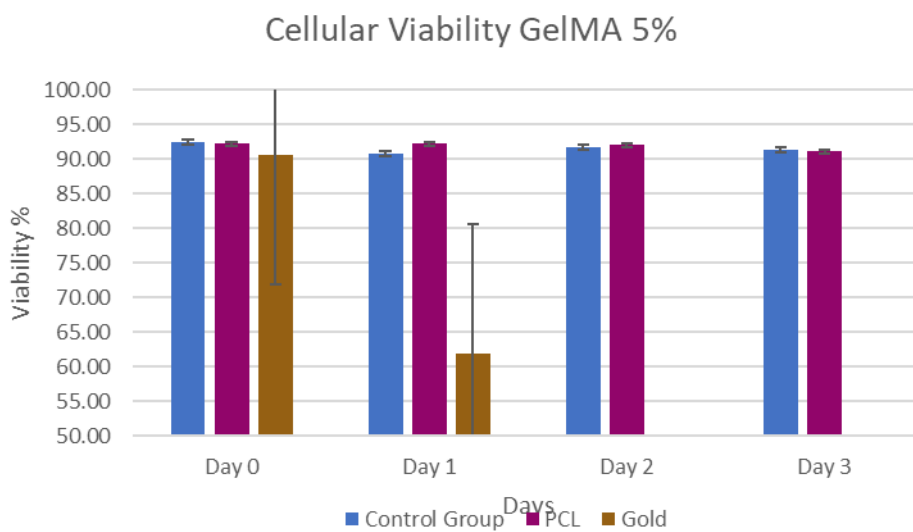**Figure 7.10** – Viability Results GelMa 4%
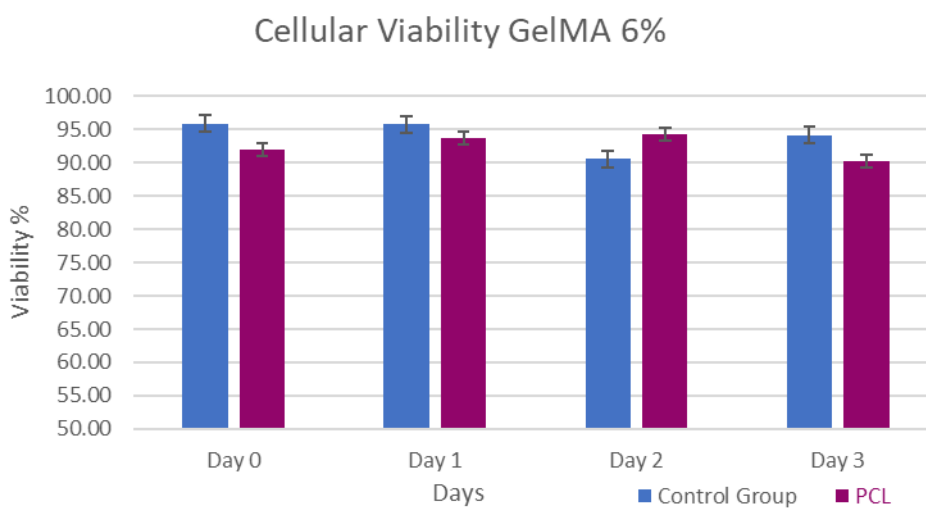
Figure 7.11 – Viability Results GelMa 5%

Figure 7.12 – Viability Results GelMa 6%

As it is possible to see, the viability data for PCL sample do not change considerably between the days, fluctuating between a viablility percentage of 90% and 96%. Due to the little availability of metallic grids and to the not encouraging results obtained with metallic grids, viability analysis for the 6% w/w of GelMa precursor solution were not performed.

7.2.1 Cells Aggregation, Elongation and Proliferation

Due to not a marked difference between the different hydrogel matrix, we decided to check on the cells' wellness, considering cellular membranes aggregation, elongation and gathering. To assay the cells behaviour and wellness, we checked on their cytoskeletons elongation and nucleus gathering through Phalloidin + DAPI. The images obtained with the fluorescence microscope are reported below in the figures. The first figure 7.13 shows how the cells appear right after 4 hours since the encapulation process.
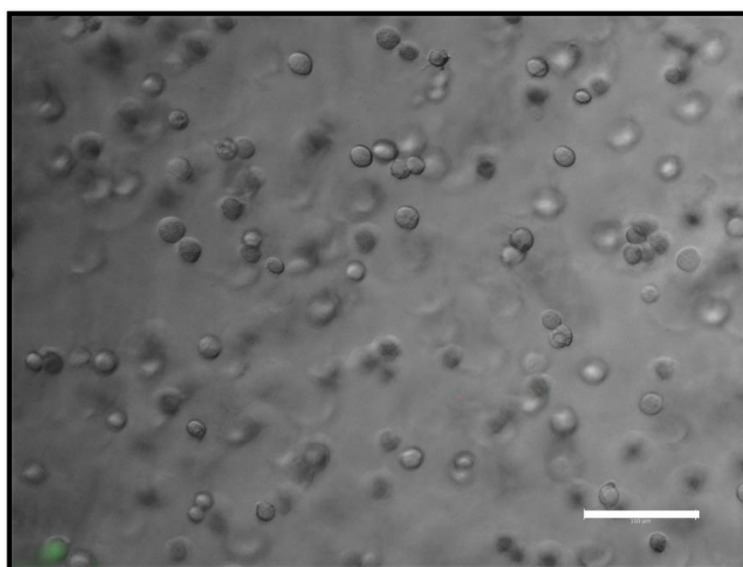
Scale bar, 150 µm.

Figure 7.13 - 4% w/w GelMA, 0,1% w/w LAP, PBS, after 4 h

After 2 Days at 37°C, in culture medium, with PCL Grids, the cells appear as showed in figure 7.14, 7.15, 7.16, for 4%, 5%, 6% w/w of methacrylated gelatine.
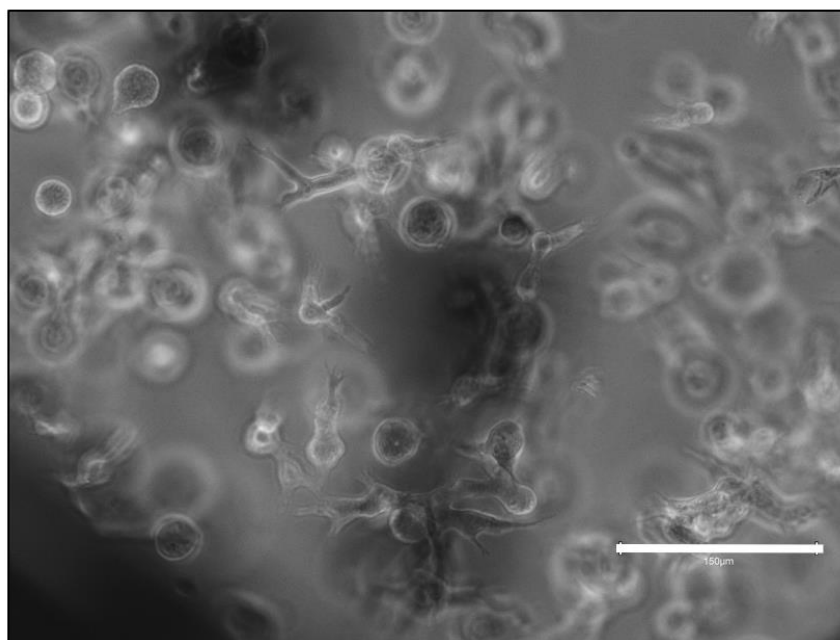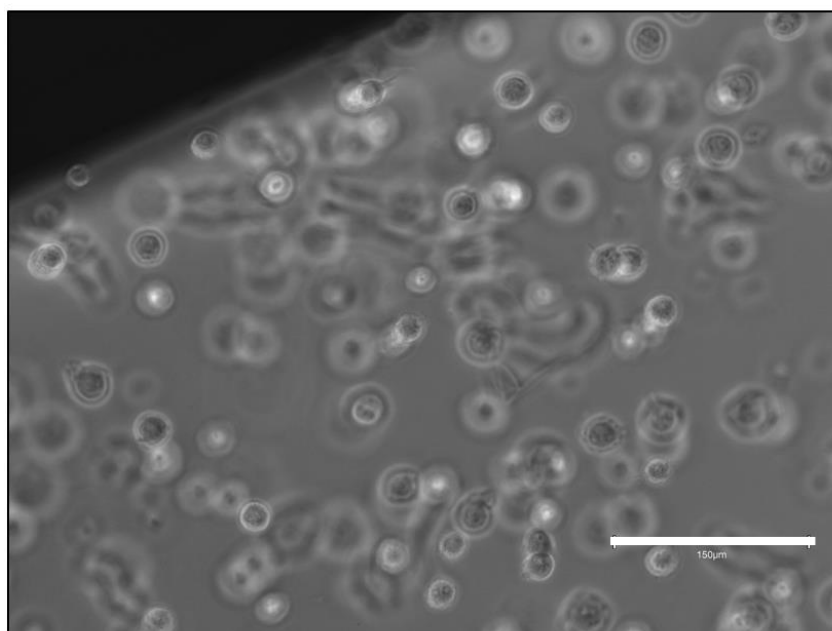

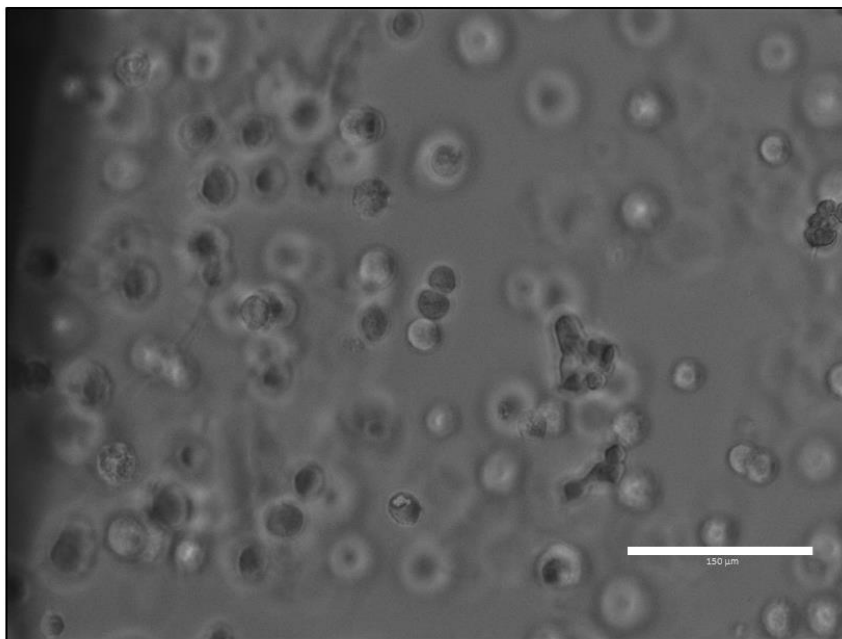**Figure 7.14** - 4% w/w GelMa

Figure 7.15 - 5% w/w GelMa

Figure 7.16 - 6% w/w GelMa

As it is possible to observe, in less stiff material, cells are able to spread and aggregate their membranes better.

On the contrary, for the metallic grids, the cellular membrane remains rounded, as it can be seen in figure 7.17 and 7.18. It means that the surrounding environment is not proper enough.
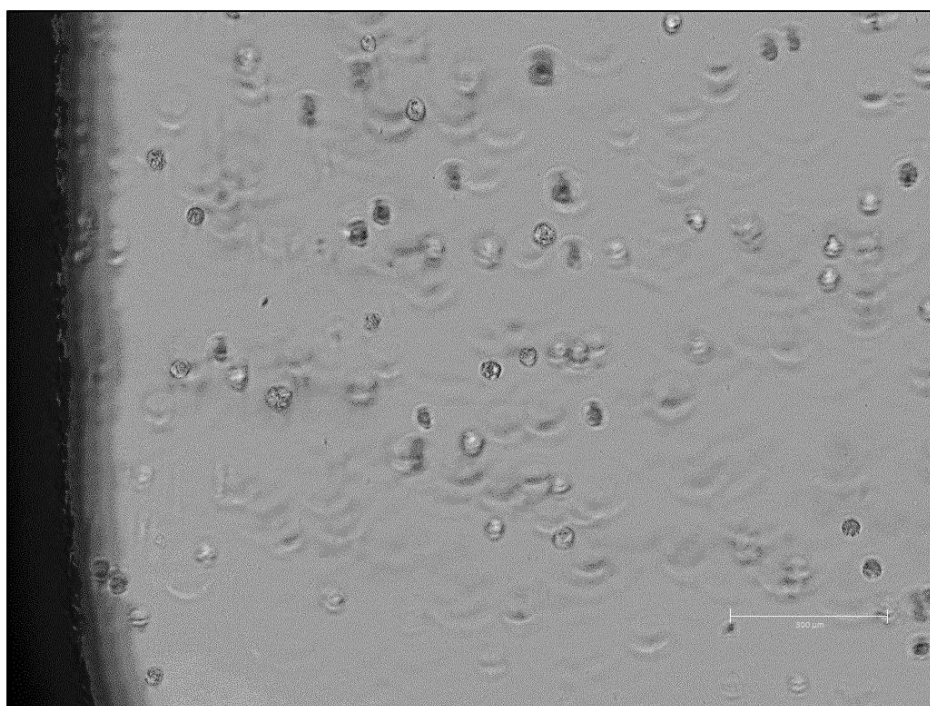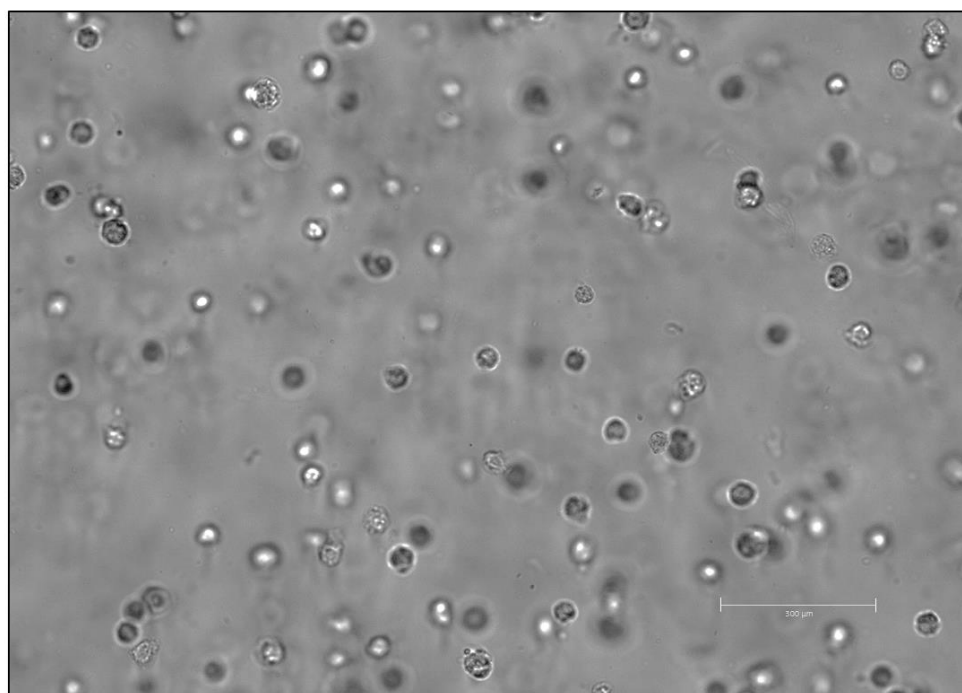
Figure 7.17 - 4% w/w GelMA day 0

Figure 7.18 - 4% w/w GelMA day 0

~ 87 ~

The two figures 7.19 e 7.20 below, obtained with Phalloidin- DAPI fluorescent staining, highlights the cellular cytoskeletons, in the 4% GelMa hydrogels.
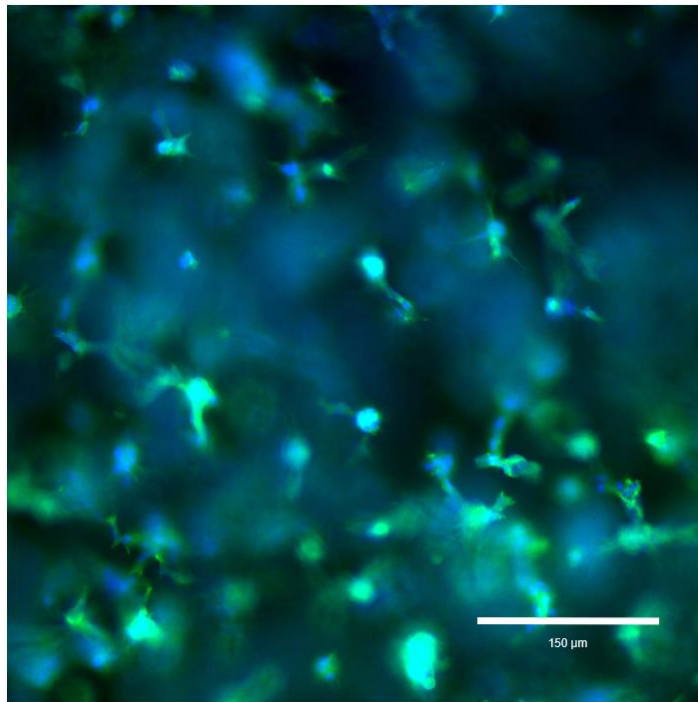

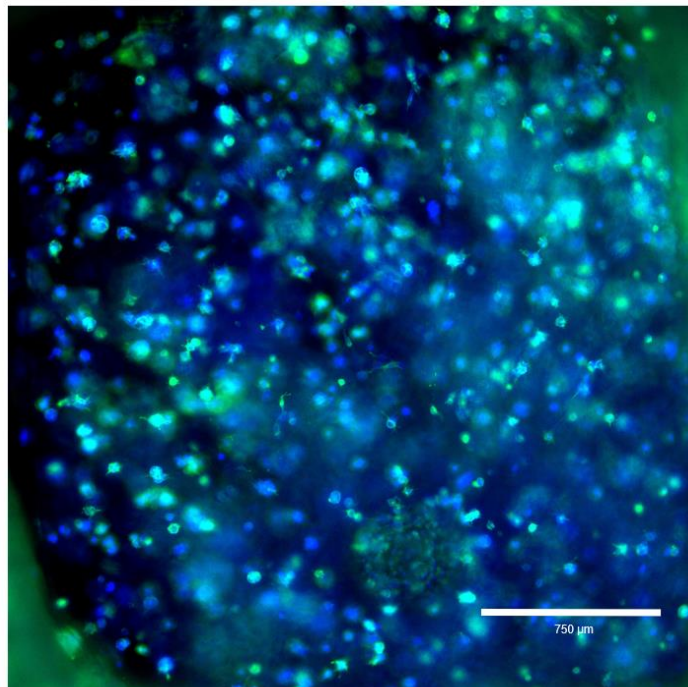**Figure 7.19**– 4% with PCL after 1 Day of Encapsulation (20x)

Figure 7.20 - 4% with PCL after 1 Day in Hydrogel (4x)

7.3 Drug Delivery

7.3.1 Hydrophobic Model Drug

Due to its non-polarity, this molecule cannot be loaded into the hydrogel just dissolving it in the precursor solution. The approach we adopted was to use polymeric nanoparticles (PNPs) to encapsulate the Oil Red O into them and then mixing the PNPs concentrated solution into the hydrogel precursor one.

7.3.1.1 Polymeric Nanoparticles Characterization

Dynamic Light Scattering (DLS) analysis have been performed on samples of PNPs with and without Oil Red O to understand the influence of the model drug on the features of the nanoparticles. The Zeta Potential (ZP), also termed as electrokinetic potential, has been examined. It is the potential at the slipping/shear plane of a colloid particle moving under electric field. The Zeta Potential reflects the potential difference between the EDL (electric double layer) of electrophoretically mobile particles and the layer of dispersant around them at the slipping plane[39]. Furthermore also the polydispersity index (PDI) and the Z-Average have been investigated. The former is dimensionless and scaled such that values smaller than 0.05 are seldom seen other than with highly monodisperse standards. Values bigger than 0.7 indicate that the sample has a very extensive size distribution and is almost certainly not appropriate for the dynamic light scattering (DLS) technique. The latter is the intensity weighted mean hydrodynamic size of the ensemble collection of particles measured by dynamic light scattering.

The data obtained are reported in the figure 7.21,7.22, 7.23, 7.24 and sum up in the table 7.4. The PDI values are optimal because largely below the threshold limit.
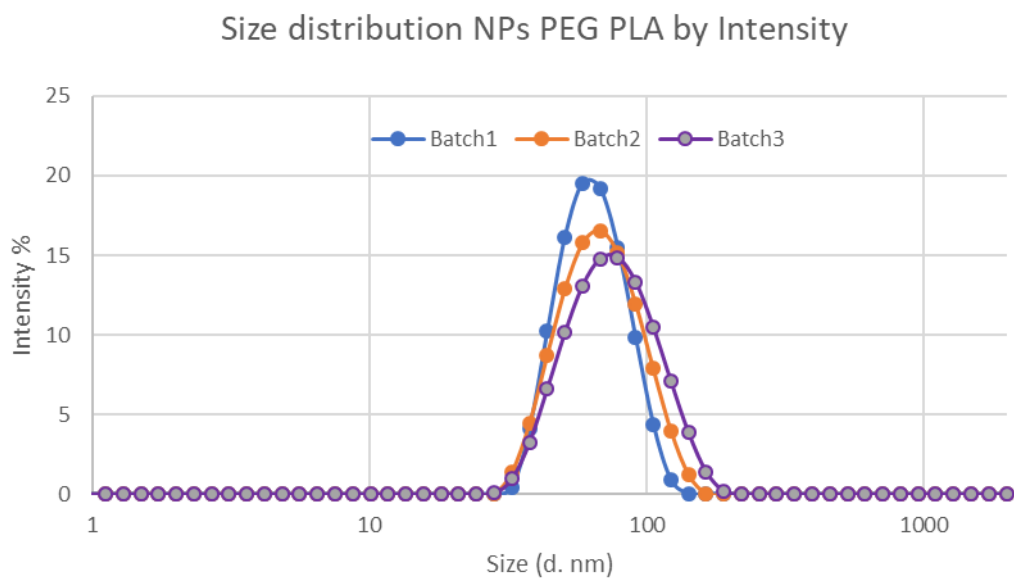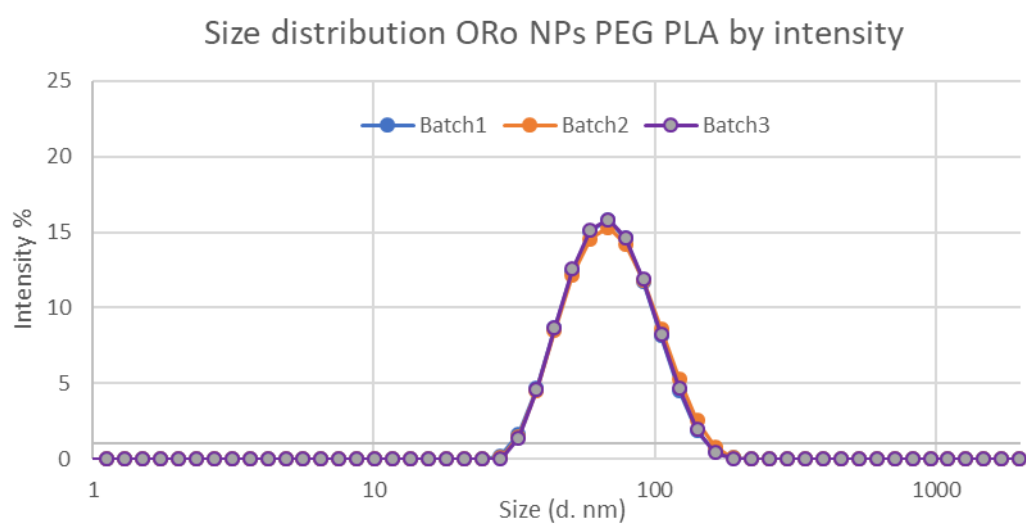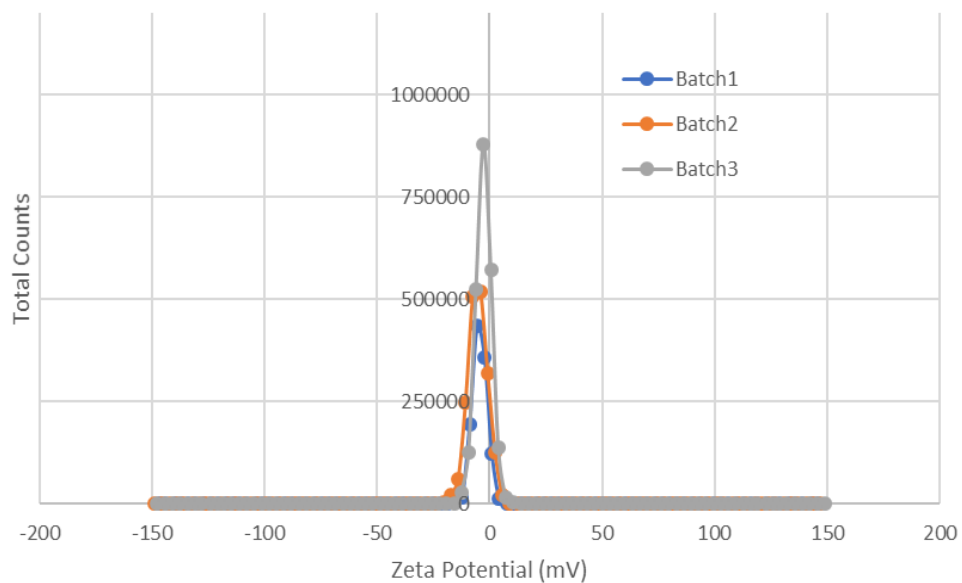
Size distribution NPs PEG PLA by Intensity

Figure 7.21 – PNPs Size Distribution (No ORo)

Size distribution ORo NPs PEG PLA by intensity

Figure 7.22 – PNPs Size Distribution (ORo Encapsulated)

Figure 7.23 – PNPs Zeta Potential Distribution (No ORo)
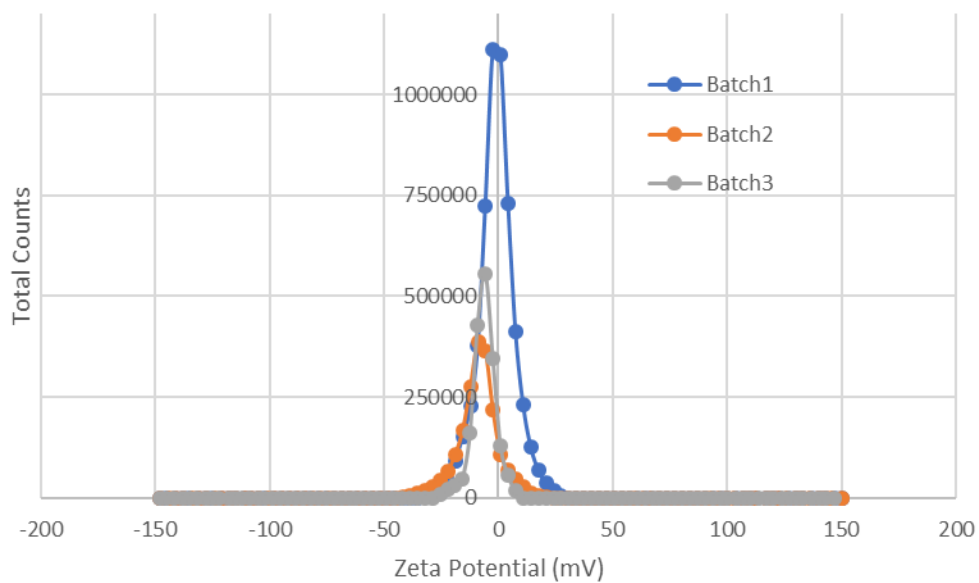
Figure 7.24 – PNPs Zeta Potential Distribution (ORo Encapsulated)

	NPs without ORo	NPs with ORo
Z-Potential [mW]	-4.15	-4.68
Z-Average [mW]	65.16	64.64
PDI	0.09	0.10

Table 7.4 – DLS Results

7.3.1.2 Rheological Characterization of GelMa with PNPs

The crosslinking kinetic of Oil Red O-Loaded hydrogel with 4% w/w of GelMa has been analysed in function of time, keeping the temperature constant, to check the time shifting respect to the hydrogel without Oil Red O loaded nanoparticles.
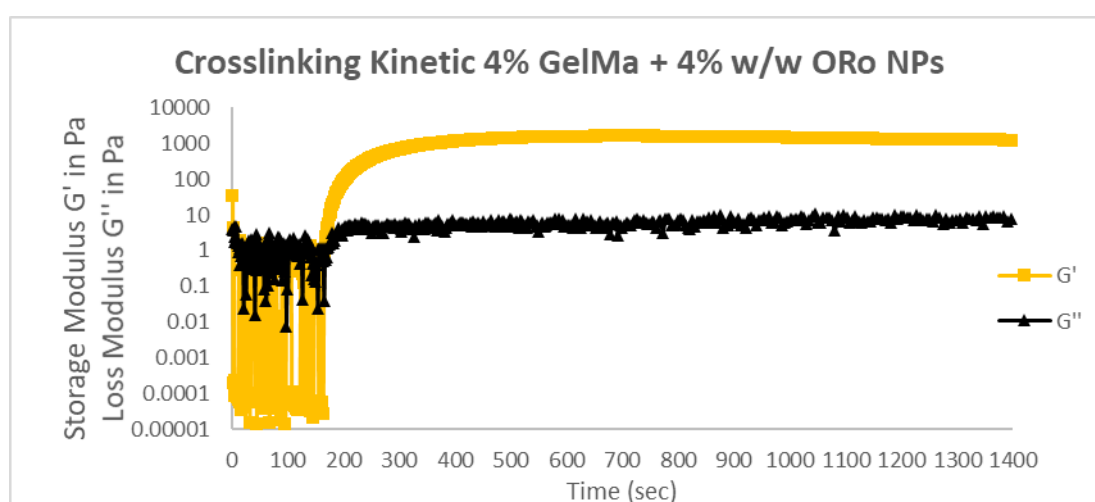

Figure 7.25 – Crosslinking Kinetic of GelMa Hydrogels with ORo loaded PNS

As shown in the figure 7.25, the cross-over time is at 168 seconds, while in the case without loaded PNPs is 75 seconds. This happens because the Oil Red O molecule has absorbance peak very close to the one of the photoinitiator LAP, has illustrated in figure 7.26 so this caused a delay in the polymerization kinetic.
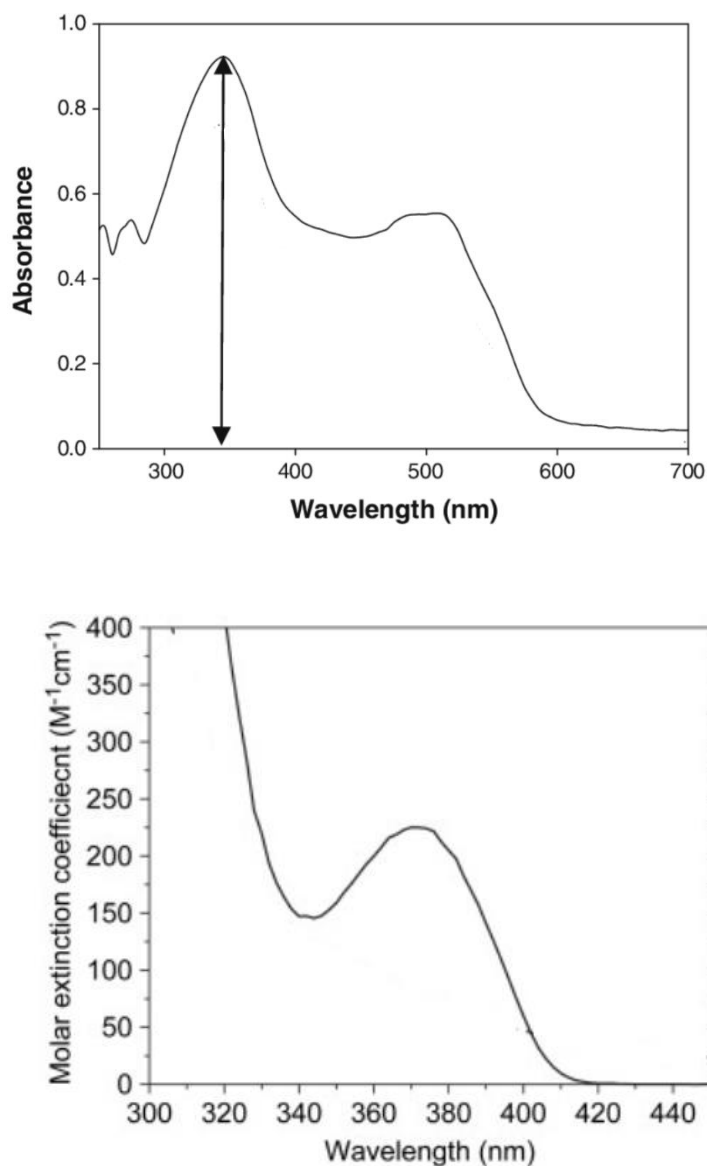

Figure 7.26 – Asorbance of Oil Red O (above) and of LAP (below)

7.3.1.3   Releasing Profile of Oil Red O

The drug release studies of the devices in PCL and metallic have been completed for both gelatin methacrylated hydrogels and sodium alginate hydrogels, for two different crosslinking times.

7.3.1.3.1   GelMa and Oil Red O

To evaluate the release of the molecule, analysis with spectrophotometer have been performed, checking absorbance between 500 and 530 nm of wavelength.

To calculate the drug release, we have exploited the Lambert – Beer relation, which is the following:

$$Abs = k * l * C$$

where:

- Abs is the dimensionless absorbance calculated before.
- k is the molar extinction coefficient or molar absorptivity (or absorption coefficient), given as a constant and varies for each molecule.
- l is the path length, known from the sample (standard) dimensions.

In addition, the calibration curve presented in figure 7.27 has been produced to extrapolate the concentration of the drug in the sample and then, knowing the initial weight of the PCL grids and the quantity of drug loaded thanks to the PNPs mass balance, we have been able to get to the amount released by the device.
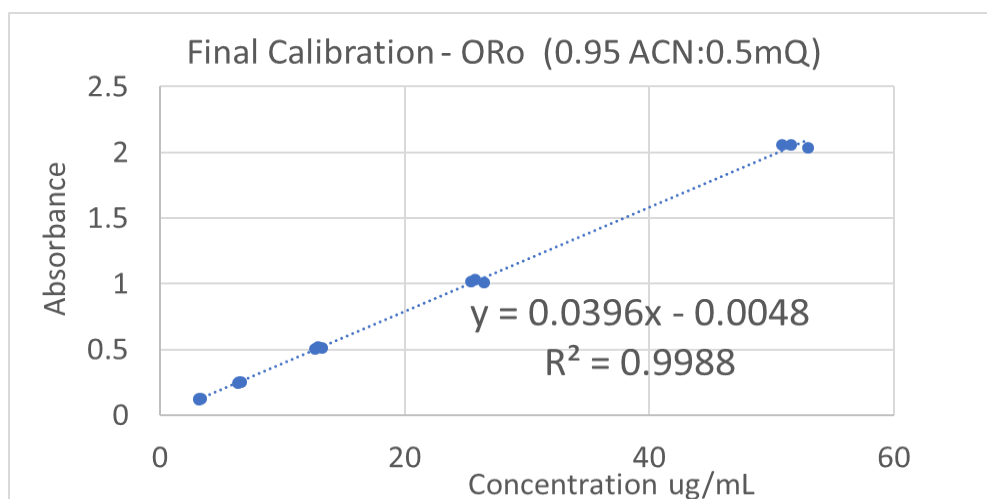
Figure 7.27 – Oil Red O calibration curve

For the analysis, two different percentages of PNPs loaded with Oil Red have been used, 4% and 8% w/w. The results obtained are shown in figure 6.39, 6.40, 6.41, 6.42 for the grid in PCL, while in figure 6.43, 6.44 for the metallic grids, for 8% w/w of nanoparticles solution.
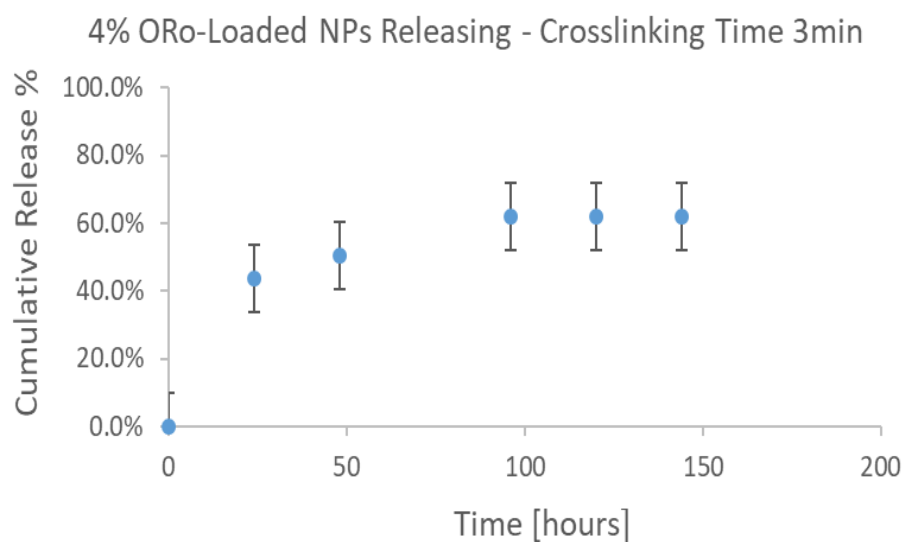

Figure 7.28 – Releasing Profile of GelMa Hydrogel 4% w/w ORo Loaded PNPs 3 min Crosslinking with PCL grids
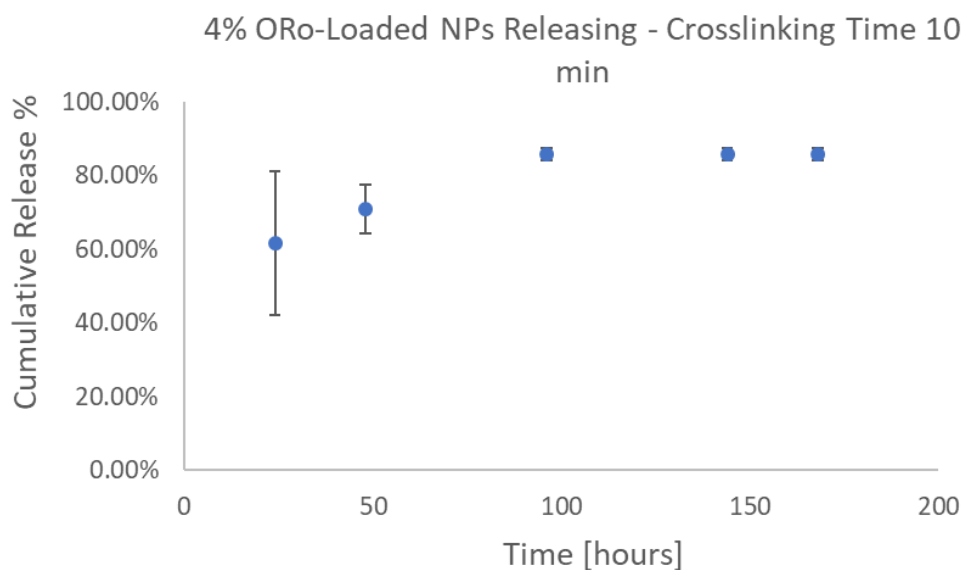
~ 95 ~

Figure 7.29 - Releasing Profile of GelMa Hydrogel 4% w/w ORo Loaded PNPs 10 min Crosslinking with PCL grids

For the two cases in the figure above, for PCL grids loaded with GelMa and 4% w/w of nanoparticles, the release appears to be better in the case of higher crosslinking time, that correspond to a thighter mesh size. Also for the case with higher PNPs concentration, the release is higher for higher crosilinkg time; for 4 minute and 8 minutes the cumulative releases are 57.57% and 60.90%, respectively.
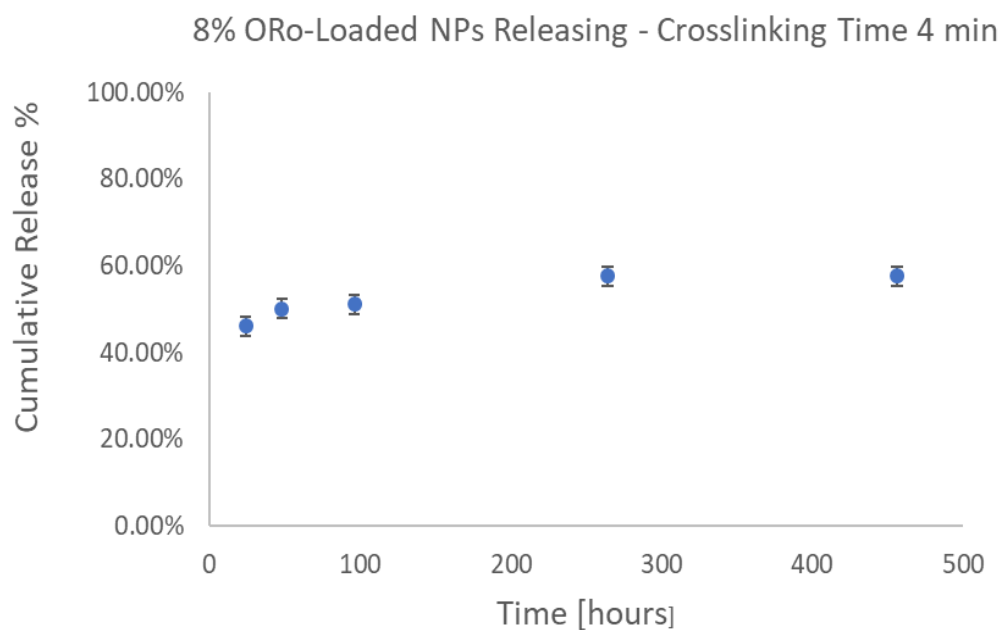
Figure 7.30 - Releasing Profile of GelMa Hydrogel 8% w/w ORo Loaded PNPs 4 min Crosslinking with PCL grids
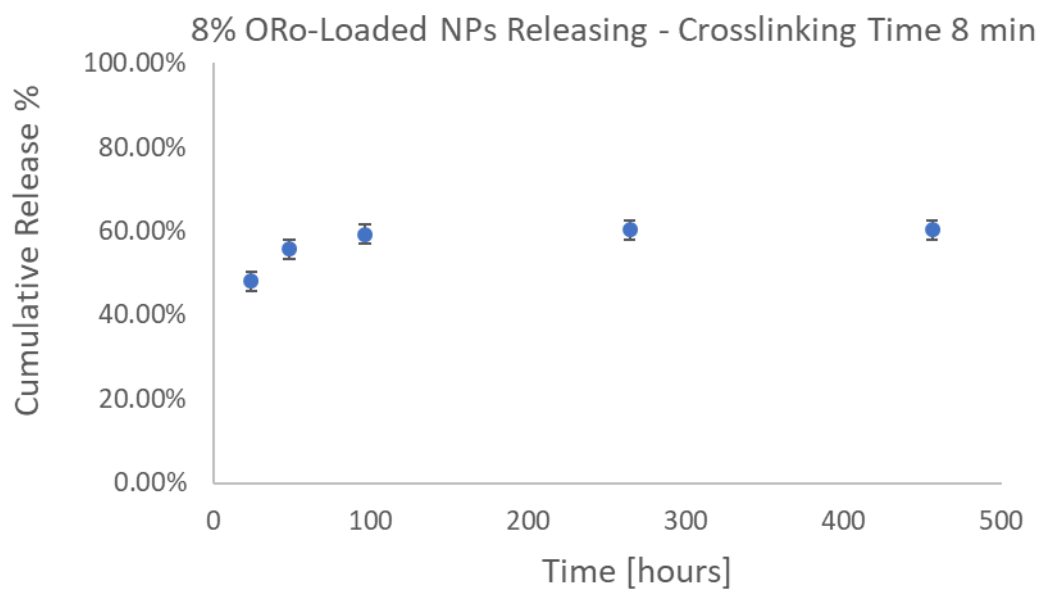

Figure 7.31 - Releasing Profile of GelMa Hydrogel 8% w/w ORo Loaded PNPs 8 min Crosslinking with PCL grids

Considering the metallic grids, as shown in figure 7.32 e 7.33 the situation about the crosslinking time is the same, the higher the crosslinking time, the higher is the molecule releasing, and the amount of drug released is superior compared to the devices in PCL. This is due to the fact that the polycaprolactone structures keep on themselves a little quantity of model drug, preventing its exiting from the gel.
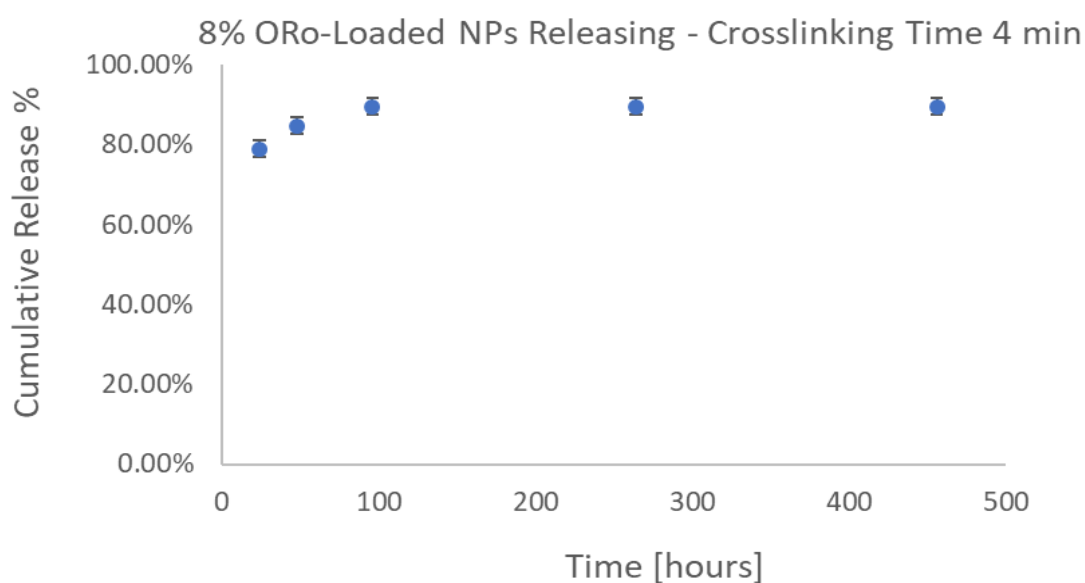

Figure 7.32 - Releasing Profile of GelMa Hydrogel 8% w/w ORo Loaded PNPs 4 min Crosslinking with Metallic Grids
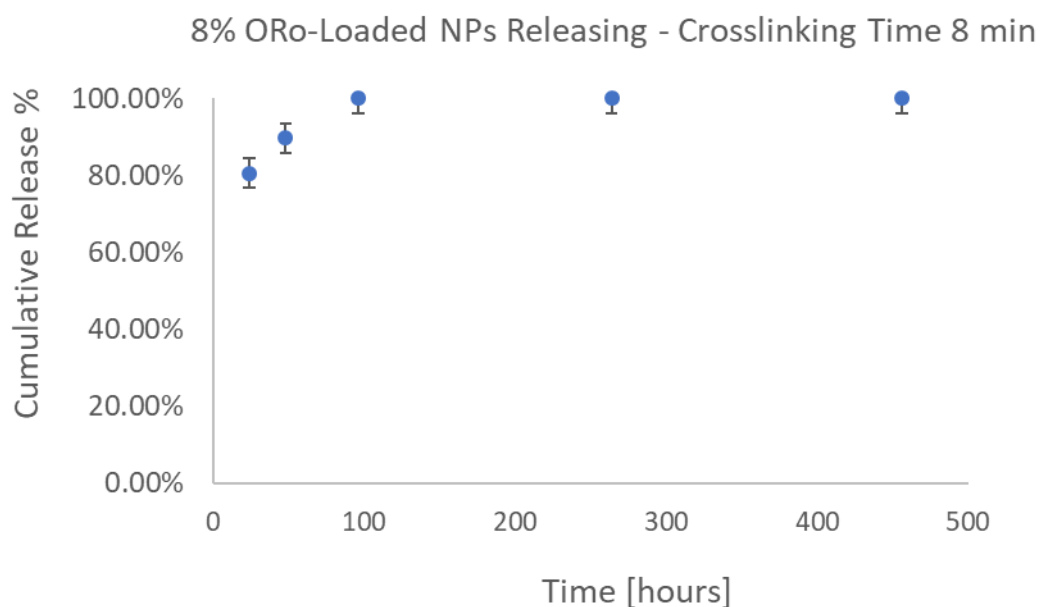
Figure 7.33 - Releasing Profile of GelMa Hydrogel 8% w/w ORo Loaded PNPs 8 min Crosslinking with Metallic Grids

7.3.1.3.2 Oil Red O and Sodium Alginate

Sodium alginate hydrogels releasing behaviour has been investigated too, in particular to highlights the differences with methacrylated gelatin and with the two devices material used for the grids.

The results obtained are shown in figure 7.34, 7.35 for the grid in PCL, while in figure 7.36, for the metallic grids, for 8% w/w of nanoparticles solution.

It can be highlighted that the final release of model drug released is 54.68% and 53.80%, practically the same for crosslinking time of 4 and 8 minutes respectively. It is probably due to the mesh size, that it does not change its dimension so fast in that interval of four minutes, so it cannot influence the release behaviour. In figure 7.36 , are reported the releasing points of the metallic grids coated with sodium alginate hydrogel, with 8% w/w of ORo Loaded PNPs, crosslinked for 8 minutes. As for methacrylated gelatin, here the released amount is higher, 60.90%, for reason that the metallic grids do not keep on themselves the same amount of Oil Red as the PCL.
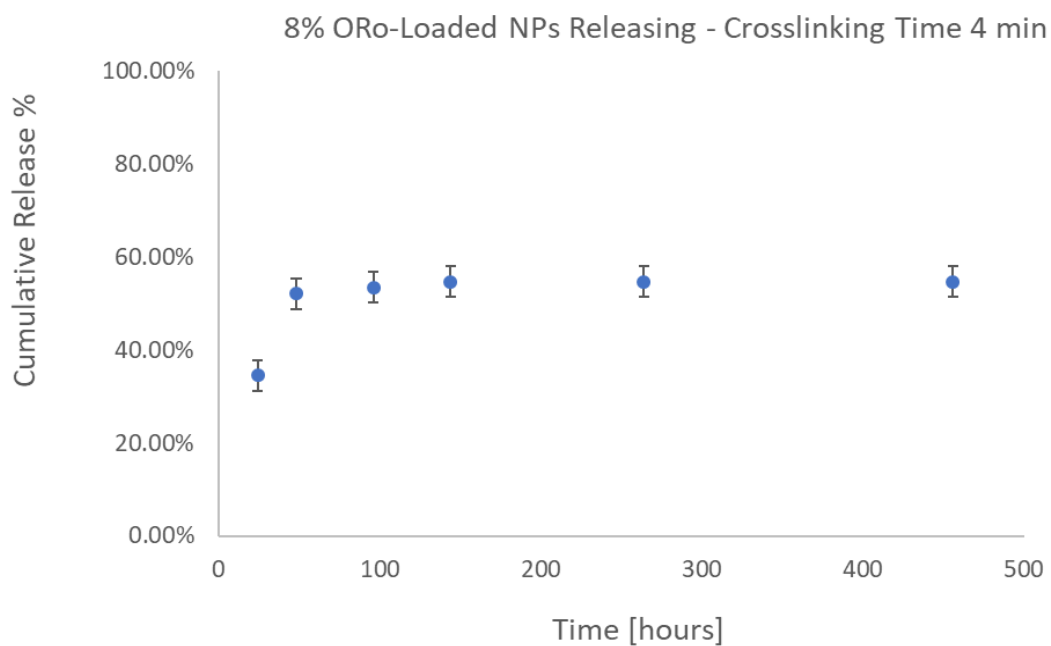
Figure 7.34 - Releasing Profile of Sodium Alginate Hydrogel 8% w/w ORo Loaded PNPs 4 min Crosslinking with PCL grids
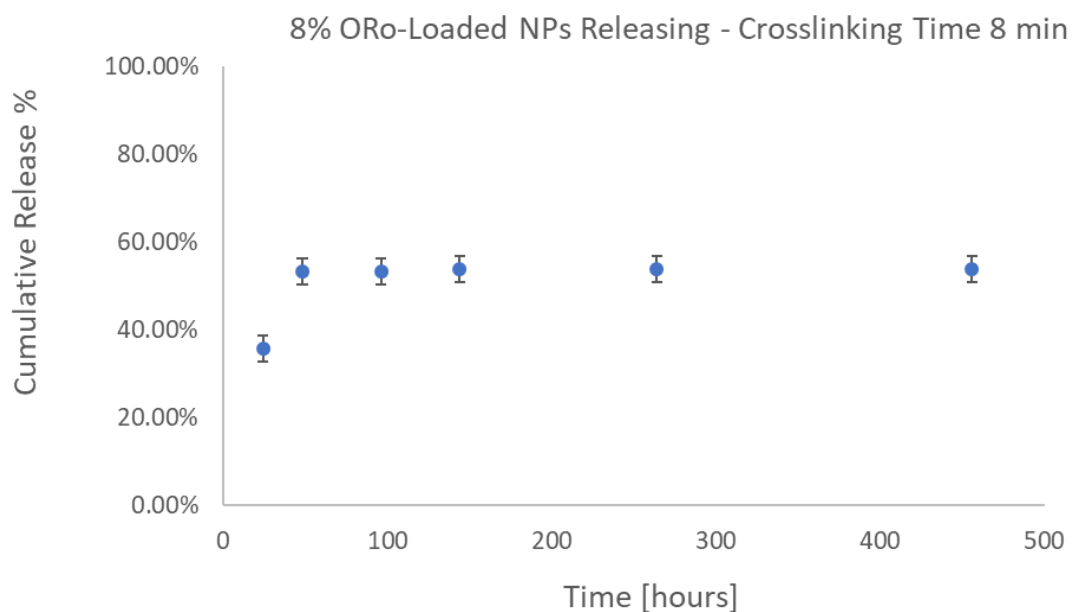
Figure 7.35 - Releasing Profile of Sodium Alginate Hydrogel 8% w/w ORo Loaded PNPs 8 min Crosslinking with PCL grids
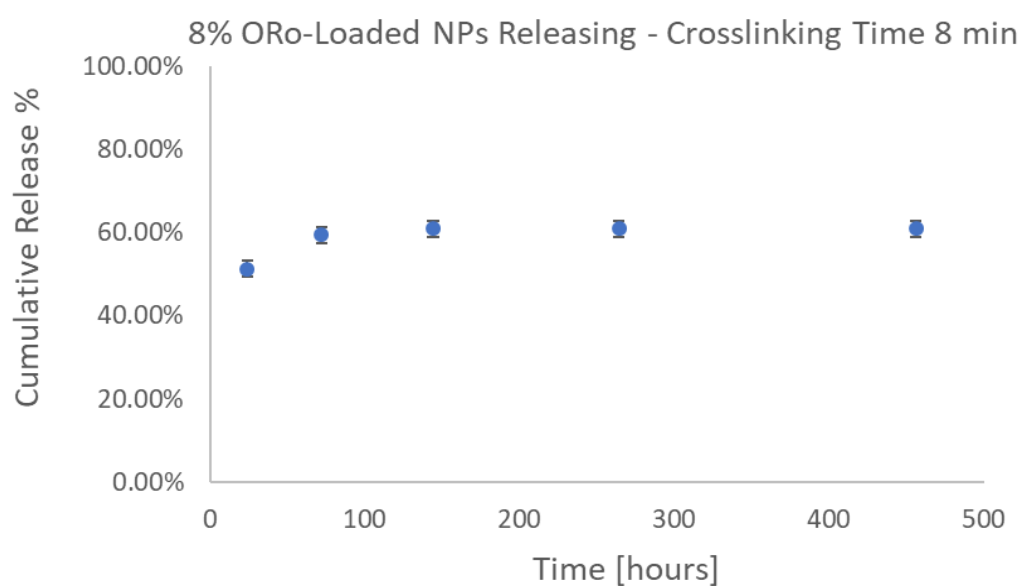

Figure 7.36 - Releasing Profile of Sodium Alginate Hydrogel 8% w/w ORo Loaded PNPs 8 min Crosslinking with Metallic Grids

7.3.2 Hydrophilic Model Drug

7.3.2.1 Rheological Characterization of GelMa with Rhodamine B Isothiocyanate

To investigate on the influence of the model drug on the crosslinking behaviour, we performed, also for this case, rheological analysis, as shown in figure x. Light intensity used to polymerized the gel was of 10 mW/cm^2 and 405 nm wavelength .
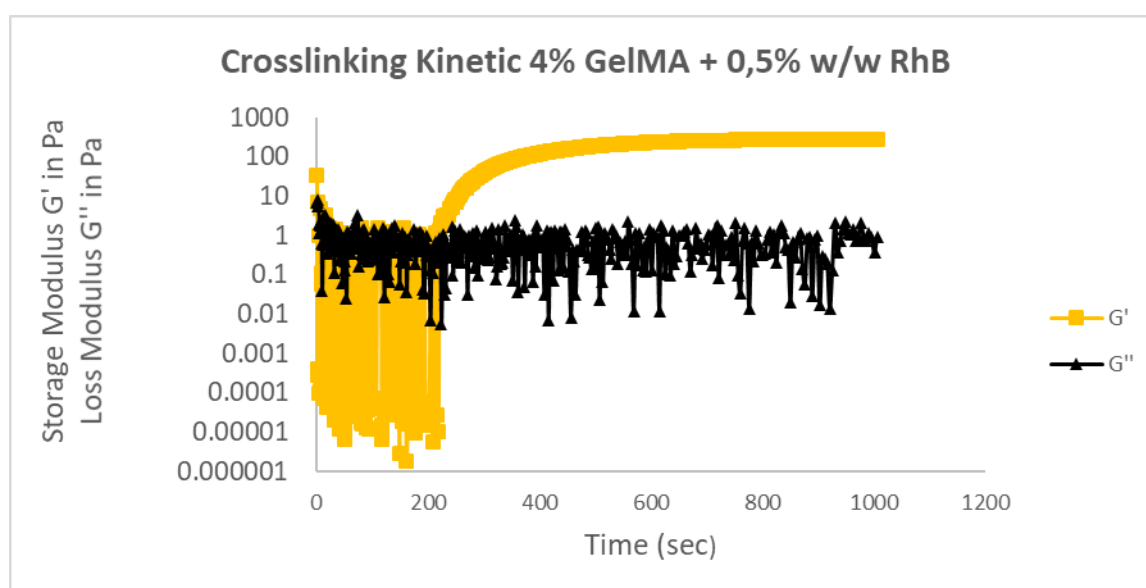

Figure 7.37 – Crosslinking Kinetic of Rhodamine B Isothiocyanate – loaded Hydrogel

The cross-over time changes from 75 sec. (case with no RhBI) to 220 sec. This happens because the RhBI molecule has absorbance peak very close to the one of the photoinitiator LAP, like in the case of Oil Red O, so this caused a delay in the polymerization kinetic.

7.3.2.2 Rhodamine B Isothiocyanate Photocatalytic Degradation Results

From the data collected using the spectrophotometric measurements, we have noticed a small degradation of RhBI in presence of UV light irradiation, in particular during the first 3 minutes of of the experiments, while in presence of the photoinitiator, the degradation is much more strong, as it can be compared in the figure 7.38 and 7.39 below.

The concentration revealed, in the case with photoinitator, starts from 50.61 µg/ml of RhBI detected and after 20 minuts of irradiation we got to a stable value of 14 µg/ml.
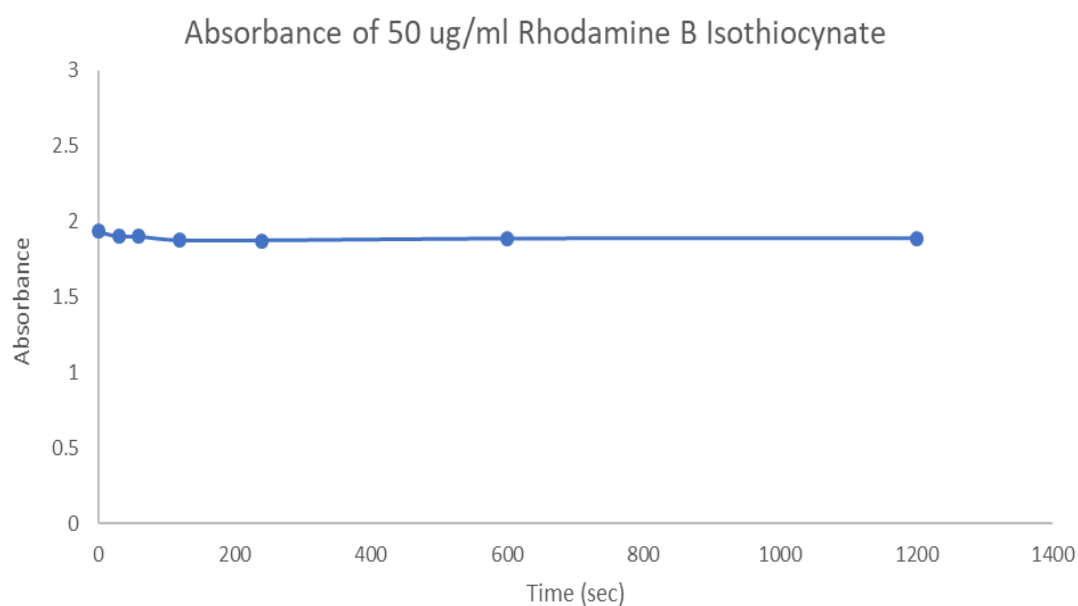
Figure 7.38– Absorbances of RhBI light up with UV light (no photoinitiator)
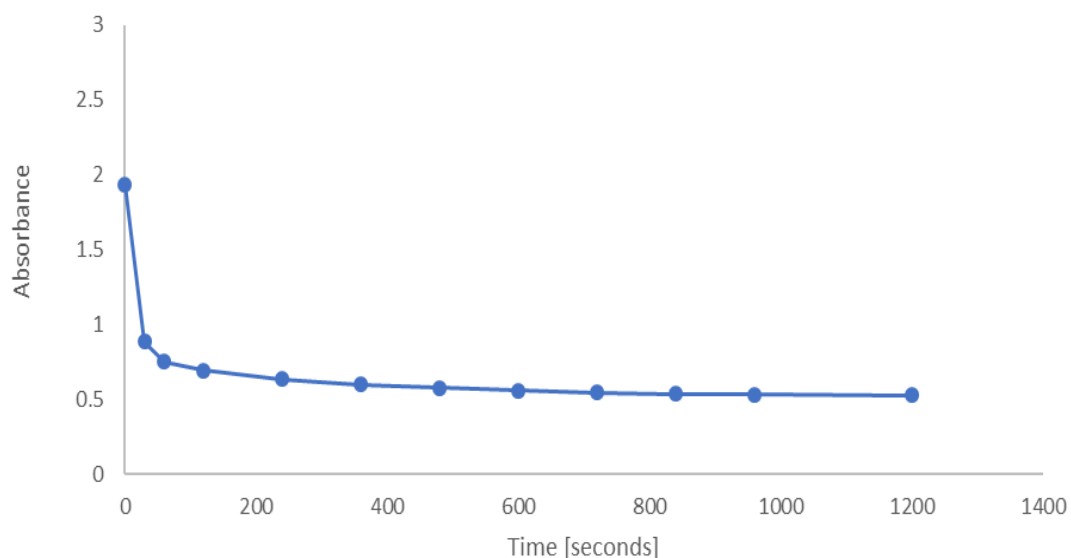
Figure 7.39– Absorbances of RhBI light up with UV light (with photoinitiator)

7.3.2.3 Rhodamine B Photocatalytic Degradation Results

The same degradation phenomena occurs with classic Rhodamine B and the same quantity of photoinitiator used for the isothiocyanated RhB. Again, the concentration of RhB switch from an inutial value of 46 µg/ml to a final one of 13 µg/ml, as demonstrated in figure 7.40.
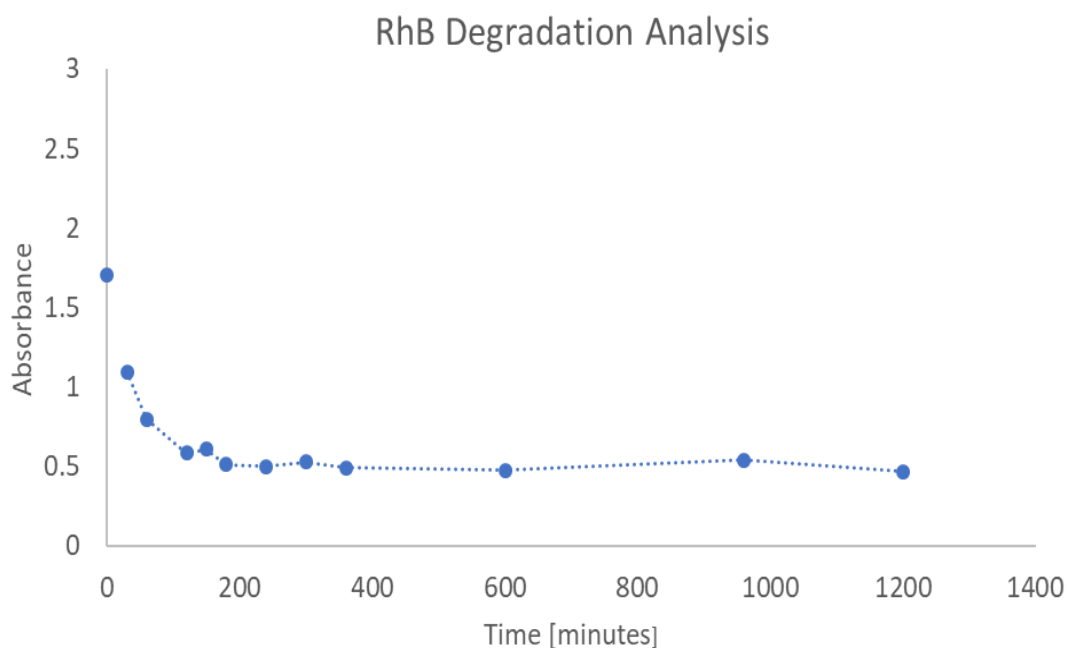
Figure 7.40 - Absorbances of RhB light up with UV light (with photoinitiator)

7.3.2.4 Rhodamine B Photocatalytic Degradation Mechanism

The photocatalytic degradation of RhB by the photogenerated active species like °OH and hole could attack the central carbon of RhB to decolorize the dye and further degraded via N-de-ethylation process.[35] A plausible degradation mechanism is reported in figure 7.41 .
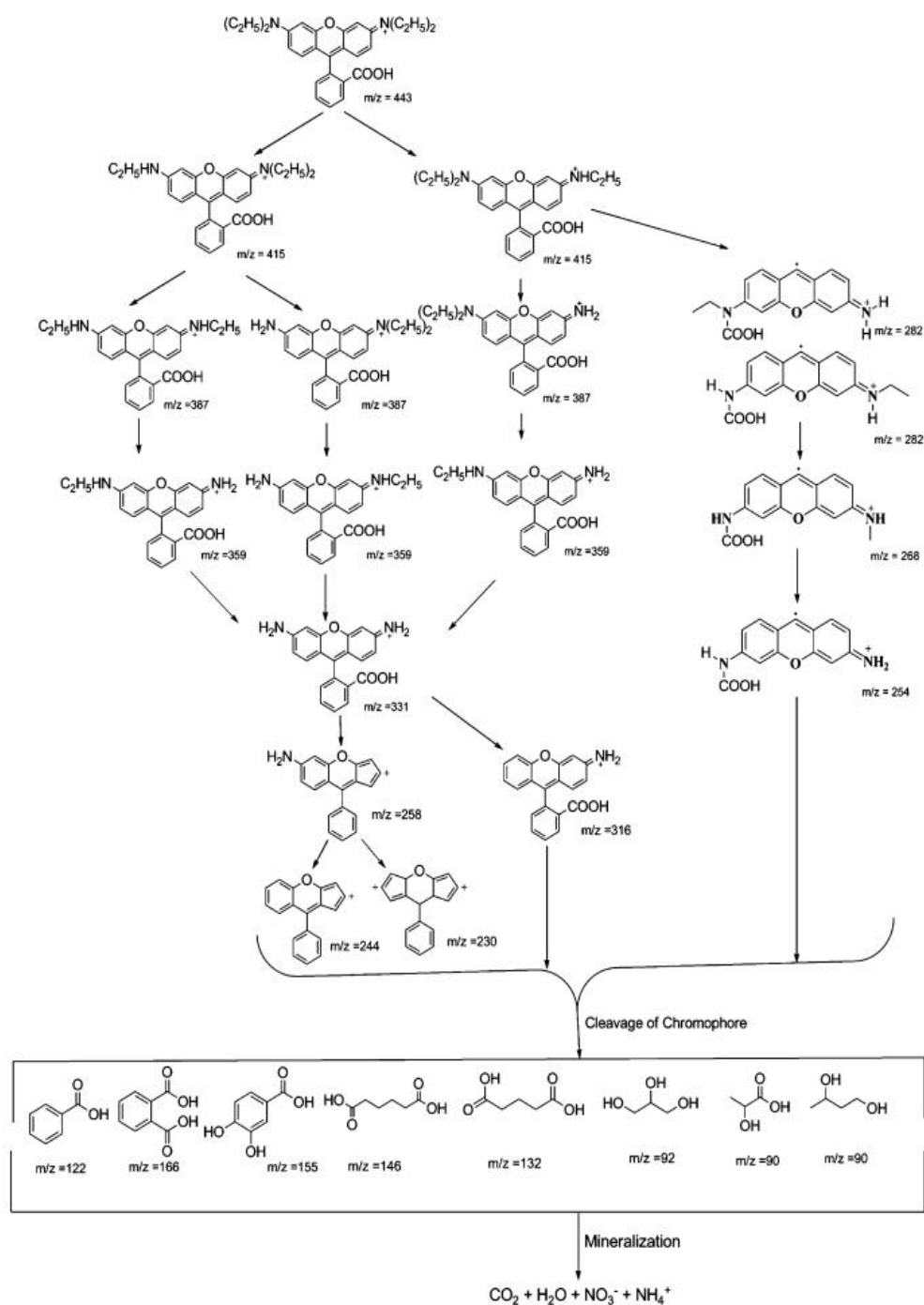
Figure 7.41 – Probable mechanism of photocatalytic degradation of RhB

7.3.2.5 Protective Effect of GelMa

To consider all the compounds in play in the drug releasing, we performed degradation conditions also in presence of GelMa itself, for the polymerization time frame, from zero to 3 minutes, to check if the compound in question screens the RhB from the damage due to the UV radiations. It is turned out, as it appears from the absorbance values registered and presented in figure 7.42, that it has a protective effect on the model drug.
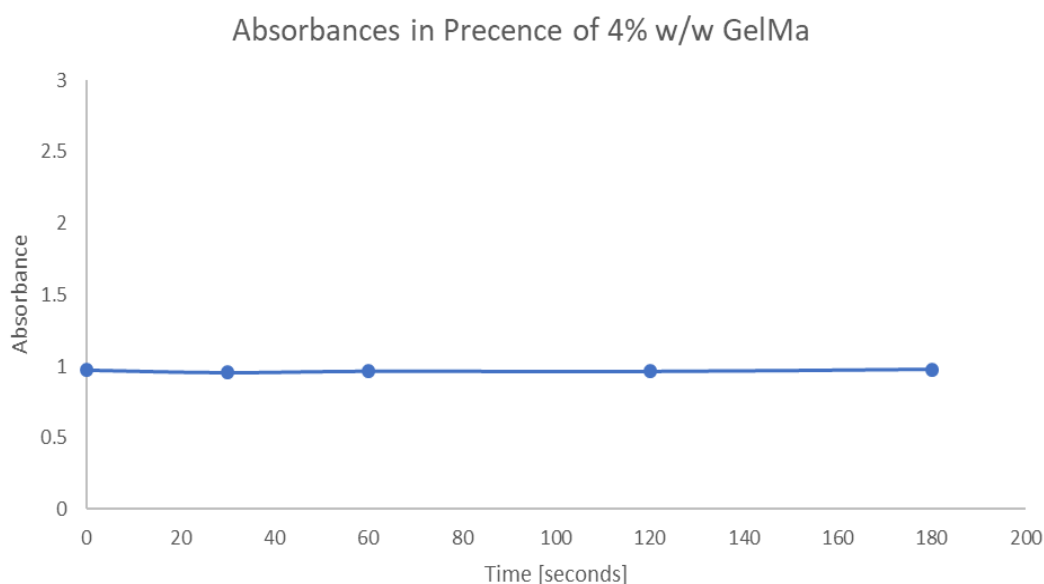
Figure 7.42 – Absorbance Values of RhB during UV Polymerization

7.3.2.6 Releasing Behaviour of Rhodamine B Isothiocyanate

For the Rhodamine B Isothiocyanate, combined with methacrylated gelatine, the release is pretty low, due to the fact that the isothiocyanate groups link themselves to the GelMa, retarding and blocking the release. This happens

due to the strong bond that is established between the isothiocyanate groups of the model drug and the NH_2 lateral groups of methacrylated gelatin. During this reaction, a thiourea is formed, as showed in figure 7.43, and its hydrolysis is much more difficult respect to normal amides.
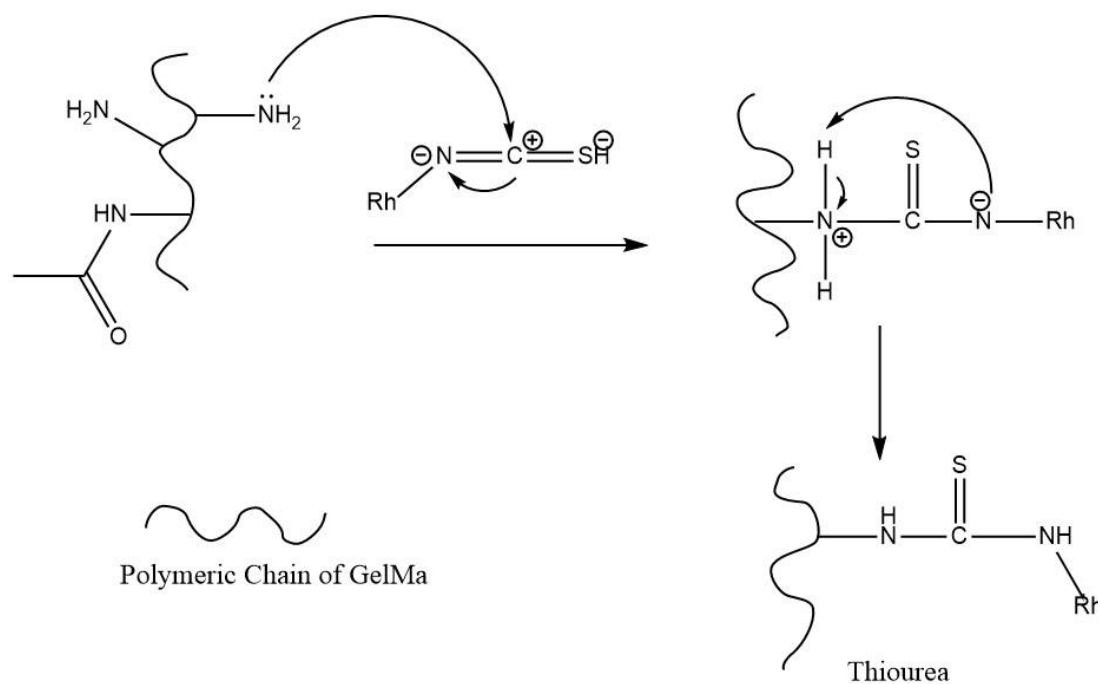
Figure 7.43 – Linking Mechanism of Rhodamine B Isothiocyanate to GelMa

Moreover, for this mimic drug, the release is a little bit higher when the crosslinking time is lower (12,87% compared to 11,47%).
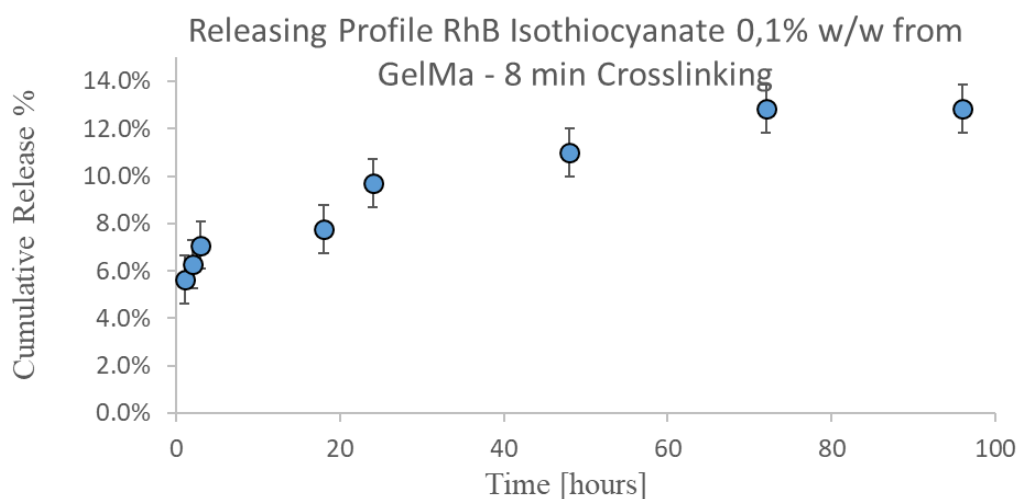
Figure 7.44 – Releasing Behaviour of RhBI after 8 minutes of crosslinking
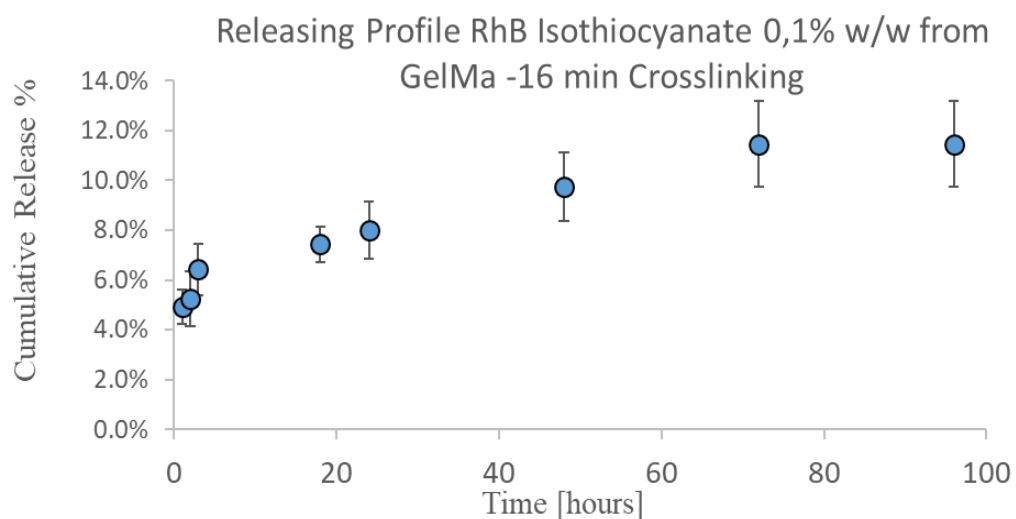
Figure 7.45 – Releasing Behaviour of RhBI after 16 minutes of crosslinking

7.3.2.7 Releasing Behaviour of Rhodamine B

Releasing studies on rhodamine B loaded in PCL GelMa-coated grids have been performed too. In the figure 7.46 below, is presented the calibration curve made for the new type of rhodamine used. As it is possible to note in figure 7.47, for this kind of rhodamine, the release has a proper releasing behaviour, due to the fact that rodamine B in this case is not linked ad tightly as rhodamine B isothiocyanate to GelMa. The maximum cumulative release is 91.36%.
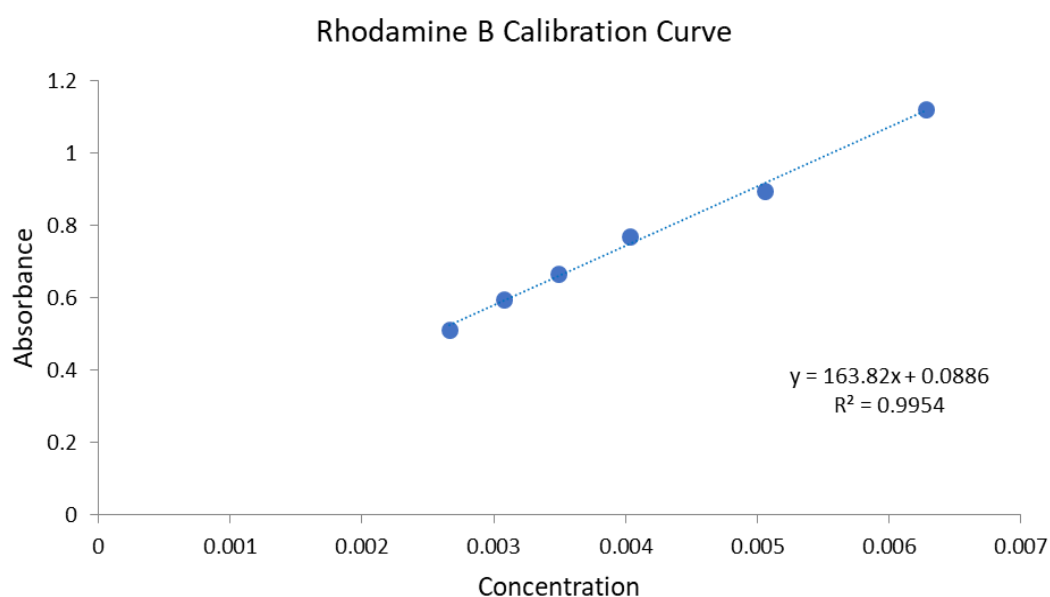
Figure 7.46 – Rhodamine B Calibration Curve
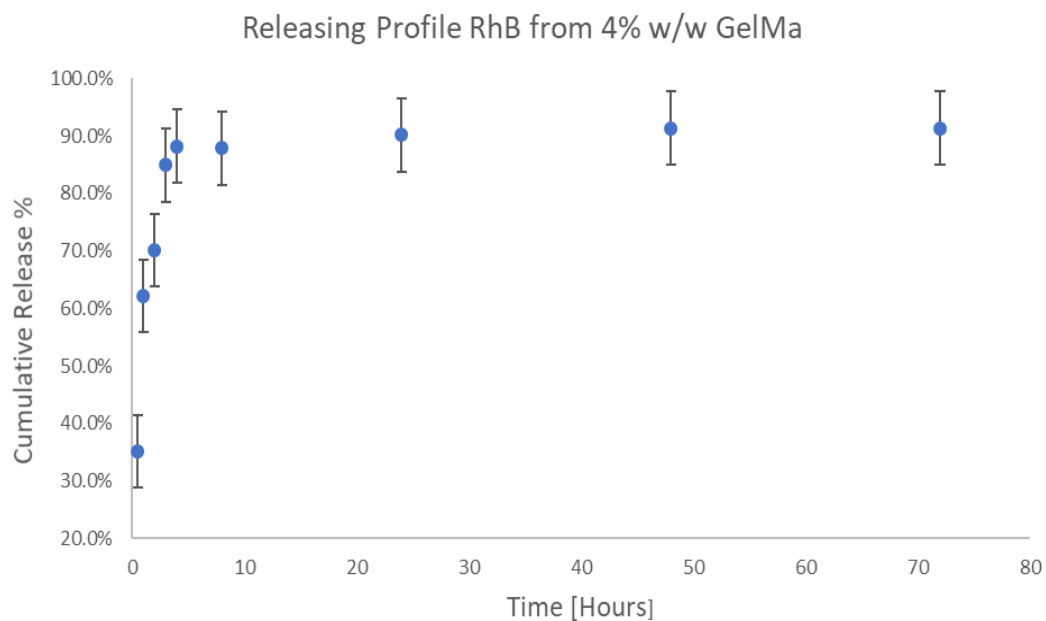
Figure 7.47 - Releasing Behaviour of RhB after 8 minutes of crosslinking

CHAPTER 8
CONCLUSIONS

This thesis work intends to focus on two important aspects that have to be considered when nowadays we think to a system that can comply both the tissue engineering field and the drug delivery one: the on-target cells and the drug delivery. With on-target delivery is meant the possibility to drive and distribute cells and drugs respectively, in a place of the body where their functionalities are requested. With a cells delivery device it is possible to transport and collect cells of whatever type or function wherever they are needed, for example for wound healing or a desease treatment. With drug delivery it is possible to tune the properties of the carrier to maintain an adequate and steady concentration for several days.

This project leads to the investigation on different phenomena and properties that influenced the two aspects mentioned above.

The first point was to control the phenomena of the superficial tension to easily coat the devices with the gel and then their fast polymerization by UV irradiation *in situ.*

Secondly, we wanted to investigate if the designed system, composed by GelMa and polycaprolactone could have been suitable for cells life; after a positive check, we tried to find the best condition for cells wellness and profliferation, which appeared to be the formulation we obtained preaparing the hydrogel with 4% wt. of methacrylated gelatin. In this case, we also tried to investigate on the effects of another material, like gold-coated metal, studied in details by Magagnin's group, but unfortunately, it did not seem to work in that specific case.

As last part, keeping in mind the hydrogel characteristics we improved for the cells environment, we studied the drug releasing behaviour of the systems, both the ones in PCL and in metal. For this part of the project, we introduced also another carrier, sodium alginate hydrogel, with the future outlook to link it with RGD peptide sequences to make it suitable for the cells attachment. We have started to syntethized it at Politecnico di Milano, to use it for future researches.

Considering the rhodamine B isothiocyanate, the results were less promising, because of a lower amount released, whereas the data obtained for the sodium alginate were satisfying, in terms of releasing efficiency, *i.e.* the amount of drug released compared to the one charged into the gels matrix.

In this investigation, we also noticed a photocatalytic degradation of rhodamine B and rhodamine B isothiocyanate, due to the photoinitiator used, as well as the protection effect of the GelMa on both the two molecules mentioned. This was important to validate our experiments and data colleted during the researches.

References

1.Ian Gibson, David W. Rosen, B. S. *Additive Manufacturing Technologies: Rapid Prototyping to Direct Digital Manufacturing*. vol. 54 (2009).

2.	Wang, X., Jiang, M., Zhou, Z., Gou, J. & Hui, D. 3D printing of polymer matrix composites: A review and prospective. *Compos. Part B Eng.* **110**, 442–458 (2017).

3.	Aal, A. A., Shaaban, A. & Hamid, Z. A. Nanocrystalline soft ferromagnetic Ni-Co-P thin film on Al alloy by low temperature electroless deposition. *Appl. Surf. Sci.* **254**, 1966–1971 (2008).

4.	Mondal, D., Griffith, M. & Venkatraman, S. S. Polycaprolactone-based biomaterials for tissue engineering and drug delivery: Current scenario and challenges. in *International Journal of Polymeric Materials and Polymeric Biomaterials* vol. 65 255–265 (2016, 2016).

5.	Hutmacher, D. W. *et al.* Mechanical properties and cell cultural response of polycaprolactone scaffolds designed and fabricated via fused deposition modeling. *J. Biomed. Mater. Res.* **55**, 203–216 (2001).

6.	Drahansky, M. *et al.* We are IntechOpen , the world ' s leading publisher of Open Access books Built by scientists , for scientists TOP 1 %. *Intech* **i**, 13 (2016).

7.	Akhtar, M. F., Hanif, M. & Ranjha, N. M. Methods of synthesis of hydrogels … A review. *Saudi Pharm. J.* **24**, 554–559 (2016).

8.	Ahmed, E. M. Hydrogel: Preparation, characterization, and applications: A review. *J. Adv. Res.* **6**, 105–121 (2015).

9.	Klouda, L. & Mikos, A. G. Thermoresponsive hydrogels in biomedical applications. **68**, 34–45 (2008).

10.	Van Den Bulcke, A. I. *et al.* Structural and rheological properties of methacrylamide modified gelatin hydrogels. *Biomacromolecules* **1**, 31–38 (2000).

11.	Zhu, M., Wang, Y., Ferracci, G., Zheng, J. & Cho, N. Gelatin methacryloyl and its hydrogels with an exceptional degree of controllability and batch- to-batch consistency. 1–13 (2019) doi:10.1038/s41598-019-42186-x.

12.	Manuscript, A. Alginate : properties and biomedical applications. **37**, 106–126 (2013).

13.	Gunasekara, N. S. *et al.* Isosorbide 5-Mononitrate A Review of a Sustained-Release Formulation. **57**, 261–277 (1999).

14.   Calcium Antagonists in Cardiology : Update on Sustained-Release Delivery Systems.

15.   Wagstaff, A. J. & Goa, K. L. Once-Weekly Fluoxetine. **61**, 2221–2228 (2001).

16.   Michel, M. C. A Benefit-Risk Assessment of Extended-Release Oxybutynin. **25**, 867–876 (2002).

17.   Julio, K. De *et al.* Sítios Geológicos e Paleontológicos do Brasil Belo promontório de rochas neoproterozoicas associadas a praias e dunas quaternárias com registros de variações do nível do mar. 22–26 (2012).

18.   Patel, A. Ocular drug delivery systems: An overview. *World J. Pharmacol.* **2**, 47 (2013).

19.   Fusco, S. *et al.* Chitosan Electrodeposition for Microrobotic Drug Delivery. *Adv. Healthc. Mater.* **2**, 1037–1044 (2013).

20.   George Chatzipirpiridis, Olgaç Ergeneman, Juho Pokki, Franziska Ullrich, Stefano Fusco, José A. Ortega, Kartik M. Sivaraman, Bradley J. Nelson, and S. P. Electroforming of Implantable Tubular Magnetic Microrobots for Wireless Ophthalmologic Applications. *Adv. Funct. Mater.* (2015).

21.   Thulasiramaraju, T. V, Kumar, B. T. & Nikilesh Babu, M. Pulmonary Drug Delivery System: an Overview. *Asian J. Res. Pharm. Sci. Biotechnol.* **1**, 16–34 (2013).

22.   Djupesland, P. G. Nasal drug delivery devices: Characteristics and performance in a clinical perspective-a review. *Drug Deliv. Transl. Res.* **3**, 42–62 (2013).

23.   Brown, M. B., Martin, G. P., Jones, S. A. & Akomeah, F. K. Dermal and transdermal drug delivery systems: Current and future prospects. *Drug Deliv. J. Deliv. Target. Ther. Agents* **13**, 175–187 (2006).

24.   Khadka, P. *et al.* Pharmaceutical particle technologies: An approach to improve drug solubility, dissolution and bioavailability. *Asian J. Pharm. Sci.* **9**, 304–316 (2014).

25.   Lee, K. Y. & Mooney, D. J. Alginate: Properties and biomedical applications. *Prog. Polym. Sci.* **37**, 106–126 (2012).

26.   Bajpai, S. K., Bajpai, M. & Saxena, S. Ion exchange resins in drug delivery. *Ion Exch. Solvent Extr. A Ser. Adv.* **18**, 103–150 (2007).

27.   Mota, J. Matrix- and reservoir-type oral multiparticulate drug delivery. *Ph. D. Diss. Freie Univ. Berlin, Ger.* (2010).

28.   Pla, P. & Bone, C. Journal of Material Sciences & Engineering Characterization of 3D Printed PLA / PCL / TiO 2 Composites for Cancellous Bone. **7**, 1–9 (2018).

29.   Hernandez, I. & Kumar, A. A Bioactive Hydrogel and 3D Printed Polycaprolactone System for Bone Tissue Engineering. (2017) doi:10.3390/gels3030026.

30.   Bernasconi, R. *et al.* Materials Horizons electroless coated 3D printed architectures †. 699–707 (2018) doi:10.1039/c8mh00206a.

31.   Tissue, L. *et al.* Synthesis and Properties of Gelatin Methacryloyl (GelMA) Hydrogels and Their Recent Applications in. (2018) doi:10.3390/polym10111290.

32.   Serafim, A. *et al.* One-pot synthesis of superabsorbent hybrid hydrogels based on methacrylamide gelatin and polyacrylamide. Effortless control of hydrogel properties through

composition design. *New J. Chem.* **38**, 3112–3126 (2014).

33.   Nichol, J. W. *et al.* Biomaterials Cell-laden microengineered gelatin methacrylate hydrogels. *Biomaterials* **31**, 5536–5544 (2010).

34.   Fairbanks, B. D., Schwartz, M. P., Bowman, C. N. & Anseth, K. S. Biomaterials Photoinitiated polymerization of PEG-diacrylate with lithium phenyl-2 , 4 , 6-trimethylbenzoylphosphinate : polymerization rate and cytocompatibility. *Biomaterials* **30**, 6702–6707 (2009).

35.   Natarajan, T. S., Thomas, M., Natarajan, K., Bajaj, H. C. & Tayade, R. J. Study on UV-LED/TiO2 process for degradation of Rhodamine B dye. *Chem. Eng. J.* **169**, 126–134 (2011).

36.   Nagaraja, R., Kottam, N., Girija, C. R. & Nagabhushana, B. M. Photocatalytic degradation of Rhodamine B dye under UV/solar light using ZnO nanopowder synthesized by solution combustion route. *Powder Technol.* **215–216**, 91–97 (2012).

37.   Hoch, E. & Hirth, T. physical properties for functional bioprinting. 5675–5685 (2013) doi:10.1039/c3tb20745e.

38.   Rogero, S. O., Higa, O. Z., Saiki, M., Correa, O. V. & Costa, I. Cytotoxicity due to corrosion of ear piercing studs. *Toxicol. Vitr.* **14**, 497–504 (2000).

39.   Bhattacharjee, S. DLS and zeta potential - What they are and what they are not? *J. Control. Release* **235**, 337–351 (2016).